THE DEVELOPMENT OF A NOVEL VACCINE AGAINST AVIAN INFLUENZA H7N9 VIRUS

A Thesis Submitted to the College of
Graduate and Postdoctoral Studies
In Partial Fulfillment of the Requirements
For the Degree of Master of Science
In the Vaccinology and Immunotherapeutics Program
School of Public Health
University of Saskatchewan
Saskatoon, SK

By

Shelby Landreth

PERMISSION TO USE POSTGRADUATE THESIS

In presenting this thesis in partial fulfillment of the requirements for a postgraduate degree from the University of Saskatchewan, I agree that the libraries of this university may make it freely available for inspection. I further agree that permission for copying of this thesis in any manner, whole or in part, for scholarly purposes may be granted by the professors who supervised my thesis work or in their absence, the Head of the Department or the Dean of the College in which my thesis work was done. It is understood that any copying or publication or use of this thesis or parts thereof for financial gain shall not be allowed without any written permission. It is also understood that due recognition shall be given to me and to the University of Saskatchewan in any scholarly use which may be made of any material in my thesis.

Request for permission to copy or to make other use of material in this thesis in whole or part should be addressed to:

Executive Director, School of Public Health,
Program Director, Vaccinology and Immunotherapeutics
University of Saskatchewan
107 Wiggins Road
Saskatoon, Saskatchewan, S7N 5B4
Canada

OR

Dean
College of Graduate and Postdoctoral Studies
University of Saskatchewan
116 Thorvaldson Building, 110 Science Place
Saskatoon, Saskatchewan, S7N 5C9
Canada

ABSTRACT

Influenza A viruses (IAV) are classified into the *Orthomyxoviridae* family and are composed of segmented, negative-sense, single-stranded ribonucleic acid (ssRNA) genomes in an enveloped particle. IAV is capable of infecting a wide variety of species, including but not limited to humans, birds, pigs, bats, and sea mammals. Up until 2013, H7N9 IAV was only prevalent in poultry; however, at this time H7N9 began infecting humans in China. Since 2013, China has seen six epidemic waves of the H7N9 virus, with human cases and deaths totaling 1,568 and 616, respectively, as of March 4, 2020. Although this virus presents high morbidity and mortality rates in humans, the majority of human cases have been a result of close contact to poultry in live poultry markets (LPMs). Fortunately, the change for sustained human-to-human transmission has not yet been acquired in this virus. However, due to IAVs evolutionary mechanisms of *antigenic shift* and *antigenic drift*, H7N9 could gain sustained transmission among humans at any time, which poses a severe threat to public health. Therefore, preventive control methods must be developed in an effort to control the spread of this influenza virus.

Vaccination is currently the main method for controlling the spread and preventing influenza infection. Currently, the two available types of vaccines are the inactivated influenza vaccines (IIV) and the live attenuated influenza vaccines (LAIV). IIVs are composed of either whole influenza virions or portions of its virion produced in large volumes, followed by inactivation of the virus with either β-propiolactone or formaldehyde. IIVs are commonly administered intramuscularly, and sometimes include adjuvants to boost their immune responses. IIVs have been countlessly demonstrated to be highly safe for all populations. LAIVs on the other hand, are composed of live viruses of which their virulence is reduced through limited replication in the vaccinated host. LAIVs are administered intranasally and do not require an adjuvant because they are capable of stimulating stronger immune responses compared to IIVs. However, one common drawback towards the use of LAIVs is the possibility of virulence reversion. On the contrary, replication-defective virus vaccines are made up of viruses defective in either viral replication, synthesis, or assembly. These replication-defective virus vaccines, therefore, consist of very limited replication in the vaccinated host and have been found to possess the advantages of both IIVs and LAIVs. These advantages include the high safety profile due to the low risk of virulence reversion, as well as the ability to induce a strong immune response. To date, no commercial vaccine is available for the H7N9 influenza viruses.

The first step in the influenza replication cycle is the binding of the virus to the host cell, which is followed by receptor-mediated endocytosis. After endocytosis occurs, in order for influenza virus to become infective, cleavage of the hemagglutinin (HA) precursor form, HA0, into HA1 and HA2 must occur. This cleavage is most often mediated by trypsin-like host proteases, inducing fusion between the viral and endosomal membranes. Therefore, this particular step is essential for determining viral pathogenicity.

For this Masters project, the goal was to generate a replication-defective virus vaccine derived from H7N9 IAV, that is composed of an altered HA cleavage site that can only be cleaved and thus activated *in vitro* by the exogenous protease elastase which is not readily available in the respiratory tract. This replication-defective virus vaccine would, therefore, be inactive during natural infection, but active *in vitro* if the appropriate protease was provided. Previous studies have proven this replication-defective nature through the mutation of the HA cleavage site from a trypsin-sensitive motif to an elastase-sensitive motif. However, these studies have only been performed with the swine influenza virus (SIV) H1N1, a human-derived H7N7 HPAI, a mouse-adapted human-derived H1N1 virus, as well as an influenza B virus (IBV) (Babiuk et al., 2011; Gabriel et al., 2008; Mamerow et al., 2019; Masic et al., 2009; Masic et al., 2010; Masic et al., 2013; Stech et al., 2011; Stech et al., 2005). Using the technique of reverse genetics, we generated a recombinant mutant H7N9 virus, BC15-HA/QTV/NA (PR8), derived from the human isolate A/British Columbia/01/2015 (H7N9) [BC15 (H7N9)] with a backbone from A/Puerto Rico/8 (H1N1) [PR8 (H1N1)]. This recombinant mutant BC15-HA/QTV/NA (PR8) virus possesses a mutant HA composed of three mutations at the HA cleavage site: lysine to glutamine at amino acid (aa) 337 (Lys-Gln), glycine to threonine at aa 338 (Gly-Thr), and arginine to valine at aa 339 (Arg-Val). In addition to the mutant HA, this recombinant mutant BC15-HA/QTV/NA (PR8) virus also contains the neuraminidase (NA) from BC15 (H7N9) and the six internal proteins from PR8 (H1N1).

In the first part of our study, we established a mouse model of BC15 (H7N9) influenza virus. BALB/c mice were intranasally infected with various doses of BC15 (H7N9) (10^3 PFU, 10^4 PFU, and 10^5 PFU), and were monitored daily for 14 days post-infection (d.p.i.). In this study, we found BC15 (H7N9) to affect mice in a dose-dependent manner: the 10^3 dose killing all mice by 8 d.p.i.; the 10^4 dose by 6 d.p.i.; and the 10^5 dose by 5 d.p.i. In addition, all doses were capable of inducing high viral replication, pathology, and proinflammatory cytokine

induction in the mouse lung. From this study, we concluded 10^3 PFU to be the chosen dose for future experiments.

In the second part of this study, we developed and characterized the recombinant mutant BC15-HA/QTV/NA (PR8) virus, which showed this virus to be entirely dependent on elastase for its replication, contain similar growth properties to its wild-type counterpart, and be genetically stable *in vitro*. In addition, when this recombinant mutant BC15-HA/QTV/NA (PR8) virus was intranasally administered in BALB/c mice, it was found to be non-virulent and replication-defective, evident by a lack of body weight loss, 100% survival rate, and no viral replication detected in the mouse lung.

Since we established this recombinant mutant BC15-HA/QTV/NA (PR8) virus to be replication-defective in mice, in order to consider this virus as a replication-defective virus vaccine candidate, we needed to test the immunogenicity and protective efficacy in BALB/c mice. To do this, we intranasally vaccinated mice twice with this recombinant mutant BC15-HA/QTV/NA (PR8) virus and then challenged the mice with a lethal dose of BC15 (H7N9). In this study, we reported that the intranasally administered BC15-HA/QTV/NA (PR8) virus induced significantly elevated levels of antigen-specific IFN-γ and IL-5 secreting cells in the splenocytes, which is evidence of a strong cell-mediated response. In addition, this virus increased the levels of neutralizing antibodies in the mouse serum, evident by both the hemagglutinin inhibition (HAI) and serum virus neutralization (SVN) assays, as well as heightened the levels of antigen-specific IgG, IgG1, and IgG2a in the mouse serum. Once the mice were challenged with BC15 (H7N9), our data showed that two intranasal vaccinations with BC15-HA/QTV/NA (PR8) were sufficient to provide complete protection of the mice from a homologous challenge. This complete protection was evident by the lack of body weight loss, 100% survival rate, lack of viral replication detected in the mouse lung, as well as the complete abolishment of proinflammatory cytokine induction in the mouse lung associated with the influenza disease. Taken together, this study demonstrates the strong potential the BC15-HA/QTV/NA (PR8) virus possesses to serve as a replication-defective virus vaccine candidate against H7N9 influenza viruses.

ACKNOWLEDGEMENTS

I would like to express my appreciation to my supervisor, Dr. Yan Zhou, for her supervision, support, and constructive criticism that allowed me to finish my study. This Master's of Science provided me with the opportunity to become experienced in a wide variety of responsibilities, which will aid in my career further down the road. I would also wish to extend my appreciation to my advisory committee member Dr. Sylvia van den Hurk, and graduate chair, Dr. Suresh Tikoo and for their suggestions on how to improve my study and keep me moving in the forward direction.

I would also like to thank my former colleague, Dr. Amit Gaba for training and assisting me with experiments I did not fully understand, as well as for his inspiration and helpful suggestions. I would also like to acknowledge my former and current colleagues, whom taught me valuable life lessons which I will carry with me forever.

Most notably, I feel thankful to the VIDO-InterVac Animal Care staff, as I could not have completed my Master's of Science without their hands-on hard work, help, advice, and guidance with regards to all the mouse work that was required for my study.

Further, I am deeply grateful for the funding sources, the Public Health Agency of Canada (PHAC) grant to Dr. Yan Zhou as well as the Vaccinology & Immunotherapeutics Program, School of Public Health, University of Saskatchewan that provided a scholarship to me.

Finally and most importantly, I thank my family and fiancé, Troy Harms, for always encouraging me to keep pursuing my goals and support me every step of the way. Without them, I could not have completed my study, and for that, I am eternally grateful. I also wish to thank Herberto.

Shelby Landreth

TABLE OF CONTENTS

PERMISSION TO USE POSTGRADUATE THESIS ..... **i**

ABSTRACT ..... **ii**

ACKNOWLEDGEMENTS ..... **v**

TABLE OF CONTENTS ..... **vi**

LIST OF FIGURES ..... **ix**

LIST OF TABLES ..... **xi**

LIST OF ABBREVIATIONS ..... **xii**

CHAPTER 1 LITERATURE REVIEW **1**

1.1 INFLUENZA VIRUS **1**

1.1.1 Classification and nomenclature 1

1.1.2 IAV virion structure 3

1.1.3 Genome structure and organization 5

1.1.4 Elastase 14

1.1.5 Replication cycle 15

1.1.6 Evolution and Genetics 18

1.1.7 Immunology of IAV 21

1.2 H7N9 INFLUENZA VIRUS **24**

1.2.1 Etiology and epidemiology 24

1.2.2 Clinical signs, pathogenesis, and diagnosis of H7N9 27

1.3 INFLUENZA VIRUS VACCINES **28**

1.3.1 Vaccination 28

1.3.2 Inactivated influenza vaccines (IIV) in Canada 29

1.3.3 Live attenuated influenza vaccines (LAIV) in Canada 31

1.3.4 Experimental live attenuated vaccines in development 35

CHAPTER 2 HYPOTHESIS AND OBJECTIVES **41**

2.1 OVERALL GOALS AND RATIONALE **41**

2.2 HYPOTHESIS **43**

2.3 OBJECTIVES **43**

CHAPTER 3 ESTABLISHMENT OF A MOUSE MODEL OF A/BRITISH COLUMBIA/01/2015 [BC15 (H7N9)] VIRUS **44**

3.1 ABSTRACT **45**

3.2 INTRODUCTION **46**

3.3 MATERIALS AND METHODS **48**

3.3.1 Cells and viruses 48

3.3.2 Ethics statement 48

3.3.3 Mouse experiments 48

3.3.4 Virus isolation and titration 49

3.3.5 RNA extraction and quantitative RT-PCR (qRT-PCR) 49

3.3.6 Histopathology 51

3.4 RESULTS **52**

3.4.1 Survival rate and body weight loss of mice infected with the HPAI H5N1 and LPAI H7N9 strain isolates 52
3.4.2 Histopathology of the mouse lung 53
3.4.3 Replication efficiency of the HPAI H5N1 and LPAI H7N9 strain isolates in different organs of mice 55
3.4.4 Cytokine and chemokine profiling in the mouse lung 56
3.5 DISCUSSION AND CONCLUSIONS 60
3.6 ACKNOWLEDGEMENTS 63

CHAPTER 4 REVERSE-GENETICS GENERATED ELASTASE-DEPENDENT BC15 (H7N9) INFLUENZA VIRUS IS REPLICATION-DEFECTIVE IN MICE 65
4.1 ABSTRACT 66
4.2 INTRODUCTION 67
4.3 MATERIALS AND METHODS 70
4.3.1 Cells and viruses 70
4.3.2 Plasmids and primers 70
4.3.3 Generation of viruses by reverse genetics 71
4.3.4 Western blot analysis 72
4.3.5 Plaque assay 72
4.3.6 Growth curve 72
4.3.7 Genetic stability of the elastase mutations 73
4.3.8 Virus purification 73
4.3.9 Ethics statement 74
4.3.10 Mouse experiments 74
4.3.11 Virus isolation and titration 74
4.4 RESULTS 75
4.4.1 The production of the mutant plasmid and recombinant mutant BC15-HA/QTV/NA (PR8) virus as a vaccine candidate against BC15 (H7N9) 75
4.4.2 The recombinant mutant BC15-HA/QTV/NA (PR8) virus is strictly dependent on elastase for its replication *in vitro* 77
4.4.3 The recombinant mutant BC15-HA/QTV/NA (PR8) virus possesses equal growth kinetics to its wild-type counterpart *in vitro* 80
4.4.4 The recombinant mutant BC15-HA/QTV/NA (PR8) virus is genetically stable *in vitro*…. 81
4.4.5 The recombinant mutant BC15-HA/QTV/NA (PR8) virus is replication-defective in mice…. 83
4.5 DISCUSSION AND CONCLUSIONS 86

CHAPTER 5 THE REPLICATION-DEFECTIVE H7N9 VIRUS ELICITED COMPLETE PROTECTION AGAINST BC15 (H7N9) VIRAL CHALLENGE IN MICE……. 90
5.1 ABSTRACT 91
5.2 INTRODUCTION 92
5.3 MATERIALS AND METHODS 95
5.3.1 Cells and viruses 95
5.3.2 Ethics statement 95
5.3.3 Mouse experiments and sampling 96
5.3.4 Isolation of splenocytes from mouse spleen 96

5.3.5 Detection of IFN-γ and IL-5 secreting cells by enzyme-linked immunospot (ELISPOT) assay 97
5.3.6 Hemagglutination inhibition (HAI) and serum virus neutralization (SVN) assay ... 98
5.3.7 Enzyme-linked immunosorbent assay (ELISA) to detect antigen-specific IgG, IgG1, and IgG2 99
5.3.8 Virus isolation and titration 100
5.3.9 RNA extraction and quantitative RT-PCR (qRT-PCR) 100
5.3.10 Statistical analysis 102
5.4 RESULTS 103
5.4.1 Vaccination with the replication-defective BC15-HA/QTV/NA (PR8) virus provides evidence of a strong cell-mediated response 103
5.4.2 The replication-defective BC15-HA/QTV/NA (PR8) virus induces a robust humoral response 105
5.4.3 The replication-defective BC15-HA/QTV/NA (PR8) virus completely protects mice from a lethal challenge of BC15 (H7N9) 109
5.4.4 Vaccination with BC15-HA/QTV/NA (PR8) eliminated virus replication in the mouse lung 111
5.4.5 Vaccination with BC15-HA/QTV/NA (PR8) reduced the production of proinflammatory cytokines in the mouse lung associated with the influenza infection 112
5.5 DISCUSSION AND CONCLUSIONS 114

CHAPTER 6 GENERAL DISCUSSION 119
6.1.1 The establishment of a mouse model of A/British Columbia/01/2015 [BC15 (H7N9)] virus 119
6.1.2 The generation and characterization of the mutant H7N9 virus with its modified HA segment *in vitro* and *in vivo* 120
6.1.3 The evaluation of the immunogenicity and protective efficacy after intranasal administration of the replication-defective virus vaccine against A/British Columbia/01/2015 [BC15 (H7N9)] virus 121
6.1.4 Future directions 123

REFERENCES 124

APPENDIX 136
A. ACHIEVEMENTS DURING THE STUDY 136
A.1 Publications 136
A.2 Presentations 136
A.3 Scholarships 137
A.4 Awards 137

LIST OF FIGURES

Figure 1.1. IAV virion structure. 5
Figure 1.2 Schematic representation of the conserved terminal regions of the eight segments of IAV vRNA and the universal primers. 6
Figure 1.3. Structures of the conformations assumed by HA during the virus life cycle. 10
Figure 1.4. Ribbon diagram of an uncleaved HA monomer from the 1918 IAV (H1N1), the causative agent of the "Spanish flu" pandemic. 11
Figure 1.5. Influenza virus life cycle. 17
Figure 3.1. Survival rate and body weight loss for the AB14 (H5N1) and BC15 (H7N9) strain isolates. 53
Figure 3.2. Lung histopathology of mice after infection with AB14 (H5N1) and BC15 (H7N9) strain isolates. 54
Figure 3.3. Viral titration of the mouse lung, spleen, and brain for the AB14 (H5N1) and BC15 (H7N9) strain isolates. 56
Figure 3.4. Innate immune receptor RIG-I, as well as cytokine and chemokine gene transcription levels in the lungs of mice infected with the AB14 (H5N1) and BC15 (H7N9) strain isolates. .. 58
Figure 3.5. Cytokine gene transcription profile in the brains of mice infected with the AB14 (H5N1) and BC15 (H7N9) strain isolates. 60
Figure 4.1. Schematic outline of the mutations introduced into the HA cleavage site of BC15 (H7N9). 76
Figure 4.2. Schematic outline displaying the rationale for the mutations introduced into the HA cleavage site of BC15 (H7N9). 76
Figure 4.3. Plaque assay illustrating the successful rescue of recombinant BC15-HA/NA (PR8) and recombinant mutant BC15-HA/QTV/NA (PR8) and BC15-HA/QSV/NA (PR8) viruses. ... 77
Figure 4.4. The replication dependency of recombinant BC15-HA/NA (PR8) and recombinant mutant BC15-HA/QTV/NA (PR8) viruses. 80
Figure 4.5. Multiple-cycle growth curves of recombinant BC15-HA/NA (PR8) and recombinant mutant BC15-HA/QTV/NA (PR8) viruses. 81
Figure 4.6. The genetic stability of the recombinant mutant BC15-HA/QTV/NA (PR8) virus. .. 82
Figure 4.7. Histogram of the sequencing analysis performed on the HA cleavage site of the recombinant mutant BC15-HA/QTV/NA (PR8) virus. 83
Figure 4.8. The survival rate and body weight loss of mice infected with the recombinant BC15-HA/NA (PR8) and the recombinant mutant BC15-HA/QTV/NA (PR8) viruses. 85
Figure 4.9. Viral titration of lungs from mice infected with the recombinant BC15-HA/NA (PR8) and the recombinant mutant BC15-HA/QTV/NA (PR8) viruses. 86
Figure 5.1. Outline of the mouse trial to evaluate the immunoprotection induced by the replication-defective recombinant mutant BC15-HA/QTV/NA (PR8) virus. 103
Figure 5.2. Antigen-specific IFN-γ and IL-5 secreting cells induced by BC15-HA/QTV/NA (PR8) vaccination in mice. 104
Figure 5.3. Humoral immune responses mounted after BC15-HA/QTV/NA (PR8) vaccination. 107
Figure 5.4. Antibody responses induced by BC15-HA/QTV/NA (PR8) vaccination. 109
Figure 5.5. The survival rate and body weight loss of vaccinated mice after homologous viral challenge with BC15 (H7N9). 110

Figure 5.6. Viral titration of the mouse lung from BC15-HA/QTV/NA (PR8) vaccinated mice after homologous viral challenge with BC15 (H7N9). 111
Figure 5.7. Cytokine production after homologous viral challenge with BC15 (H7N9). 113

LIST OF TABLES

Table 3.1. List of primers used in qRT-PCR studies in mice. 50
Table 4.1. Outline of mouse trial to evaluate the virulence of the recombinant mutant BC15-HA/QTV/NA (PR8) virus. 84
Table 5.1. Grouping within the mouse trial to evaluate the immunoprotection of the replication-defective recombinant mutant BC15-HA/QTV/NA (PR8) virus..... 104

LIST OF ABBREVIATIONS

A	Adenosine
aa	Amino acid
AB14 (H5N1)	A/Alberta/01/2014 (H5N1)
ADCC	Antibody-Dependent Cellular Cytotoxicity
AP	Alkaline phosphatase
APC	Antigen-presenting cell
AREB	Animal Research Ethics Board
ASC	Adapter protein apoptosis associated speck-like protein containing a CARD
BALF	Bronchoalveolar lavage fluid
BC15 (H7N9)	A/British Columbia/01/2015 (H7N9)
BC15-HA/NA (PR8)	Recombinant H7N9 influenza virus rg-(6+2)-BC15-HA/NA
BC15-HA/QTV/NA (PR8)	Recombinant mutant H7N9 influenza virus rg-(6+2)-BC15-HA/QTV/NA
BSA	Bovine serum albumin
CCAC	Canadian Council on Animal Care
cDNA	Complimentary DNA
CFIA	Canadian Food Inspection Agency
CFR	Case fatality rate
CLSs	Cord-like structures
CNS	Central nervous system
CPSF	Cleavage and polyadenylation specificity factor
cRNA	Complimentary RNA
CTL	Cytotoxic T lymphocytes
DCs	Dendritic cells
DI	Defective-interfering viral particles
DMEM	Dulbecco's Modified Eagle Medium
d.p.i.	Days post-infection
dsRNA	Double-stranded RNA

DTT	Dithiothreitol
EDTA	Ethylenediaminetetraacetic acid
ELISA	Enzyme-linked immunosorbent assay
ER	Endoplasmic reticulum
FBS	Fetal bovine serum
G	Guanine
GFP	Green fluorescent protein
GISRS	Global Influenza Surveillance and Response System
HA	Hemagglutinin
HAI	Hemagglutinin inhibition assay
HCV	Hepatitis C virus
HEK	Human embryonic kidney
HI	Hemagglutinin inhibition
HPAI	Highly pathogenic avian influenza
h.p.i.	Hours post-infection
H&E	Hematoxylin and eosin
IAV	Influenza A virus
IBV	Influenza B virus
ICV	Influenza C virus
IDV	Influenza D virus
IFN	Interferon
IFN-α	Interferon alpha
IFN-β	Interferon beta
IFN-γ	Interferon gamma
IgA	Immunoglobulin A
IgG	Immunoglobulin G
IgM	Immunoglobulin M
IIV	Inactivated influenza vaccines
IL-1β	Interleukin-1 beta
IL-1	Interleukin-1

IL-2	Interleukin-2
IL-4	Interleukin-4
IL-5	Interleukin-5
IL-6	Interleukin-6
IL-9	Interleukin-9
IL-10	Interleukin-10
IL-13	Interleukin-13
IL-18	Interleukin-18
IP-10	Interferon-gamma-inducing protein 10
IRF3	Interferon response factor-3
IRF7	Interferon response factor-7
ISGs	IFN-stimulated genes
IWG	Influenza Working Group
LAIV	Live attenuated influenza vaccines
LD100	Lethal dose 100
LPAI	Low pathogenic avian influenza
LPMs	Live-poultry markets
LRT	Lower respiratory tract
M	Matrix protein
M1	Matrix 1 protein
M2	Matrix 2 protein
M2e	M2 ectodomain
MAVS	Mitochondrial antiviral signaling protein
MDCK	Madin-Darby canine kidney
MDV	Master donor virus
MEM	Minimal Essential Medium
MHC	Major histocompatibility complex
m.o.i.	Multiplicity of infection
mRNA	Messenger RNA
NA	Neuraminidase

NACI	National Advisory Committee on Immunization
NCR	Non-coding regions
NEAA	Non-Essential Amino Acids
NEP	Nuclear export protein
NF-κB	Nuclear factor kappa-light-chain-enhancer of activated B cells
NK	Natural killer
NLRP3	NLR family pyrin domain-containing protein 3
NLRs	Nucleotide-binding domain and leucine-rich repeat-containing proteins
NLS1	Nuclear localization sequence 1
NLS2	Nuclear localization sequence 2
NLS	Nuclear localization signal
nm	Nanometers
NP	Nucleoprotein
NS2	Non-structural protein 2
ORF	Open reading frame
PA	Polymerase acidic protein
PABII	Poly (A)-binding protein II
PAGE	Polyacrylamide gel electrophoresis
PAMPS	Pathogen-associated molecular patterns
PB1	Polymerase basic protein 1
PB2	Polymerase basic protein 2
PBS	Phosphate buffered saline
PFU	Plaque-forming unit
PHAC	Public Health Agency of Canadian
PKR	Protein kinase R
PNPP	p-nitrophenyl phosphate
PRRs	Pattern recognition receptors
PR8 (H1N1)	A/Puerto Rico/8 (H1N1)
QIV	Quadrivalent inactivated vaccines

qPCR	Quantitative PCR
qRT-PCR	Quantitative RT-PCR
RANTES	Regulated on activation normal T cells expressed and secreted
RBC	Red blood cell
RBD	RNA-binding domain
RDE	Receptor destroying enzyme
RIG-I	Retinoic acid-inducible gene-I
RNA	Ribonucleic acid
RNP	Ribonucleoprotein
RdRp	RNA-dependent RNA polymerase
SAVE	Synthetic Attenuated Virus Engineering
sciIAVs	Single cycle infectious IAVs
SDS	Sodium dodecyl sulfate
SD191 (H1N2)	A/Swine/Alberta/SD0191/2016 (H1N2)
SD69 (H3N2)	A/Swine/Saskatchewan/SD0069/2015 (H3N2)
sIgA	Secretory IgA
SIV	Swine influenza virus
SVN	Serum virus neutralization
ssRNA	Single-stranded RNA
$TCID_{50}$	Fifty-percent tissue culture infective dose
TGN	Trans-Golgi network
Th	T-helper cells
Th1	T-helper cell type 1
Th2	T-helper cell type 2
Th17	T-helper cell type 17
TIV	Trivalent inactivated vaccines
TLR	Toll-like receptor
TNFα	Tumor necrosis factor alpha
TNFβ	Tumor necrosis factor beta

TPCK	L-[(toluene-4-sulphonamido)-2-phenyl] ethyl chloromethyl ketone
Treg	Regulatory T cell
UACC	University Animal Care Committee
URT	Upper respiratory tract
VIDO-InterVac	Vaccine International Disease Organization, International Vaccine Centre
VLP	Virus-like particle
vRNA	Viral RNA
vRNP	Viral ribonucleoprotein
WHO	World Health Organization
µm	Micrometer

CHAPTER 1 LITERATURE REVIEW

1.1 INFLUENZA VIRUS

1.1.1 Classification and nomenclature

Influenza viruses contain segmented, negative-sense, single-stranded ribonucleic acid (ssRNA) genomes and are members of the *Orthomyxoviridae* family (Bouvier and Palese, 2011). Interestingly, the *Orthomyxoviridae* family also contains the genera's *Thogotovirus*, *Isavirus*, and *Quaranjavirus*. *Thogotovirus* and *Quaranjavirus* are transmitted by ticks and infect a variety of mammalian species, including humans, where *Isavirus* primarily infects the fish population, specifically salmon (Acheson, 2011). Influenza viruses are categorized into four genera (Influenza A virus [IAV], Influenza B virus [IBV], Influenza C virus [ICV], and Influenza D virus [IDV]) based on the antigenic variances found on the two main structural components of the virion, the nucleocapsid (NP) and matrix (M) proteins (Couch, 1996; Noda, 2011). Among the four genera of influenza viruses, IAV is the most prevalent due to its ability to produce variants through mechanisms such as *antigenic shift* and *antigenic drift*. These variants of IAV are grouped into subtypes based on the antigenic differences found on the hemagglutinin (HA) and neuraminidase (NA) glycoproteins. *Antigenic shift* and *antigenic drift* have also led to different variants within the HA subtypes, known as group 1 and group 2 for IAV. Within IAV, group 1 includes the H1 clade (H1, H2, H5, H6, H11, H13, and H16), and the H9 clade (H8, H9, and H12). Group 2 includes the H3 clade (H3, H4, and H14) and the H7 clade (H7, H10, and H15). The two other HA subtypes (H17 and H18) have only been recently discovered in bats (Shao et al., 2017). Currently, 18 HA subtypes and 11 NA subtypes have been identified for IAV, although it is hypothesized that more will arise in the upcoming years (Subbarao, 2019).

The categorization of IAV, IBV, ICV, and IDV viruses is not only based on the antigenic variances found on the NP and M proteins, but also the permissive species and the severity of the disease. The permissive species IAV infects comprises a range of mammalian hosts, including wild birds, bats, pigs, whales, horses, seals, cats, dogs, and humans, whereas the permissive species for IBV although mainly restricted to humans, has also been isolated from dogs, pheasants, seals, and pigs (Shao et al., 2017; Subbarao, 2019). IAV and IBV have been the main subtypes during the human seasonal epidemics, whereas IAV has been the main subtype during pandemics. This lack of IBV prevalence during pandemics has been attributed to its lack of

antigenic diversity and minimal reassortment potential; it is categorized into two distinct lineages: the Victoria-like lineage (B/Victoria/2/1987) and the Yamagata-like lineage (B/Yamagata/16/1988) (Subbarao, 2019). The permissive species of ICV, like IBV, has been mainly limited to humans, except for some cases found in pigs and dogs. Although ICV frequently infects humans, its severity and proportion compared to IAV and IBV infections is lower (Subbarao, 2019; Webster et al., 1992a). The permissive species of IDV has mainly been cattle, with studies showing cattle to be the original host. Interestingly, although cattle are the primary host for IDV, antibodies have also been detected among sheep, goat, equine, and camel populations. These antibodies against IDV have also been isolated among humans who work with cattle, raising the concern for the potential of IDV to infect humans (Ferguson et al., 2016; Subbarao, 2019).

Besides the antigenic variances, the permissive species, and the severity of the disease, the different types of influenza virus can also vary both morphologically and genetically. Morphologically, IAV and IBV can be spherical or filamentous, and thus cannot be differentiated by electron microscopy (Bouvier and Palese, 2011). However, ICV has been found to form ICV-specific cord-like structures (CLSs) inside infected cells besides spherical and elliptical virions, allowing them to be differentiated from IAV and IBV (Nakatsu et al., 2018). Genetically, IAV and IBV are composed of an RNA genome with eight segments, whereas the genomes of ICV and IDV are comprised of only seven segments. However, the single-stranded, negative-sense RNA nature is consistent among the four types of influenza virus (Bouvier and Palese, 2011; Ferguson et al., 2016; Nakatsu et al., 2018).

For the nomenclature system of influenza virus, a World Health Organization (WHO) standard was developed in the 1980s. This system uses the following information in consecutive order: virus type; species of isolation (for non-human); place of isolation; isolate number; isolate year; and for IAV, the HA and NA subtype (CDC, 2017). For example, the nomenclature: A/British Columbia/01/2015 (H7N9) denotes this IAV was isolated from humans in British Columbia, Canada as isolate number 1 in the year 2015, and has the H7N9 subtype based on the HA and NA characteristics.

1.1.2 IAV virion structure

IAVs are enveloped virions that can be spherical or filamentous, ranging in a diameter of 80 to 120 nanometers (nm) if in the spherical form, and up to 300 nm if in the filamentous form, with filaments about 20 micrometers (μm) in length (Acheson, 2011; Bouvier and Palese, 2011). Interestingly, the shape of IAV is partly determined on whether the strain is laboratory-adapted, egg-adapted, or directly isolated from clinical samples. If a strain is laboratory-adapted its shape is predominately spherical or elliptical, whereas strains found in clinical isolates are mostly filamentous, and egg-adapted strains lose this filamentous morphology to become spherical (Bouvier and Palese, 2011). Although the underlying biological functions of these morphologies are currently unknown, researchers have attempted to understand these functions by focusing on the various viral and host determinants. For example, researchers have alluded to the matrix 1 (M1) and matrix 2 (M2) proteins being essential components for the development of the filamentous morphology (Noda, 2011). It has also been demonstrated that a filamentous clinical isolate can become a spherical virus through repetitive passaging in chicken eggs (Badham and Rossman, 2016). These findings, along with many others, have led researchers to believe the filamentous morphology to be vital for influenza's existence in the environment (Noda, 2011).

The outer lipid envelope of IAV is formed during the budding process of the replication cycle (Acheson, 2011; Noda, 2011). Embedded and protruding from this envelope to form distinctive spikes are the two proteins, HA and NA, found at a four to one proportion. While HA and NA are both composed of identical subunits, HA forms a spike-like trimer, and NA forms a mushroom-like tetramer (Gamblin and Skehel, 2010). The M2 protein that spans the lipid envelope is found at a smaller ratio compared to the HA and NA, specifically, there is one M2 ion channel per 10^1 - 10^2 HA molecules (Badham and Rossman, 2016; Bouvier and Palese, 2011; Chlanda et al., 2015). These three proteins, HA, NA, and M2 overlie M1, a virion protein that surrounds the virion core. The M1 protein is essential for the virions morphology and is found at the highest abundance compared to the other proteins (Bouvier and Palese, 2011; Noda, 2011). The M1 protein can also associate with influenza's genome within the ribonucleoprotein (RNP) complex, acting as an anchor to hold HA, NA, and M2 in place (Badham and Rossman, 2016).

Within the virion core of IAV resides the nuclear export protein (NEP, formerly known as non-structural protein 2, NS2) and the RNP complex. Although NEP is a non-structural protein, research has shown that it also possesses structural properties within the virion. For

example, the C-terminal domain of NEP has been shown to aid in the release of progeny viral RNP (vRNP) from the nucleus by binding to the M1 protein (Shimizu et al., 2011; Yasuda et al., 1993). The RNP complex is composed of viral RNA (vRNA) and an RNA-dependent RNA polymerase (RdRp) that is coated with several NP (Figure 1.1). More precisely, each viral segment is encapsulated within several NP to generate an RNP complex. Each RNP complex contains its own heterotrimeric RdRp, made up of the polymerase basic protein 2 (PB2), the polymerase basic protein 1 (PB1), and the polymerase acidic protein (PA) (Baudin et al., 1994; Bouvier and Palese, 2011). These components contribute to maintaining the virion structure of IAV.

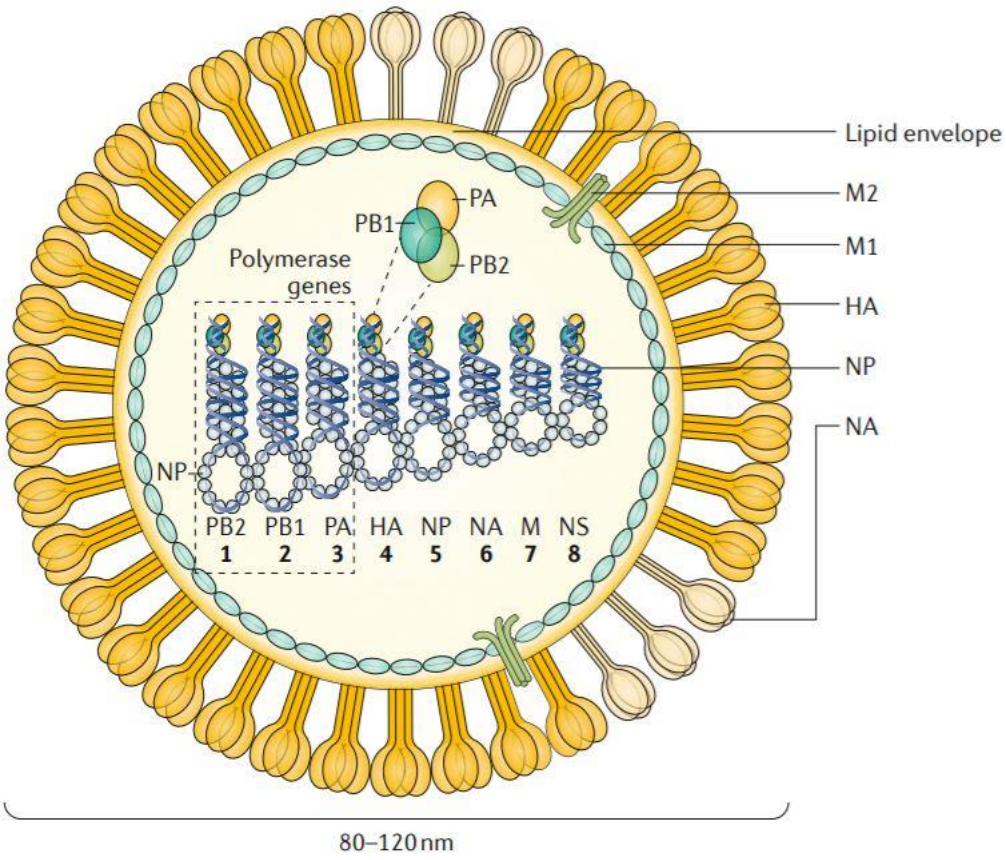

Reprint with permission from [**RightsLink®**]: [**Springer Nature**] [**Nature Reviews Disease Primers]** [Influenza, Florian Krammer, Gavin J. D. Smith, Ron A. M. Fouchier, Malik Peiris, Katherine Kedzierska, Peter C. Doherty, Peter Palese, Megan L. Shaw, John Treanor, Robert G. Webster & Adolfo García-Sastre], [**License Number 4690830306430**] [2018]. Figure description modified from the original article.

Figure 1.1. IAV virion structure.
IAVs are composed of negative-sense RNA within an enveloped virus particle, with genomes composed of eight ssRNA segments. The viral genome of IAV is derived from the following viral proteins that possess precise functions; (i) PB2, PB1, and PA generate the viral RdRp. They are the three largest RNA segments and function in RNA synthesis and viral replication; (ii) HA and NA are the two glycoproteins, where HA functions as a sialic acid receptor binding protein, and NA aids in the release of viruses; (iii) NP binds the RNA genome; (iii) M1, M2, NS1 (not shown), and NEP protein. The M1 protein supports the structure of the virion. The M1 and NEP monitor the movement of vRNA segments. The M2 protein acts as a proton ion channel that maintains the pH across the viral envelope and trans-Golgi membrane. The NS1 protein functions as a virulence factor by inhibiting the antiviral response induced in the host.

1.1.3 Genome structure and organization

IAV is a negative-sense, ssRNA virus that consists of eight different segments (PB2, PB1, PA, HA, NP, NA, M1, M2, and NS1) numbered according to their length, in decreasing order (Figure 1.1). These segments encode at least 17 gene products: PB2, PB1, PB1-F2, PA, HA, NP, NA, M1, M2, NS1, NEP/NS2, PB1-N40, PA-X, PA-N155, PA-N182, M42, and NS3 (Vasin et al., 2014). Interestingly, each IAV segment is composed of conserved sequences at the 5’ and 3’ non-coding regions (NCR) that enable universal amplification of all IAVs with a single primer set (Figure 1.2). The 5’ NCR has 13 conserved nucleotides, while the 3’ NCR has 12 conserved nucleotides. These conserved sequences are followed by a segment-specific NCR that allows the individual amplification of the different segments (Hoffmann et al., 2001).

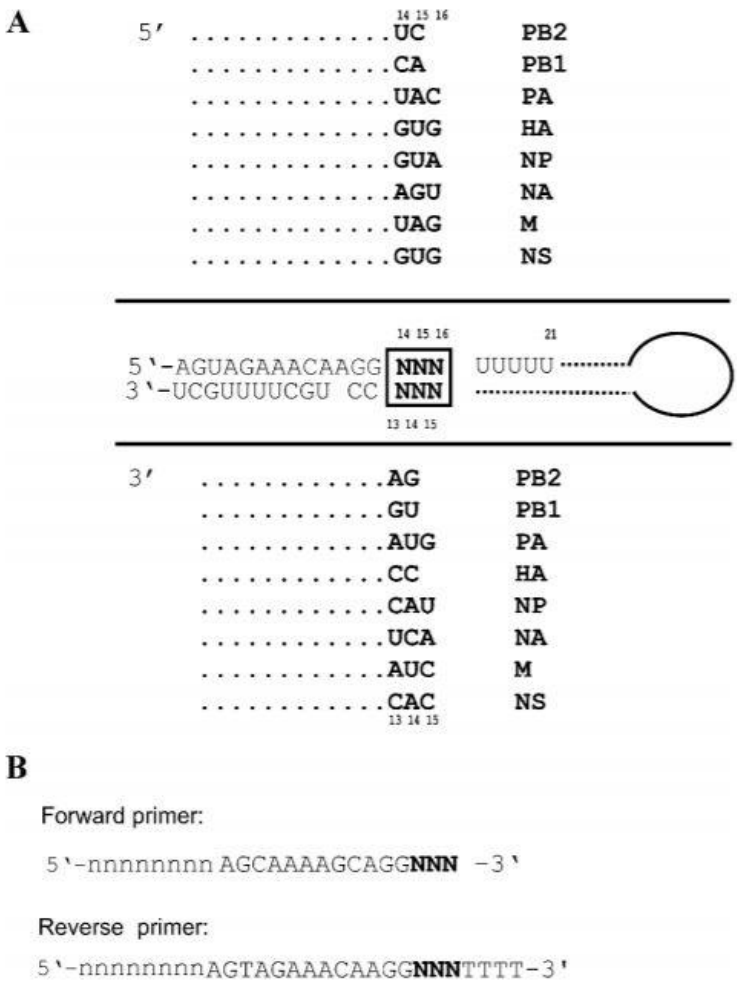

Figure 1.2 Schematic representation of the conserved terminal regions of the eight segments of IAV vRNA and the universal primers.
A. Each NCR of the vRNA segments is different by length and sequence, although each is unique for the eight segments. There are 13 conserved nucleotides at the 5' terminus, and 12 conserved nucleotides at the 3' terminus. The dotted line for each vRNA segment parallels to the NCR of the vRNA segment.
B. These primers were created to contain complementary sequences to the conserved sequences of the segment-specific influenza virus.

The PB2 protein is the largest protein found within IAV and is encoded by the RNA segment 1. This enzymatic protein is part of the RdRp and is capable of undergoing a mechanism

known as cap snatching. This mechanism entails PB2 binding to the hosts 5'-capped structure found on eukaryotic messenger RNA (mRNA), and then using this host structure as a primer to initiate viral transcription (Acheson, 2011; Graef et al., 2010). The PB2 protein also seems to play a role in determining the viral replication efficiency in various hosts; for example, if PB2 possesses the amino acid (aa) glutamic acid (E) at position 627, it preferentially replicates in avian species, while a lysine (K) at this position results in the preferential amplification in mammalian species (Hatta et al., 2001b). In conjunction with the viral replication efficiency, PB2 may also affect the virulence of IAV through its interaction with the mitochondrial antiviral signalling (MAVS) protein to inhibit interferon-beta (IFN-β) expression. This role is supported by research that has found PB2 to not only accumulate in the nucleus but also in the mitochondria (Graef et al., 2010).

RNA segment 2 was originally known to encode at least two proteins, the PB1 protein, and in some IAV strains, a small 87-aa protein, PB1-F2 (Bouvier and Palese, 2011). However, a third protein, PB1-N40, was recently discovered to be an N-terminally truncated form of PB1 (Wise et al., 2009). In addition to the PB2 protein, the PB1 protein is the second polymerase subunit found within the RdRp. This protein functions mainly as a nuclease, cleaving cellular pre-mRNAs at either adenosine (A) or guanine (G) approximately 10 to 13 nucleotides from the 5'-cap. This cleavage results in the PB2 complex, coupled to the capped structure that binds viral genome RNA, to initiate RNA elongation (Acheson, 2011).

A second reading frame in a +1 open reading frame (ORF) orientation translates the other protein encoded by RNA segment 2, PB1-F2. Although this protein is only found in some IAV strains, it has been found to have pro-apoptotic activity, contribute to viral pathogenicity, and be localized to the mitochondria (Acheson, 2011; Bouvier and Palese, 2011). The PB1-F2 protein co-localizes with MAVS to inhibit IFN production and potentially increases viral pathogenicity. The influenza pandemics that occurred in 1918, 1957, and 1968, along with the H5N1 pandemic all possessed the PB1-F2 protein. Interestingly, the increased virulence associated with the 1918 and H5N1 pandemics could be associated with an asparagine (66N) to serine (66S) mutation at aa-66 (Varga et al., 2011). However, not all influenza pandemic strains possess this protein: the 2009 H1N1 pandemic influenza virus lacks the PB1-F2 protein due to three stop codons within its genome that prevent it from being expressed (Hai et al., 2010). The PB1-F2 protein has also not been found in IBV or ICV (Bouvier and Palese, 2011).

The third protein encoded by RNA segment 2, PB1-N40, is an N-terminally truncated form of PB1 that is 718 aa in length. This protein has been detected in several IAV, including human, equine, and avian strains. PB1-N40, translated because of leaky ribosomal scanning, is undistinguishable from PB1 apart from the 39 aa deleted at the N-terminal that play an essential role in the interaction with PA. Although there are conflicting hypotheses on the functionality of PB1-N40, research has agreed that while PB1-N40 expression is essential for virus replication *in vitro* and *in vivo*, it is dispensable for the viability of IAV. Therefore, PB1-N40 plays an essential role in controlling the balanced expression of PB1 and PB1-F2 so that influenza virus can maintain its viral fitness (Tauber et al., 2012; Wise et al., 2009).

RNA segment 3 encodes the third member of the RdRp, the PA protein (Acheson, 2011). This segment is also capable of translating three other proteins, PA-X, PA-N155, and PA-N182 (Vasin et al., 2014). Although the definite function of PA is currently unknown, there are many hypotheses. For example, certain regions of the PA protein might be involved in vRNA and complementary RNA (cRNA) promoter binding (Maier et al., 2008). The PA protein may also play an essential role in transcription and replication through the proper assembly and packaging of vRNA into the IAV virions (Regan et al., 2006). Other studies have alluded to the PA protein possessing proteolytic activity through the introduction of point mutations, although the overall importance of this activity for influenza virus is unknown (Huarte et al., 2001).

A second reading frame in a +1 ORF translates the second protein encoded by RNA segment 3, PA-X (Vasin et al., 2014). PA-X is generated through the fusion of the 191 aa N-terminal domain of PA with the 61 aa C-terminal domain produced by the second reading frame in a +1 ORF, called X-ORF (Jagger et al., 2012). The X-domain of PA-X has been found to be highly conserved among all IAV strains and all host species, alluding to its importance for the viral life cycle (Shi et al., 2012). PA-X has been shown to be involved in modifying the host response to influenza viral infection in a variety of manners. Some of these modifications include the degradation of host mRNA, the ability to shut-off host-cell gene expression to decrease the antiviral response mounted, and the ability to switch host ribosome functionality from the translation of host mRNA to viral mRNA (Jagger et al., 2012; Weber and Haller, 2007). The two other proteins encoded by RNA segment 3, PA-N155 and PA182, are N-terminal truncated forms of PA that are translated in-frame because of leaky ribosomal scanning (Muramoto et al.,

2013). The functionality of these two proteins likely resides within the replication cycle of IAV, however, the exact mechanisms have yet to be discovered (Muramoto et al., 2013).

RNA segment 4 encodes one of the major glycoproteins found on the exterior surface of the virus, HA. HA has three major roles: (i) it enables attachment of the virus to the cell by interacting and binding to the sialic acid receptors found on the surface of the host cell (Bouvier and Palese, 2011); (ii) it enables the fusion of the viral envelope to the host endosomal membrane, allowing IAV to enter the cytoplasm and continue its replication cycle; and (iii) HA is the major antigen to which the immune system produces neutralizing antibodies against. For IAV to become infectious, cleavage of the HA single polypeptide precursor, HA0, must occur. The cleavage of HA0 is not only essential for infectivity but it also determines the pathogenicity and tissue tropism. The cleavage of HA0 most often occurs in the trans-Golgi network (TGN) or on the surface of the cell, and is induced by various host trypsin-like proteases to result in the formation of HA1 and HA2 connected by disulfide linkages. Two such trypsin-like proteases include TMPRSS2 (transmembrane protease serine S1 membrane 2) and HAT (human air-way trypsin-like protease). HA1 is composed of the N-terminus of HA0, while HA2 is composed of the C-terminus (Böttcher et al., 2006; Masic et al., 2008; Skehel and Wiley, 2000). The cleavage of HA0 into HA1 and HA2 enables the exposure of a hidden fusion peptide found within HA2. Therefore, when HA undergoes its conformational change as a result of the low pH within the endosomes, the now exposed fusion peptide can induce fusion of the virus to the endosomal membrane (Figure 1.3) (Böttcher-Friebertshäuser et al., 2013).

As mentioned above, the cleavage of HA0 results in the formation of HA1 and HA2 connected by disulfide linkages. These two portions, HA1 and HA2, make up the globular head and stalk domain of HA in a homotrimer formation (Figure 1.4). More specifically, the globular head is composed of HA1 and contains the sialic acid receptor binding site, while the stalk domain is composed of the entire HA2 and some portions of HA1 (Bouvier and Palese, 2011). Unlike the globular head, the stalk domain is highly conserved among different IAV subtypes, which has been strongly taken into account with the development of a universal vaccine (Gao et al., 2017).

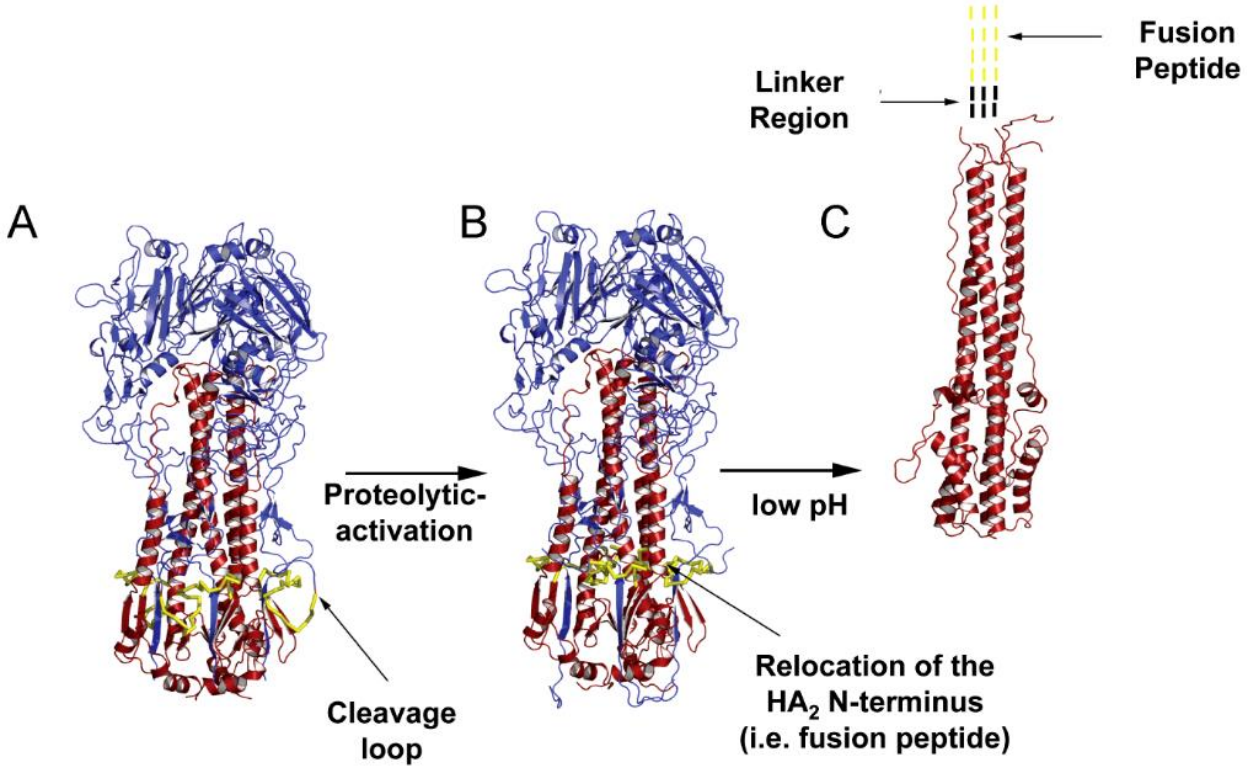

Reprint with permission from (Influenza HA Subtypes Demonstrate Divergent Phenotypes for Cleavage Activation and pH of Fusion: Implications for Host Range and Adaptation. Galloway S.E. et al. *PLOS Pathogens*. 2013. 9(2): e1003151. https://doi.org/10.1371/journal.ppat.1003151. Figure description modified from the original article.

Figure 1.3. Structures of the conformations assumed by HA during the virus life cycle. The HA protein is a trimer. The HA1 subunit is blue, whereas the HA2 subunit is red. The fusion peptide region is yellow. (**A**) The arrow parallels to the cleavage loop that encloses the HA cleavage site. (**B**) Once proteolytic activation occurs, the N-terminus of HA2 subunit moves to form an intertwined connection with the fusion peptide pocket, priming for fusion. (**C**) Once a low pH occurs HA undergoes a conformational change to result in membrane fusion between the virus and endosomal membranes.

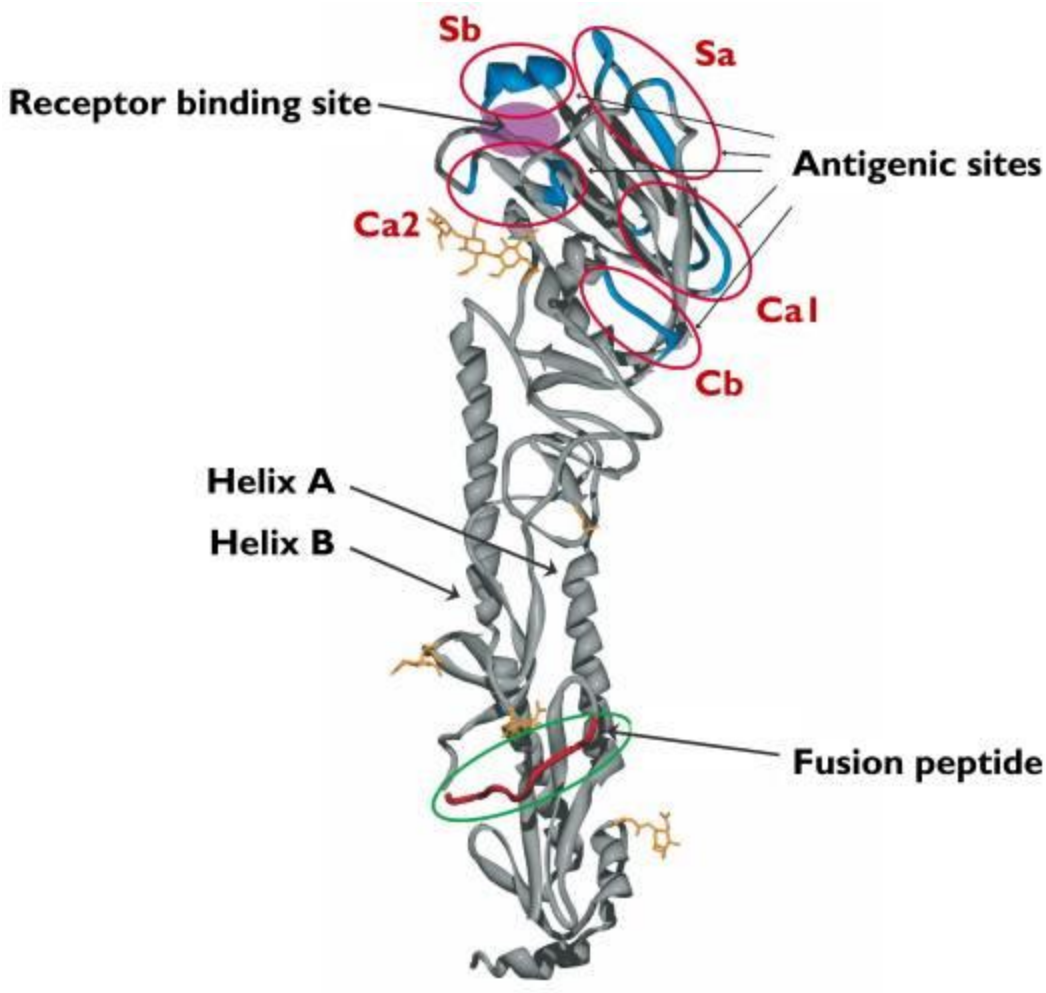

Reprint with permission from [**RightsLink®**]: [**Vaccine**] [**Elsevier**] [The biology of influenza viruses, Nicole M. Bouvier, Peter Palese], [**License Number 4690870265128**] [2008]. Figure description modified from the original article.

Figure 1.4. Ribbon diagram of an uncleaved HA monomer from the 1918 IAV (H1N1), the causative agent of the "Spanish flu" pandemic.
The HA head is composed of the sialic acid receptor binding site. The stem is composed of helices A and B as well as the fusion peptide. The five antigenic sites around the HA head are Sa, Sb, Ca1, Ca2, and Cb.

RNA segment 5 encodes the NP, which functions to bind and encapsidate newly synthesized vRNA (Acheson, 2011). There has also been evidence of NP playing a role in switching RNA synthesis from the production of mRNAs through transcription to the production of cRNA and vRNA through genome replication (Portela and Digard, 2002). NP also plays a major role in importing nucleocapsids from the cytoplasm to the nucleus by using a nuclear

localization signal (NLS) that interacts with the cellular importin-α factor. When the NP protein interacts with importin-α, it forms a complex which then interacts with importin-β, facilitating the entry of the nucleocapsids into the nucleus to promote transcription (Acheson, 2011).

RNA segment 6 encodes the NA protein, the other major surface glycoprotein in addition to HA. The NA protein is a mushroom-shaped integral membrane glycoprotein tetramer that traverses as well as protrudes from the viral envelope. The major role of NA is to release newly budded virions from the cell through cleavage of the sialic acid receptors, allowing the virions to spread to neighbouring cells. Interestingly, NA may also play a role in the entry of the virus into host cells (Bouvier and Palese, 2011). The NA protein is primarily known to intensify infectivity by reducing the virus aggregate formation through its removal of sialic acid residues on the viral envelope. Various antibodies and NA inhibitors, like oseltamivir and zanamivir, function in blocking the release of the budded virus to prevent infection of the neighbouring cells (Bouvier and Palese, 2011).

RNA segment 7 encodes two proteins, the M1 and M2 proteins. For IAV, the M1 protein is transcribed from RNA segment 7, while the M2 protein is transcribed by RNA splicing. The M1 protein is involved in the nuclear export of vRNA through its interaction with NEP, and is thought to play a role in the recruitment and assembly of various proteins at the plasma membrane. The M1 protein is also the bridge between vRNA and NP, allowing these two components to come together to form the RNP complex. Lastly, the M1 protein may be important for the initiation of the budding process, conceivably from the build-up of this protein underneath the lipid bilayer (Bouvier and Palese, 2011).

The M2 protein spans the lipid bilayer membrane and functions as an ion channel, essential for many processes of the influenza replication cycle (Bouvier and Palese, 2011). The M2 protein is a small 97-aa protein found as a tetramer composed of a short periplasmic domain, a transmembrane domain, and a cytoplasmic tail (Acheson, 2011; Cady et al., 2009). The M2 protein is found at a lower abundance compared to HA (1:10 - 100), and its primary function is to allow protons to travel through the viral envelope so that the desired pH can be maintained for viral entry, replication, and maturation. For example, when the endosome activates its low pH, this triggers the M2 channel to open and allow protons to enter the virion, resulting in acidification. This acidification has been hypothesized to dwindle the interaction between M1 and RNP so that when fusion occurs, the RNPs can be released into the cytosol (Bouvier and

Palese, 2011). The M2 protein is also the main target for the anti-influenza drugs amantadine and rimantadine. These drugs block the proton channels from functioning and thus block the release of nucleocapsids and the continuation of infection. Interestingly, the M2 protein possesses a conserved region essential for its functionality that is composed of a His-XXX-Trp motif (with X being any aa). This motif functions as a proton gate, controlling the flow of protons across the channel to maintain the desired pH. This conserved region has not only been found in IAV but also in IBV as well as some genotypes of hepatitis C virus (HCV) (Acheson, 2011; Cady et al., 2009). An additional protein that is encoded by RNA segment 7 is the M42 protein, which is generated by leaky ribosomal scanning (Wise et al., 2009). This protein is capable of acting in place of the M2 protein when it is functionally absent (Vasin et al., 2014).

RNA segment 8 encodes at least two non-structural proteins by alternative splicing, NS1 and NEP (Vasin et al., 2014). The NS1 protein is known as an antagonist of IFN, while the NEP is known for its involvement in the exportation of vRNP from the nucleus (Bouvier and Palese, 2011). The NS1 protein is collinearly expressed and consists of 230-aa, while the NEP protein is formed by alternative splicing and contains 121-aa. The N-terminal RNA-binding domain (RBD, aa 1 - 73) and the C-terminal effector domain (aa 74 - 237) are the two domains of the NS1 protein whose functionalities are essential for the replication of IAV (Lin et al., 2007). The N-terminal domain of the NS1 protein functions in binding to double-stranded RNA (dsRNA) to suppress the antiviral state induced by dsRNA-dependent protein kinase R (PKR) and 2', 5'-oligoadenylate synthetase. The C-terminal domain is composed of three functional domains: eIF4GI, the 30 kDa subunit of the host cell proteins cleavage and polyadenylation specificity factor (CPSF30), and the poly (A)-binding protein II (PABII) domain. These domains function by interacting with host cellular proteins such as CPSF or PABII to result in cellular mRNAs unable to cleave the 3'-end and perform polyadenylation. The NS1 protein has also been implicated in suppressing the innate cellular antiviral response by inhibiting the cytoplasmic and nucleic sensor, retinoic acid-inducible gene-I (RIG-I), which blocks the IFN response factor-3 (IRF3) from inducing IFNs and thus the antiviral response (Acheson, 2011; Lin et al., 2007; Liu et al., 2018).

A third protein recently found to be encoded by RNA segment 8, NS3, is a protein expressed in only some IAV strains (Vasin et al., 2014). This protein arises due to a D125G mutation that creates a third novel donor splice site in NS1 that allows NS3 to be expressed

(Selman et al., 2012). The NS3 protein is very similar to the NS1 protein, with the only difference being that the NS3 has a deletion from codons 126 - 128 in NS1 that causes a three antiparallel beta-strand motif to be deleted (Selman et al., 2012). Interestingly, this particular mutation has been shown to have a replicative gain-of-function, with viruses that have recently jumped to a new species acquiring this protein. Specifically, this protein was discovered in 33 IAV strains that recently jumped from avian to mammalian hosts, such as human, swine, and canine. These findings, therefore, allude to the potential role NS3 plays in both host adaptation and spilling over into new species (Selman et al., 2012).

1.1.4 Elastase

Elastase, a serine protease, was first discovered in the 1950s and was found to be capable of hydrolyzing elastin fibres found within the aorta. In mammals it is known to primarily reside within the pancreas and pancreatic juice, although it has also been found in human serum (Appel, 1974; Kuhn and Senior, 1978). The lung neutrophils and alveolar macrophages are the two main sources from which endogenous elastase originates in the human serum. The neutrophil elastase is found intracellularly within granule cells, and is primarily involved in immune responses against bacteria (Gramegna et al., 2017; Kuhn and Senior, 1978). The biological function of elastase is to digest a major protein, elastin, that functions in maintaining tissue elasticity (Tamada et al., 2009). This digestion occurs through elastase cleaving elastin at its peptide bond, allowing the digestion of various foods, such as meat (Berg et al., 2007). Elastin also enables the skin to become flexible yet maintain its rigidity during various activities, such as the contracting of a muscle. Elastin, together with collagen, another important structural protein found within connective tissue, muscle, and skin, both aid in the mechanical functions of the various tissues (Tamada et al., 2009). Maintaining the proper enzymatic activity of elastase is, therefore, vital for the health of the host, as an overactive elastase can result in detrimental effects. These detrimental effects are rooted in the mass breakdown of elastin throughout the body, which can lead to conditions such as pulmonary emphysema or vessel wall aneurysms, which are characterized by lower tissue stiffness (Black et al., 2008). Equally, the use of elastase within science has immensely proven its usefulness towards the development of influenza virus vaccines. Researchers have created elastase-sensitive HA cleavage sites within the influenza viruses, and these viruses have proven their immunogenicity and protective efficacy in both mice

and pigs (Babiuk et al., 2011; Gabriel et al., 2008; Masic et al., 2008; Masic et al., 2009; Masic et al., 2010; Stech et al., 2011; Stech et al., 2005). Moreover, studies have shown immunizations derived from elastase to have enhanced antibody responses compared to immunizations derived from other proteases, such as trypsin (Darani and Doenhoff, 2009; Sokol et al., 2000).

1.1.5 Replication cycle

IAV initiates infection in the respiratory tract by entering through aerosols or fomites (Racaniello, 2009). After entry into the respiratory tract, the HA homotrimer spikes on the surface of IAVs lipid membrane attach to the sialic acid receptors (also known as *N*-acetylneuraminic acid) on the host epithelial cells to initiate entry into the cell (Figure 1.5) (Skehel and Wiley, 2000). Sialic acid can be bound to carbohydrates in two forms: α-2,3 or α-2,6-galactose linkages, which can influence which influenza strains can bind and enter the host cell. IAVs of human origin prefer the α-2,6- galactose linkage present in the bronchiolar epithelial cells of the human upper respiratory tract (URT), while IAVs of avian origin identify with the α-2,3-galactose linkage present on the epithelial cells of both bird intestines and the human lower respiratory tract (LRT) (Bouvier and Palese, 2011; Lee et al., 2018; Samji, 2009; Shao et al., 2017). On the other hand, pigs and a number of avian species (pheasants, turkeys, and quails) are considered "mixing vessels," because they have both the α-2,3 and α-2,6-galactose linkage receptors, and thus pose risks towards the generation of reassortant viruses that may be of pandemic potential (Scholtissek, 1995; Shao et al., 2017). Interestingly, humans have also been proposed as a potential mixing vessel for the reassortment of influenza virus. In 2013, a patient from China had tested positive for both H7N9 and H3N2 influenza viruses, which was previously unheard of (Zhu et al., 2013). This individual, therefore, underlies the theory of humans acting as a mixing vessel and aiding human-to-human transmission.

After influenza has bound to the sialic acid residues, the next step is receptor-mediated endocytosis. The most common method is clathrin-mediated endocytosis, although other clathrin/caveolin-independent mechanisms, as well as macropinocytosis, have been demonstrated (Edigner et al., 2014; Grove and Marsh, 2011; Sieczkarski and Whittaker, 2002; Vries et al., 2011). Macropinocytosis is a process where large endocytic vesicles called macropinosomes form to absorb the incoming virus through an actin-dependent formation (Edigner et al., 2014).

Interestingly, the mode of entry may vary depending on the cell-type, thus warranting further research to answer these findings (De et al., 2011).

After internalization of IAV into the host cell through receptor-mediated endocytosis, the low pH inside the endosome (pH 5.0 – 6.0) induces a conformational change on the HA protein, altering its precursor form, HA0. This conformational change results in HA1 and HA2 shifting such that HA2 is visible at the N-terminus, enabling the insertion of the fusion peptide to the endosomal membrane, and thus fusion between the virus and the endosome (Hamilton et al., 2012; Stegmann, 2000). When the low pH within the endosome occurs, not only does fusion result between the virus and endosome, but it also aids the release of vRNP to the cytoplasm through the opening of the M2 ion channel (Samji, 2009). This activation of the M2 ion channel occurs in the early endosome environment, consisting of a pH 6.0 - 6.5, as well as in high sodium and low potassium concentrations (Manzoor et al., 2017). When the M2 ion channel is activated, there is an influx of protons from the endosome to the virion, which enables the dissociation of the M1 protein from the vRNP and the viral envelope, and allows vRNP to be released into the cytoplasm to complete the uncoating process (Pinto et al., 1992).

Once the vRNP have entered the cytoplasm, they are transported to the nucleus of the host cell where transcription and replication occur (Herz et al., 1981). IAV is unique in its transcription and replication process such that it takes place entirely in the host cell nucleus, unlike other RNA viruses where these processes occur in the cytoplasm (Shao et al., 2017). The vRNP are transported to the nucleus by both the nuclear localization sequence 1 (NLS1) and nuclear localization sequence 2 (NLS2) found on NP (Wu et al., 2007). In the nucleus, the RdRp initiates transcription by binding to the 5'-caps of host pre-mRNA, a process called 'cap snatching,' to transcribe negative sense vRNA into viral mRNA (Neumann et al., 2000; Reich et al., 2014). The viral mRNA is then transported to the cytoplasm through the NXF1 pathway, where it is used as a template for the translation of the viral proteins (Hay et al., 1977; York and Fodor, 2013).

As the viral proteins are being translated, PB2, PB1, PA, and NP are transported back to the nucleus where they are used in the formation of progeny vRNP (Li et al., 2015). Simultaneously, as the viral proteins are translated the negative sense vRNA is replicated into intermediate cRNA. The cRNA is encapsulated within PB2, PB1, PA, and NP and used to

replicate the influenza genome and create progeny vRNP (York and Fodor, 2013). The progeny vRNP then form a complex with NEP and M1 to aid in the exportation of the vRNP from the nucleus to the cytoplasm by the CRM1 pathway (Paterson and Fodor, 2012; Watanabe et al., 2014). Concurrently, as HA, NA, and M2 proteins are translated at the endoplasmic reticulum (ER), they are transported to the plasma membrane through the TGN (Ohkura et al., 2014). Once the vRNP reach the plasma membrane, they are packaged into progeny virions and released from the cell by budding and cleavage of the sialic acid residues by NA, allowing the virions to infect the neighbouring cells (Matrosovich et al., 2004; York and Fodor, 2013).

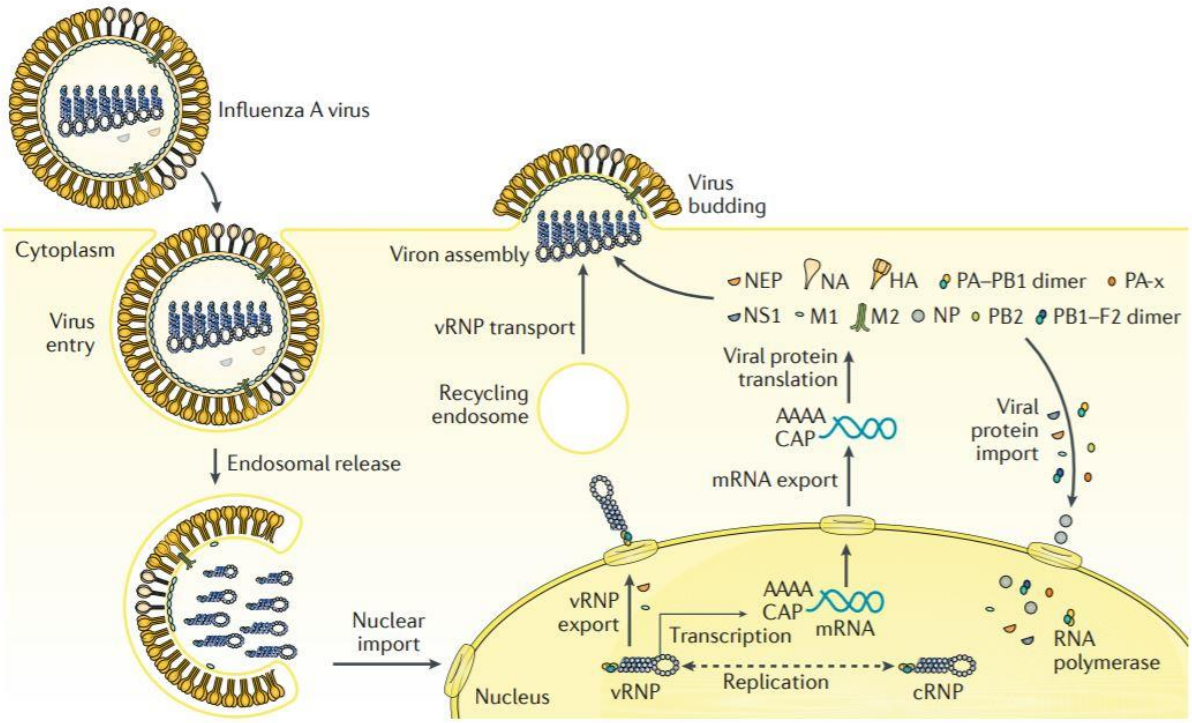

Reprint with permission from [**RightsLink®**]: [**Springer Nature**] [**Nature Reviews Disease Primers]** [Influenza, Florian Karmmer, Gavin J. D. Smith, Ron A. M. Fouchier, Malik Peiris, Katherine Kedzierska, Peter C. Doherty, Peter Palese, Megan L. Shaw, John Treanor, Robert G. Webster & Adolfo García-Sastre], [**License Number 4690830306430**] [2018]. Figure description modified from the original article.

Figure 1.5. Influenza virus life cycle.
The entry of the influenza virus occurs through endocytosis, which is followed by transport of the vRNP to the nucleus. These vRNP then undergo transcription into mRNA or replication through a cRNP intermediate. The mRNA is translated into the various viral proteins in the cytoplasm, where these proteins are assembled at the plasma membrane with the newly synthesized vRNP to create progeny virions.

1.1.6 Evolution and Genetics

IAV is a challenging virus for public health control measures because of its complex evolutionary characteristics, both internal and external. The mechanisms by which IAV internally evolves includes *antigenic drift*, *antigenic shift*, and less often, recombination. *Antigenic drift* is a subtle evolutionary mechanism where mutations gradually accumulate on its segmented genome, while *antigenic shift* is a dramatic mechanism where different strains of IAV reassort to produce an entirely new strain (Bouvier and Palese, 2011; Shao et al., 2017). These evolutionary changes are the primary reason for the annual epidemics and less frequent pandemics that affect public health. Besides these complex internal evolutionary characteristics, IAV is also capable of evolution through external factors, such as the environment and the susceptibility of its host. One of the environmental features includes China's live-poultry markets (LPMs), while one of the host features include the classification of IAV as a zoonotic virus (Su et al., 2017). IAV uses its wide range of permissive species to evolve through spillovers from an animal restricted pathogen to humans or to generate novel variants through the mixing of different influenza subtypes (Shao et al., 2017; Webster et al., 1992b). Therefore, IAV poses a serious threat to public health, where the complex internal and external evolutionary characteristics hinder the progress towards controlling the spread and developing effective annual and universal vaccines (Shao et al., 2017).

One of the internal evolutionary mechanisms, *antigenic drift*, enables IAV to escape the immune system, alter the binding preference, and enhance its overall fitness. This mechanism occurs through the accumulation of point mutations in HA and NA from the error-prone RdRp. These point mutations accumulate at a rate of 10^{-3} - 10^{-4}, which eventually results in the hosts neutralizing antibodies becoming ineffective against that particular strain. These neutralizing antibodies become ineffective because of the point mutations changing the antigenic sites on the virus, allowing IAV to escape the immune system (Acheson, 2011; Bouvier and Palese, 2011; Shao et al., 2017).

Antigenic drift has also been implicated in altering the binding preference of HA to α-2,3 or α-2,6 sialic acid residues on the host cell by introducing aa substitutions (Shao et al., 2017). For example, one study found that the aa substitutions G186V and Q226L enabled the avian influenza H7N9 virus that preferentially binds to α-2,3 sialic acid receptors, to bind to human-

like α-2,6 sialic acid receptors (Dortmans et al., 2013). These substitutions among aa can also occur in viral proteins other than HA if it is advantageous for the overall fitness and evolution of IAV. For example, the E627K mutation in PB2 has been associated with enhancing the polymerase activity and replication ability in human cells and is one of the main factors that determines the host range of avian IAV (Shao et al., 2017). More detrimentally, some aa mutations can result in a low pathogenic avian influenza (LPAI) virus becoming a highly pathogenic avian influenza (HPAI) virus. In general, LPAI viruses are only capable of causing mild disease in avian species, whereas HPAI viruses are capable of causing severe disease in avian species. HPAI viruses also more frequently cause epidemics, with the most common HPAI viruses in nature being the H5 or H7 HA subtypes (Spickler, 2016). The classification of IAV into LPAI or HPAI is determined by both the severity of the virus and specific genetic features found on the HA cleavage site. Classification based on the severity of the virus is determined by the lethality in young chickens that are intravenously inoculated in a laboratory (Spickler, 2016). Classification based on specific genetic features is determined by the composition of aa found on the HA cleavage site. LPAI viruses are composed of one basic aa at the HA cleavage site (ex. PEKQT**R**/GLF) restricting HA cleavage to a limited number of cellular proteases (Offlu, 2019). These cellular proteases are often trypsin-like proteases, such as TMPRSS2 (transmembrane protease serine S1 membrane 2) and HAT (human air-way trypsin-like protease) which have restricted tissue tropism to the respiratory and intestinal systems, limiting the spread of IAV throughout the body (Böttcher-Friebertshäuser et al., 2013). Conversely, HPAI viruses are composed of a multiple basic aa HA cleavage site (ex. PQRES**RRKK**/GLF), enabling HA cleavage by multiple cellular proteases (Offlu, 2019). These cellular proteases capable of cleaving the multiple basic aa are ubiquitously found throughout the body (ex. furin), which increases the capability of IAV to systemically spread throughout the body (Böttcher-Friebertshäuser et al., 2013). Interestingly, *Qi et al.* discovered that the LPAI H7N9 virus evolved to an HPAI H7N9 virus through the insertion of four basic aa on the HA cleavage site, which is characteristic of HPAI viruses. They also found several other mutations, including S31N of M2 and E627K, A588V, and K526R of PB2, all of which enhanced the overall fitness of H7N9 IAV (Qi et al., 2018).

The second internal mechanism IAV possesses, *antigenic shift*, is another major contributor to the evolution of IAV. *Antigenic shift* enables the generation of entirely new strains

and/or subtypes through the reassortment of the segmented genomes of genetically diverse IAVs. This mechanism is a rapid change, most often occurring through IAV obtaining either the HA, NA, or both segments from an entirely different subtype. Less often, *antigenic shift* can involve subtypes from both human and animal viruses. Unfortunately, if mixing of two or more IAV strains from different species occurs, it can cause pandemics because of the lack of pre-existing immunity (Acheson, 2011; Bouvier and Palese, 2011). *Antigenic shift* is most often the primary reason for the generation of pandemic viruses, such as the 2009 H1N1 virus (Shao et al., 2017). This IAV pandemic virus was generated through the reassortment of the European H1N1 and North American H1N2 swine influenza virus (SIV), the North American avian IAV, and the H3N2 IAV (Dawood et al., 2009).

The third internal evolutionary mechanism of IAV, genetic recombination, is a rarer occurrence compared to *antigenic drift* and *antigenic shift*. Genetic recombination in IAV occurs by two mechanisms: non-homologous recombination and controversial homologous recombination. Out of the two mechanisms, non-homologous recombination is the more frequent occurrence (Shao et al., 2017). Interestingly, although a rare event, it has been hypothesized that the H7N9 IAV pandemic in China may have arisen due to recombination. Phylogenetic analysis found a 291-nucleotide fragment from the HPAI H5N1 virus that had recombined inside the PB1 segment of H7N9 (Chen et al., 2016). Similarly, evidence has alluded to recombination being essential for the evolution of various H5N1 viruses (Shao et al., 2017). Therefore, although a rare event, recombination may play a bigger role in the evolution of IAV than previously thought.

Even though IAV possesses many internal evolutionary mechanisms, such as *antigenic drift*, *antigenic shift*, and recombination, the evolution of IAV is also facilitated through external factors, such as the environment and the susceptibility of the host. Research has shown China's environment to be favourable for the generation of novel influenza subtypes as well as spillovers into new species. China's favourable environment is partly attributed to its LPMs, where poultry are housed in small quarters with poor hygiene. These LPMs facilitate the transportation and mixing of IAV strains to generate novel variations through either the long-distance transportation of poultry to their destination or the close contact between poultry and other species (Su et al., 2017). Another external factor that can contribute to the evolution of IAV is the diversity of China's ecosystem. The ecosystem of China is unique because it is home to a variety of species

that often come in close contact to humans and poultry, such as birds, dogs, cats, pigs, and ferrets (Guan and Smith, 2013). Some species, such as pigs, can serve as 'mixing vessels,' to aid in the generation of novel influenza subtypes, and thus, contribute to the evolution of IAV (Ma et al., 2009). This combinatorial effect of the close contact among poultry, humans, and other species in the LPMs enables the potential for novel influenza variants to arise and potentially infect humans, posing a substantial public health threat. One example that illustrates this threat is the H7N9 influenza virus because most human infections have resulted from close contact with poultry (Su et al., 2017). Therefore, the complex evolutionary mechanisms of IAV, both internal and external, have challenged the progress towards the development of both the annual seasonal vaccines and a universal vaccine candidate.

1.1.7 Immunology of IAV

IAV initiates infection by entering the respiratory tract of various animals through either aerosols or fomites (Racaniello, 2009). After IAV enters the respiratory tract, the airway mucosa epithelial cells are infected through the interaction between the sialic acid receptors found on the host epithelial cells and IAVs HA (Skehel and Wiley, 2000). IAV infection further advances to the lung macrophages and dendritic cells (DCs) found in the alveoli or lung epithelium where the inflammatory immune response is triggered. Throughout this process, various pattern recognition receptors (PRRs) can sense IAV and initiate an immune response. These PRRs include toll-like receptors (TLR), RIG-I, and the nucleotide-binding domain and leucine-rich repeat-containing proteins (NLRs) that consists of the NLR family pyrin domain-containing protein 3 (NLRP3). The TLR group encompasses four distinct types that function within the cytoplasmic endosomes: TLR3, TLR7, TLR8, and TRL9 (found in humans). TLR3 recognizes foreign dsRNA, which activates a cascade of events that ultimately leads to the activation of the nuclear factor kappa-light-chain-enhancer of activated B cells (NF-κB) and IRF3. TLR7 and TLR8 recognize foreign ssRNA, which initiates the activation of NF-κB and IFN response factor-7 (IRF7). The cascade of events initiated by these TLR eventually leads to the production of various proinflammatory cytokines, type I IFNs, and IFN-stimulated genes (ISGs) (Iwasaki and Pillai, 2014; Kreijtz et al., 2011). Unlike TLR3, TLR7, and TLR8, which function inside the cytoplasmic endosomes, RIG-I possesses a dual capability to function within the cytosol and the nucleus of the cell (Liu et al.,

2018). RIG-I functions by recognizing 5'-triphosphate viral dsRNA produced after viral replication, which activates MAVS and leads to the activation of IRF3 and IRF7, as well as the production of various proinflammatory cytokines and type I IFNs (Chen et al., 2018; Iwasaki and Pillai, 2014). NLRP3 is expressed in many cell types including macrophages, DCs, and neutrophils. NLRP3 is activated upon IAV infection and requires two signals to result in the production of interleukin-1 beta (IL-1β) and interleukin-18 (IL-18) by the inflammasome (Chen et al., 2018; Iwasaki and Pillai, 2014). Interestingly, it has been found that when the NLRP3 inflammasome is activated, a cascade of events including adapter protein apoptosis associated speck-like protein containing a CARD (ASC) speck formation and caspase-1 activation is induced, ultimately resulting in the production of IL-1β (Park et al., 2018).

As previously mentioned, the epithelial cells of the respiratory tract are the first cells infected with IAV. Upon infection, the alveolar macrophages are activated, which enables not only phagocytosis of the IAV infected cells, but also initiation of the antiviral response to result in the production of various proinflammatory cytokines such as tumour necrosis factor alpha (TNFα), IL-6, and interleukin-1 beta (IL-1β) (Chen et al., 2018; Park et al., 2018). These cytokines are paramount for the elimination of IAV and the control of inflammation because they aid in the recruitment of various innate immune effector cells such as macrophages, natural killer (NK) cells, DCs, monocytes, and neutrophils to the site of infection by increasing the adhesion of leukocytes to the endothelium. DCs constantly survey the area for pathogen-associated molecular patterns (PAMPS), and upon encounter, they phagocytize the virus, functioning as an antigen-presenting cell (APC). These APCs then migrate from the lungs to the lymph nodes where they present their viral antigens in the form of peptides (epitopes) to naïve T lymphocytes, thereby activating the T cells and the adaptive immune response. Therefore, DCs are essential for linking the innate and adaptive immune responses (Chen et al., 2018).

The epitopes found on the APCs can be presented to naïve T lymphocytes through either the major histocompatibility complex (MHC) class I or II molecules. MHC class I molecules present endogenous antigens that originate in the cell's cytoplasm, whereas MHC class II molecules present exogenous antigens that originate extracellularly. Specifically, MHC class I molecules present peptides from IAV that were degraded in the proteasome, whereas MHC class II molecules present IAV peptides that were degraded in either the endosomes or lysosomes. The type of MHC molecule that is presented to a naïve T lymphocyte will dictate whether $CD4^+$ T-

helper (Th) cells or $CD8^+$ cytotoxic T cells (CTL) are generated. In general, MHC class II molecules are presented to $CD4^+$ Th cells and MHC class I molecules are presented to $CD8^+$ CTLs (Kreijtz et al., 2011). The $CD4^+$ Th cells can be divided into two different groups based on the predominant cytokines generated: T-helper cell type 1 (Th1) and T-helper cell type 2 (Th2). Th1 cells predominately generate antiviral cytokines such as IFN-gamma (IFN-γ), interleukin-2 (IL-2), and tumour necrosis factor beta (TNFβ), which function in the cellular immune response against IAV. Conversely, Th2 cells produce interleukin-4 (IL-4), interleukin-5 (IL-5), interleukin-6 (IL-6), interleukin-9 (IL-9), interleukin-10 (IL-10), and interleukin-13 (IL-13) which function to induce antibody responses and activate B cells involved in the humoral immune response against IAV. T-helper cell type 17 (Th17) and regulatory T cells (Treg) have also been implicated in regulating the cellular immune response against IAV (Kreijtz et al., 2011; Romangnani, 2000). Upon activation of the $CD8^+$ T cells, they differentiate into CTLs. Once differentiated they travel to the site of infection and function to contain viral replication and kill virus-infected cells through either the induction of apoptosis or Fas/FasL interactions. Apoptosis occurs through the release of perforin and granzymes from CTLs; perforin punches holes into in the virus-infected cells, allowing granzyme to enter and induce apoptosis (Chen et al., 2018; Kreijtz et al., 2011; Romangnani, 2000).

After clearance of the IAV infection, memory $CD4^+$ and $CD8^+$ T cells act as a surveillance system for IAV epitopes they have previously mounted an immune response against. This surveillance system aids the rapid response against reinfections, potentially protecting against IAV infection. When a memory T cell recognizes an epitope, it activates naïve B cells to produce antibodies and block infection, a mechanism known as humoral immunity. Conversely, memory CTLs continue to circulate in the blood, lymphoid organs, and the site of initial infection, a phenomenon known as cellular immunity (Cheng et al., 2017; Kreijtz et al., 2011). Interestingly, research has shown that memory CTLs may aid in the reduction of IAV disease and death in the absence of humoral immunity if the N subtype is the same between the two different subtypes. One study emphasized this concept, such that pigs vaccinated against H1N1 and subsequently challenged with H5N1 were completely protected, providing evidence of the dual properties these memory CTLs can possess (Van Reeth et al., 2009).

Humoral immunity is initiated through a primary infection or a memory T cell activating a naïve B cell. When a naïve B cell becomes a mature B cell, this leads to the generation of

antibodies against HA and NA, with the production of these antibodies often associated with protection. Since HA is involved in the virus's attachment to the cell, HA-specific antibodies block viral entry. Furthermore, since the primary function of NA is to release newly budded virions by cleaving sialic acid residues, NA-specific antibodies block the further spread of IAV infection. Both HA and NA antibodies also initiate Antibody-Dependent Cellular Cytotoxicity (ADCC), which further helps to remove the virus-infected cells (Kreijtz et al., 2011; Wong and Webby, 2013).

Humoral immunity induced by IAV leads to the production of immunoglobulin A (IgA), immunoglobulin M (IgM), and immunoglobulin G (IgG) isotypes. IgA, also known as mucosal or secretory IgA (sIgA) is the main antibody detected at mucosal surfaces and is the first line of defence against infection because of its capability to eliminate IAV before it enters the respiratory tract. Interestingly, the non-inflammatory properties of IgA may play an important role in the control of HPAI strains because these strains characteristically present unrestrained proinflammatory responses (Kreijtz et al., 2011; van Riet et al., 2012). In comparison, IgG is the predominant antibody responsible for preventing the systemic dissemination of IAV, whereas IgM can indicate an active influenza infection. IgG and IgM can activate the inflammatory complement pathway, leading to the initiation of various inflammatory responses (Muramatsu et al., 2014; Skountzou et al., 2014; van Riet et al., 2012). Thus, induction of the various immunoglobulins is essential for the control of IAV infection.

1.2 H7N9 INFLUENZA VIRUS

1.2.1 Etiology and epidemiology

The LPAI H7N9 virus potentially originated in the Yangtze River Delta Region of China in 2013, with the first identifications occurring in Zhejiang, Jiangsu, and Shanghai. The Yangtze River Delta Region has had the largest amount of H7N9 cases, while the Pearl River Delta Region, specifically in Guangdong, has had the second-largest amount of cases. Since its initial identification in 2013, there have been six epidemic waves in China (occurring each year from 2013 to 2017). The WHO has defined each epidemic wave to begin on October 1 and end September 30 of the following year. Several studies have analyzed H7N9 to decipher its origin, concluding that H7N9 contains incredible genetic diversity. Some studies have concluded that

H7N9 originated from the reassortment of the H7 and N9 surface genes from wild birds, and the internal genes from poultry H9N2 viruses (Su et al., 2017). However, one study discovered that H7N9 potentially originated from the reassortment of H5N6 and H6N6 (Jin et al., 2017). These findings, along with others, have contributed to the conclusion that H7N9 is more diverse than previously thought.

During the first four epidemic waves, there was a total of 798 cases and 328 deaths with a case fatality rate (CFR) of 40.6%. However, during the fifth wave, there was 766 cases and 288 deaths, almost as many cases as the first four waves combined. The fifth wave also contained the emergence of the HPAI H7N9, resulting in quicker hospitalization rates and fewer days to onset of illness than the first four waves (Su et al., 2017; Yang et al., 2019). In the fifth wave, H7N9 underwent a geographic expansion to China's Western provinces, such as Chongqing city, Gansu, Sichuan, and Tibet. This geographic expansion highlights the threat that H7N9 poses, and the importance of vaccination programs to control the spread. The threat H7N9 poses is also highlighted in the high morbidity and mortality rates; as of April 9, 2017, 35% of patients who contracted H7N9 died, with CFR's ranging from 33% to 45% for the LPAI H7N9 and HPAI H7N9, respectively (Su et al., 2017). As of March 4, 2020, H7N9 had resulted in 1,568 human cases and 616 deaths (FAO, 2020).

Concerning the epidemiology of H7N9, most infections in the first four waves were in males (69%) over the age of 40 years. Interestingly, that prevalence shifted in the fifth wave, during which primarily male and female elderly to middle-aged adults were infected. Of note, most patients that died from infection had previous underlying medical conditions; ~53% of patients in waves one through four, and 63% of patients infected with the HPAI H7N9. Most patients who contracted H7N9 had previous exposure to live poultry (85 - 100% of infections), indicating the risk LPMs play in the spread and generation of new reassortment influenza viruses (Su et al., 2017).

Although most H7N9 infections have been mainly due to the exposure to the influenza virus through LPMs in China, other regions of the world are also at risk for contracting this disease. In January 2015, two individuals from Canada that had recently travelled to China contracted H7N9 (Skowronski et al., 2016). Luckily, these patients recovered; however, their infections highlight the risk of influenza spreading throughout the world due to increased travel, which stresses the importance of vaccination programs to help control the disease.

Throughout the six epidemic waves, most infections were attributed to the LPAI H7N9 virus. However, the fifth epidemic wave in 2017 resulted in the emergence of the HPAI H7N9, which began infecting humans. The HPAI H7N9 virus possesses the insertion of four basic aa at the HA cleavage site ("KRTA," "KRIA," or "KRAA"). This insertion of a multibasic aa HA cleavage site is a characteristic feature for high virulence in HPAI viruses, such as H5N1 (Qi et al., 2018; Yang et al., 2019). Although there have only been a few human cases of the HPAI H7N9, there is a great potential of H7N9 gaining sustained transmission through *antigenic shift* and *antigenic drift*, which could cause a devastating pandemic. Apart from the HPAI H7N9 possessing a multiple basic aa HA cleavage site, unique aa mutations exist that are distinct from the LPAI H7N9 virus. These mutations include Q226L, R292K, E627K, A588V, and K526R, which all seem to favor mammalian binding and enhance replication efficiency. The Q226L mutation is found in HA, where the occurrence of Q or L can dictate the receptor binding preference. Specifically, the 226Q mutation favours mammalian receptor binding and is prevalent in the HPAI H7N9 human infections, whereas the 226L mutation favours avian receptor binding. The R292K mutation in NA has been found in up to at least 75% of HPAI H7N9 cases (Qi et al., 2018). This mutation has been linked to the resistance towards various NA inhibitors, such as oseltamivir, which can decrease the effectiveness of these antiviral agents (Su et al., 2017). Other mutations such as E627K, A588V, and K526R found in the PB2 segment support increased replication ability in mammalian hosts, and have been found in up to 75% of the HPAI H7N9 human infections (Qi et al., 2018). For the A/British Columbia/01/2015 [BC15 (H7N9)] strain isolate, the virus of study for my thesis, out of the aa mutations mentioned above, the only one present is E627K. This mutation on PB2, E627K, is known to be a key adaptation and virulence marker for influenza viruses. Research has shown that avian IAVs retain a glutamic acid (E) at this position, and mammalian IAVs retain a lysine (K). In order for an avian IAV to become infective in mammals, the 627E needs to be mutated to a 627K (Hatta et al., 2001a). These mutations are important determinants for the viral replication efficiency in various hosts, with the 627K mutation allowing IAV to be more active in mammalian cells due to its strong interaction with the mammalian importin-α isoforms. These importin-α isoforms are important for the nuclear import of vRNP so that transcription and replication can occur, with the strong interactions with 627K enhancing these abilities (Gamblin and Skehel, 2010; Lee et al., 2017b). Moreover, it has been found that the PB2 627 domain is not only vital for transcription

and replication of IAV, but also for the collection of the cRNA intermediates required for replication (Nilsson et al., 2017). Therefore, this E627K mutation on PB2 may aid in the pathogenesis of BC15 (H7N9), and may explain its ability to proficiently replicate in the human respiratory tract.

Therefore, the generation of these aa substitutions through *antigenic drift* and *antigenic shift* highlight the importance of the development of a vaccine protective against the H7N9 IAV. Development of this vaccine could ultimately result in protection against the LPAI H7N9, and prevent the HPAI H7N9 from gaining sustained human-to-human transmission, which could result in a devastating pandemic.

1.2.2 Clinical signs, pathogenesis, and diagnosis of H7N9

Like most influenza viruses, H7N9 infection begins through the entry into the respiratory tract where it binds to sialic acid receptors on the host epithelial cells, enters the host, and then continues its replication cycle inside the host (Racaniello, 2009; Skehel and Wiley, 2000). Once H7N9 has initiated infection, progression between the onset of illness to admission to a hospital, laboratory confirmation, and death has been found to vary between the different epidemic waves and whether the infection is from the LPAI H7N9 or HPAI H7N9. The time between the onset of illness and hospitalization was 5 days, 4 days, 3 days, and 2 days for waves 1-3, wave 4, wave 5, and the HPAI H7N9, respectively. The time between the onset of illness and laboratory validation was 8 days and 6 days for waves 1-3, and the HPAI H7N9, respectively. Lastly, the time between the onset of illness and death was 21 days, 19 days, 16 days, 15 days, 14 days, and 6 days for wave 1, wave 2, wave 3, wave 4, wave 5, and the HPAI H7N9, respectively (Su et al., 2017).

The main clinical symptoms of H7N9 infection are fever, cough, weakness, muscle soreness, shortness of breath, chest distress, nausea, chills, and pneumonia (Su et al., 2017). Other more severe symptoms and outcomes associated with H7N9 infection can include high hospitalization rates (99%), pneumonia or respiratory failure (90%), acute respiratory distress syndrome (ARDS) (34%), severe pulmonary disease, and the requirement to be admitted to an intensive care unit (63%) (Zeng et al., 2015).

Although the LPAI H7N9 and HPAI H7N9 viruses both induce severe symptoms, they seem to differ in their transmissibility, tropism, pathology, and induction of the inflammatory

response. The transmission of the LPAI H7N9 has been found to mainly occur through direct contact, whereas the HPAI H7N9 can transmit through both direct contact and aerosols. Concerning the tropism, studies have shown the replication of both the LPAI H7N9 and HPAI H7N9 viruses to be mostly restricted to the human respiratory tract, unlike other subtypes (ex. H5N1) capable of systemic infection (Belser et al., 2013; Lu et al., 2019; Zeng et al., 2015). The LPAI H7N9 and HPAI H7N9 viruses both undergo very prominent replication. The LPAI H7N9 is characterized by high viral loads in the lungs and hydrothorax (Yang et al., 2019), while the HPAI H7N9 possesses higher virulence and tropism for the brain tissue (Lu et al., 2019). The HPAI H7N9 has also been detected in the intestinal and ocular tissues, sparking concern that the HPAI H7N9 may become systemic (Sun et al., 2018). The different tropisms of the LPAI H7N9 and HPAI H7N9 viruses also correlate to the different pathologies induced. The LPAI H7N9 is a potent inducer of pathology in the lungs of mice, causing strong inflammatory responses such as the infiltration of inflammatory cells to the walls of the arterioles, alveoli, and bronchiolar epithelium. This infiltration results in damage through methods such as degeneration and necrosis (Lu et al., 2019). Conversely, the HPAI H7N9 is a potent inducer of pathology to the brain. Ferret models have shown the HPAI H7N9 infection to cause meningoencephalitis with the severity directly correlated to the duration of infection. This pathology can entail neuronophagia, neuronal necrosis, glial nodules, extensive haemorrhage, and substantial inflammatory infiltration in the meninges, perivascular areas, and parenchyma (Sun et al., 2018).

When diagnosing influenza virus in human patients, although there are several tests available throughout Canada, the most recommended test is the nucleic acid amplification test (NAAT). This test is recommended over other tests because of its performance, automation, and scalability. Other tests such as the direct immune-fluorescence assays (DFA), indirect immune-fluorescence assays (IFA), and rapid influenza detection tests (RIDT) are available but are less sensitive than NAAT and are incapable of subtyping (PHAC, 2018).

1.3 INFLUENZA VIRUS VACCINES

1.3.1 Vaccination

Since the primary method for protection against influenza viruses is through vaccination, the WHO has developed annual meetings in February whereby they meet and discuss the recommended influenza subtypes to be included for the next flu season (PHAC, 2019). Before

these annual meetings occur, the Global Influenza Surveillance and Response System (GISRS) network performs a cumbersome screening over 500,000 virological samples followed by genetic and antigenic analysis of 8,000 samples. The results generated from this analysis are then sent to the WHO for review at these annual meetings (Wong and Webby, 2013). Once the WHO releases their recommendations for the next flu season, in Canada, Canada's Influenza Working Group (IWG) considers the recommendations, develops the annual vaccine, and then sends this vaccine for review to the National Advisory Committee on Immunization (NACI). Once the annual vaccine is approved, it is offered to health care providers to distribute in vaccination programs in the fall. The exact timing of these vaccination programs can vary based on several factors, such as the recent activity of influenza, predicted severity of the upcoming flu season, the best timing of vaccination for communities, and logistical factors such as staffing, equipment, and the availability of infrastructures. Interestingly, because of other factors such as money, shelf-life, and implementation strategies, different jurisdictions might not distribute the same vaccines (PHAC, 2019).

In Canada, there are two types of vaccines available: inactivated influenza vaccines (IIV) and live attenuated influenza vaccines (LAIV). These vaccines are recommended for everyone above and including the age of 6 months, with the type of vaccine available for use determined by both the age of the individual as well as the individual's overall health conditions (PHAC, 2019).

1.3.2 Inactivated influenza vaccines (IIV) in Canada

IIVs have been widely available for use since the 1940s, and have since improved through the addition of adjuvants and advancements to the production technologies (Sridhar et al., 2015). The production of an IIV can include either the whole influenza virus or portions of it produced in large volumes, followed by inactivation of the virus (PHAC, 2017b). The generation of IIVs begins with co-transfection of the eight viral segments into cells to recover the vaccine seed strain. Once this vaccine seed strain is generated, it is amplified in embryonated chicken eggs to obtain high titers of the virus. The HA and NA viral segments are chosen based on the WHO recommendations, whereas the remaining six segments are from a virus capable of replicating to high titers, such as the A/Puerto Rico/8 H1N1 [PR8 (H1N1)]. This combination results in a 6:2

reassortment virus, which is then concentrated, purified, and inactivated with either β-propiolactone or formaldehyde (Blanco-Lobo et al., 2019). The IIVs approved for Canada are a combination of both split virus and subunit vaccines (PHAC, 2019). Split viruses are made the same way as whole IIVs, with the difference being the addition of a detergent to disrupt the viral envelope to expose its internal components, such as its viral proteins. In comparison, subunit vaccines contain portions of the influenza virus, most commonly the surface proteins HA, NA, or both. In these vaccines, the surface proteins undergo further purification steps to remove all other components except the desired proteins (PHAC, 2019; Wong and Webby, 2013).

An IIV is then further classified into whether it is a trivalent inactivated vaccine (TIV) or a quadrivalent inactivated vaccine (QIV). These two vaccine types are currently used in Canada, where the TIV contains two human subtypes of IAV (H1N1 and H3N2) and one lineage of IBV (B/Yamagata/16/88-like or B/Victoria/2/87-like), while the QIV contains both IBV lineages. The TIVs authorized for Canada are an adjuvanted TIV, unadjuvanted TIV, and a high-dose TIV. There are two types of adjuvanted TIV, Fluad® and Fluad Pediatric®, both containing the adjuvant MF59 (an oil-in-water emulsion) and recommended for children aged 6-23 months and adults over the age of 65. The unadjuvanted TIV is recommended for all ages. The high-dose TIV called Fluzone® High-Dose is approved for adults over the age of 65. The only authorized QIV in Canada is a QIV without an adjuvant which is recommended for all ages (Moore, 2018; PHAC, 2019).

In Canada, the current standard dosage for IIVs is 15 µg of HA per strain, delivered intramuscularly. However, some IIVs have higher dosages to accommodate their target population. For example, the Fluzone® High-Dose comprises 60 µg of HA per strain, four times more the standard dosage. Since this IIV targets adults over the age of 65, this high-dose is required to stimulate a robust immune response. This robust immune response is essential because adults in this age range often have a waning immune system, and are at a higher risk for complications, morbidity, and mortality (PHAC, 2019; Wong and Webby, 2013). However, a downside of using this high-dose IIV is that more resources are required for a single dose, so that in the event of a pandemic, vaccine shortages may occur. These vaccine shortages can result in not being able to meet demand, making this vaccine impractical for a large-scale vaccination program (Wong and Webby, 2013).

When an individual is vaccinated with an IIV, this leads to the induction of both the local and systemic immune responses. The antibodies produced by an IIV are predominately IgG, composed mainly of IgG1, followed by IgM and IgA. Within 2 - 6 days post-vaccination, the serum antibody responses increase, and within 2 weeks after vaccination, these responses peak in primed individuals. However, after approximately 6 months, this response decreases around 2-fold, which is why boosters are recommended. Unfortunately, the duration of the antibody response induced by an IIV is still unknown, and the traditional responses generated from both $CD4^+$ and $CD8^+$ T cells are still up for debate (Sridhar et al., 2015).

In Canada, IIVs are advantageous and thus more widely available than LAIVs because of their precise standardization methods and the induction of antibodies specific to the vaccine seed strains. This induction of antibodies is measured as a correlate of protection through the hemagglutinin inhibition (HAI) assay (Krammer et al., 2018; Sridhar et al., 2015). IIVs are also advantageous compared to LAIVs because they have an exceptional safety profile, can be used in children from 6 months of age, and can be used in the elderly, asthmatics, and high-risk individuals (ex. pregnant women and healthcare workers). However, a disadvantage of IIVs is that the vaccine seed strain must often closely match the current circulating strain to be efficacious (ex. homologous vaccine) and that this efficacy is often lower compared to LAIVs (Sridhar et al., 2015). IIVs also often require the use of adjuvants to boost their immunogenicity, because these vaccines frequently stimulate lower immune responses to the viruses present in nature (PHAC, 2017b). Only a few adjuvants are licensed for commercial use in Canada, because of the rigorous safety and efficacy trials required to be used in humans (Isakova-Sivak and Rudenko, 2017). The efficacy rates of IIVs are anywhere from 40% - 60% in adults aged 18 - 65 years, and around 60% in children. Conversely, LAIVs have efficacy rates of approximately 83% in 6 months to 7-year-old children (Osterholm et al., 2012; Sridhar et al., 2015).

1.3.3 Live attenuated influenza vaccines (LAIV) in Canada

LAIVs are a newer type of vaccine that have been used in Russia for over 50 years and more recently licensed for use in North America and Europe around 2003. LAIVs are modified live viruses such that their virulence is reduced because they have restricted replication within the vaccinated host. The LAIVs currently licensed for use are attenuated, temperature-sensitive, and cold adapted such that they can rapidly replicate at 33°C, but cannot replicate at higher

temperatures. This temperature sensitivity permits the replication of the LAIV in the colder URT, where temperatures are around 25°C - 33°C, but inhibits replication in the warmer LRT, where temperatures are around 37°C - 39°C. This phenotype inhibits the virus from undergoing its complete replication cycle to result in the influenza disease (Sridhar et al., 2015).

To produce a LAIV, two main techniques may be used: (i) sequential passage of the virus at colder temperatures, an older technique, and; (ii) reverse genetics, a more recently developed technique. Both techniques use a backbone Master Donor Virus (MDV), either A/Ann Arbor/6/60-H2N2 for IAV, or the B/Ann Arbor/1/66 for IBV. In order to generate a LAIV by sequential passages, the viruses were sequentially passaged at a low temperature of 25°C, with the added selection pressure of neutralizing antibodies against the MDV surface glycoproteins. These MDV underwent sequencing analysis, which led to the discovery of five genetic alterations that explained their attenuated, temperature-sensitive, and cold-adapted phenotype: one found on the PB2 protein (N265S), three on the PB1 protein (K391E, D581G, and A661T) and one on the NP protein (D34G). In order to generate a LAIV by reverse genetics, the six internal genes (PB2, PB1, PA, NP, M, and NS) from one of the MDVs and the HA and NA from the currently circulating strains undergo co-transfection to rescue the viable virus. This viable virus is then propagated with the appropriate environmental conditions (Blanco-Lobo et al., 2019; Cox et al., 1998; Maassab and Bryant, 1999).

Unfortunately, for Canada, as of 2019, there is no commercially available LAIV. In previous years, the FluMist®Quadrivalent (AstraZeneca) was available, but there was a vaccine shortage for the 2019-2020 season (PHAC, 2019). This vaccine is normally composed of four reassortment viruses in a 6:2 arrangement, with two IAV strains and two IBV strains. For the two IAV strains, the six corresponds to the six internal segments from A/Ann Arbor/6/60-H2N2 and the HA and NA from influenza A/H1N1 and influenza A/H3N2 strains, respectively. For the two IBV strains, the six corresponds to the six internal segments from B/Ann Arbor/1/66 and the HA and NA from the Victoria-like lineage (B/Victoria/2/1987) and the Yamagata-like lineage (B/Yamagata/16/1988), respectively (Blanco-Lobo et al., 2019; Jin et al., 2003).

LAIVs are administered intranasally using a nasal spray at a vaccine dose of approximately 10^7 fifty-percent tissue culture infective dose ($TCID_{50}$). This dosage is generally used for all age groups, and similar to the IIV, the influenza strains vary each year depending on

the recommendations by the WHO (Belshe et al., 2004; PHAC, 2019). When a LAIV is administered the virus replicates in the URT, but not the LRT. This replication leads to an immune response similar to that to a natural infection. Therefore, similar to a natural infection, the immune response generated to a LAIV is multifaceted, stimulating both the humoral and cell-mediated immune responses. This multifaceted response is composed of influenza-specific IgA nasal antibodies, serum antibodies, T cells, and IFNs (Belshe et al., 2004). LAIVs also induce higher amounts of memory B cells, $CD4^+$ T cells, and $CD8^+$ T cells compared to IIVs, with the T cell responses being more diverse in children. This T cell diversity, therefore, could aid in the high cross protection efficacy that LAIVs are known to possess. In addition, the production of the nasal IgA antibody is thought to be an essential correlate of protection against the influenza virus. This antibody can be found in nasal secretions for up to 6 - 12 months post-vaccination and works by blocking future infections from entering the mucosal sites (Mohn et al., 2018). Therefore, unlike the immune response that is produced after administration of an IIV, the immune response induced by LAIVs encompass a multitude of components that aid in the protection of the host from the influenza disease.

LAIVs have a long list of advantages compared to IIVs, with some of these including their needle-free properties, ease of administration, patient approval, general lack of opposition from children, acceptability in clinical trials, and preference over the intramuscular route which aids in compliance rates (Belshe et al., 2004). LAIVs are also cheaper to manufacture and may only require a single dose (Isakova-Sivak and Rudenko, 2017). Interestingly, although LAIVs are not yet approved for use in high-risk individuals in Canada, some studies have demonstrated the safety and tolerability of LAIVs in these high-risk populations (Belshe et al., 2004; PHAC, 2019). LAIVs have also demonstrated to be safe and genetically stable for use in the general population, in both immunocompetent children and adults (Blanco-Lobo et al., 2019; Cha et al., 2000; Sridhar et al., 2015).

Not only do LAIVs possess many administrative advantages over IIVs, but they also possess many immunological advantages. The ability of LAIVs to induce the cell-mediated immune response leads to the production of virus-specific cytotoxic $CD8^+$ T lymphocytes, which may be a contributing factor in the protection against heterosubtypic influenza strains (Isakova-Sivak and Rudenko, 2017). In addition, because LAIVs are capable of stimulating the mucosal immune system, this aids in the vaccine mimicking a natural infection, which helps to limit viral

replication and spread through the induction of nasal IgA, local and systemic antibodies, and T cell responses (Isakova-Sivak and Rudenko, 2017; Lorenzo and Fenton, 2013; Sridhar et al., 2015). Lastly, LAIVs are adept in inducing 'herd' immunity, that is, vaccinated individuals aid in the protection of unvaccinated individuals by blocking the spread of influenza among populations (Isakova-Sivak and Rudenko, 2017).

Albeit the abundance of advantages LAIVs possess over IIVs, there are still disadvantages that need to be overcome before LAIVs can become as frequently administered as IIVs. Some of these disadvantages include the lack of a correlate of protection, restricted use to select populations, and safety concerns. Although the immune response generated after LAIV vaccination is multifaceted, to date, there are no definite correlates of protection that can be accurately measured for their efficacy. This lack of measurement is one of the major drawbacks for LAIV vaccination programs, resulting in IIV vaccination programs predominating the field because of their definite correlates of protection through the HAI assay (Sridhar et al., 2015). Researchers have attempted to use the HAI assay to define correlates of protection for LAIVs, however, the results generated varied between children and adults. *King et al.* found a direct correlation between the dosage of a LAIV and serum HAI titers in children, while *Treanor et al.* found no correlation among adults (King et al., 1998; Treanor et al., 1999). However, *Belshe et al.* found that although a high serum HAI antibody response correlated with a high protection efficacy, a low response did not always reflect a lack of protection (Belshe et al., 2004). Therefore, using solely an HAI assay to measure protection efficacy paints an incomplete picture, because the immune response generated from a LAIV is so complex. Thus, much more research is required to establish a correlate of protection so that LAIVs can be more widely licensed throughout the world (Mohn et al., 2018; Sridhar et al., 2015).

Another disadvantage of using LAIVs in vaccination programs is that there is not enough research associated with the health and safety risks to support the administration in all population types. For example, because LAIVs are produced in the allantoic fluid of embryonated hen's eggs, individuals with egg allergies are not recommended to use this vaccine. Moreover, pregnant women and children with chronic health conditions, children under the age of two, immunocompromised individuals, and health care workers surrounded by severe influenza disease are also not permitted to use this vaccine, due to the lack of safety research (Belshe et al., 2004; PHAC, 2019; Sridhar et al., 2015). Other disadvantages of the use of LAIVs include minor

side effects such as a runny nose, nasal congestion, low-grade fever, and a scratchy throat (Belshe et al., 2004). Lastly, for LAIVs to become widespread in vaccination programs, they must overcome the safety concerns associated with reversion or reassortment with the current circulating IAV strains (Mamerow et al., 2019).

More importantly, throughout three seasonal epidemics, although previous studies had countlessly demonstrated LAIVs to possess high efficacy rates, the quadrivalent LAIV, FluMist®Quadrivalent, did not fit this criterion. Despite the high efficacy rates in previous years, children vaccinated with FluMist®Quadrivalent possessed low efficacy rates in the 2013-2014 (18%), 2014-2015 (28%), and 2015-2016 (48%) seasons. There are several proposed factors that may have contributed to these low rates: (i) pre-existing immunity could have existed in adults; (ii) viral infection could have been reduced due to the HA from IAV H1N1 not being fully adapted to humans; (iii) the pH stability could have been altered from the introduction of mutations in the M segment of the MDV A/Ann Arbor/6/60 H2N2; (iv) increased susceptibility of the IAV H1N1 strain to heat degradation; and, (v) high volumes of defective-interfering (DI) viral particles in the vaccine leading to lower immune responses (Blanco-Lobo et al., 2019). Therefore, before LAIVs become the predominant vaccine strategy throughout vaccination programs, they must overcome these limitations so that they can adequately protect all types of individuals.

1.3.4 Experimental live attenuated vaccines in development

Although there is currently no commercially available LAIV for use in Canada for the 2019-2020 season, several other experimental LAIV vaccines are in development. These experimental vaccines were developed through reverse genetic strategies to allow manipulation of portions of the influenza genome to generate recombinant influenza viruses that can be used as LAIVs. Some experimental LAIV vaccines that have been generated include NS1 truncated viruses, suboptimal codon usage viruses, and single-cycle infectious IAVs (sciIAV).

The NS1 protein is expressed in the early stages of IAV infection, where its primary role is to antagonize IFN. This role results in suppressing the antiviral response and type I IFN production, which enables the replication of IAV. Therefore, viruses that lack NS1 or have truncated NS1 proteins can serve as LAIVs in IFN-competent hosts due to their inability to block the antiviral response against infection, resulting in the attenuation of the virus (Blanco-Lobo et

al., 2019). These NS1 truncated viruses hold strong promise as LAIV candidates because several studies have proven their attenuation, cross protection ability, safety, and immunogenicity. For example, one study demonstrated that not only was an NS1 truncated SIV completely attenuated in pigs, this attenuation was directly correlated to the level of IFN-α and IFN-β in the pig cells (Solorzano et al., 2005). Another study performed in healthy humans demonstrated the safety of an NS1 truncated IAV H1N1 virus. This truncated virus was well tolerated and induced both strain-specific and cross-neutralizing antibodies against heterologous variants of IAV (Wacheck et al., 2010). Therefore, NS1 truncated viruses hold strong promise as safe, immunogenic, and protective LAIVs to administer to IFN-competent hosts.

Another experimental LAIV approach researchers have developed was manipulation of the codon usage found among all species. The genetic code is redundant such that most aa are encoded by more than one codon, termed synonymous codons. Researchers have discovered that not all synonymous codons are expressed equally, a phenomenon termed codon usage bias (Blanco-Lobo et al., 2019). For example, the codon pair CAG-GGC might be expected to occur 3000 times in an ORF but is only observed 200 times. This codon usage bias results in each species possessing different preferential codons (Mueller et al., 2011). These preferential codons have been demonstrated to alter many functions, such as gene expression, translation, and protein folding. For IAV, the codon usage bias is often parallel to the codon usage bias of the permissive host, for translation to occur most efficiently. Specifically, an avian IAV will possess a similar codon usage bias to a permissive avian species, but will not possess this same bias in a permissive mammalian species. Researchers have exploited this finding to create LAIVs through the manipulation of these codons in either specific viral proteins or the entire viral genome (Blanco-Lobo et al., 2019). LAIVs in which a specific viral protein is targeted is deoptimized for a specific codon found on a specific viral segment of the influenza virus, such as the NS protein. For example, if the NS protein possesses a codon usage bias of AAA to code for lysine, one could mutate the codons to AAG so it still codes for lysine, but these codons are not the preferential codons for that particular position (Nogales et al., 2014). Conversely, LAIVs that use codon deoptimization to target the entire viral genome entails a more cumbersome approach, such as using a technique called Synthetic Attenuated Virus Engineering (SAVE). This technique calculates the frequency of the various codons throughout the genome and then changes the high-frequency codons to ones that are least frequently observed in nature. This

genome alteration can cause attenuation of the virus, with the hypothesis being that the alteration of the nucleotides changes the translation of the virus (Mueller et al., 2011). Manipulation of the entire genome can also be performed without the SAVE technique. For example, the genome of a human seasonal A/Brisbane/59/2007 H1N1 IAV was manipulated by mutating over 300 nucleotides such that it could replicate in eggs but was attenuated in human cells. This approach allowed the virus to be propagated, and still administered as a LAIV in humans (Fan et al., 2015). Overall, these suboptimal codon usage LAIVs are capable of quick production, are highly attenuated, and are safe regarding reversion because of the high number of mutations introduced into the genome (Blanco-Lobo et al., 2019).

The third experimental LAIV approach researchers are developing are IAVs defective in some part of the replication cycle, namely, single-cycle infectious IAVs (sciIAVs). These sciIAVs can be defective in features such as viral genome synthesis, assembly, or release of the virion to infect the neighbouring cells. Scientists have created these sciIAVS through molecular biology techniques by modifying specific viral proteins such that they are: (i) substituted with another viral component, whether it is from the same or a different pathogen; (ii) partially or entirely deleted; or (iii) mutated in some manner. However, when developing these sciIAVs, researchers must retain the packaging signals and NCRs to preserve the optimal fitness of the virus. Although these viruses do not possess all the necessary components to undergo more than a single cycle of replication, this can be overcome *in vitro* or *in vivo* by providing the necessary component (Blanco-Lobo et al., 2019).

One sciIAV developed through the substitution technique was generated through substitution of the coding region of the PB2 protein on the PR8 (H1N1) virus with the green fluorescent protein (GFP), creating a PR8 sciIAV ΔPB2 virus. When administered to mice intranasally, this LAIV did not cause disease, was protective against lethal challenges of IAV, and induced antibodies against both PR8 and GFP, illustrating the potential of this vaccine to be used against different pathogens (Victor et al., 2012). The generation and efficiency of protective sciIAVs through the substitution technique was also demonstrated in other species. Specifically, *Masic et al.* developed a sciIAV for pigs through the fusion of the H3 HA ectodomain of A/Swine/Texas/4199-2/98 H3N2 to the NA segment of A/Swine/Saskatchewan/18789/02 H1N1. When this sciIAV was administered intratracheally, it was not only found to be completely

attenuated but also generated antibodies against both the H1 and H3 antigens, illustrating the potential of this sciIAV to act as a bivalent vaccine (Masic et al., 2013).

When generating a sciIAV through the mutagenesis technique, the purpose is to alter specific viral proteins to generate either a non-functional virus, a non-expressible virus, or a virus that cannot be efficiently processed. This method is, therefore, less invasive than deleting or substituting an entire viral protein, because only a few mutations are performed. For example, the HA protein is initially found in its precursor form, HA0, and must be cleaved into HA1 and HA2 by specific host proteases to become active and continue its replication cycle. A sciIAV can be generated by introducing mutations to the HA cleavage site such that the host proteases can no longer recognize and cleave HA. This results in IAV unable to continue its replication cycle to cause the influenza disease (Blanco-Lobo et al., 2019). This concept was tested by mutating the HA cleavage site from arginine to glutamine at aa position 329. This single mutation resulted in a lack of cleavage by the host protease trypsin, and thus rendered the virus unable to continue its replication cycle (Chen et al., 1998). The HA cleavage site can also be mutated such that although it can no longer be cleaved by a specific host protease, cleavage can still occur through the supplementation of an exogenous protease. For example, the HA cleavage site found on an SIV strain A/Swine/Saskatchewan/18789/02 (H1N1) was mutated from a trypsin-sensitive motif to an elastase-sensitive motif by mutating arginine to valine at aa position 345. This SIV mutant strain was protective, immunogenic, and genetically stable when administered intranasally in pigs. This virus could be amplified *in vitro* when provided the protease elastase (Masic et al., 2008). Therefore, the mutagenesis of a single aa can generate stable, safe sciIAVs that possess strong potential to serve as LAIV candidates against various IAV strains and subtypes.

These molecular biology techniques to generate sciIAVs can be used in combination to generate potential LAIV candidates. For example, *Mamerow et al.* demonstrated that a double-mutant virus composed of the elastase-sensitive HA cleavage site and an NS1 truncated protein was attenuated and protective against homologous challenge in both pigs and mice. The goal for this double-mutant LAIV is to improve the safety concerns associated with reversion and reassortment with the standard cold-adapted LAIVs, such as the FluMist® vaccine (Mamerow et al., 2019).

Conversely, replication-defective viruses are a newer type of vaccine independent of IIVs and LAIVs such that they are composed of viruses that lack one or more essential functions

required for replication, synthesis, or viral assembly. These replication-defective viruses can be propagated *in vitro* through the supplementation of the missing gene product by complementing cell lines, however, they cannot properly replicate *in vivo* (Dudek and Knipe, 2006). This feature allows the replication-defective virus to produce viral antigens within the infected cells. Unlike IIVs and LAIVs, which both contain disadvantages towards their use replication-defective viruses seem to combine the advantages of both IIVs and LAIVs. More specifically, like IIVs, replication-defective viruses have been shown to be extremely safe due to their very limited replication within the host (Dudek and Knipe, 2006). This is in contrast to LAIVs, where virulence reversion is a major safety concern towards their widespread use (Watanabe et al., 2001). Replication-defective viruses have also been shown to induce the same immune responses LAIVs induce, namely, $CD4^+$ T cells, $CD8^+$ T cells, and humoral immune responses (Dudek and Knipe, 2006). This induction is explained through the ability of the replication-defective viruses to enter the cells, followed by the presentation of the viral antigens through both the MHC class I and II pathways (Dudek and Knipe, 2006).

The advantages of using replication-defective viruses as vaccines have also been assessed through *in vivo* protection efficacy experiments. *Watanabe et al*. demonstrated mice vaccinated with replication-defective influenza virus-like particle (VLP) composed of a NEP-knockout to have a 94% protection efficacy against an antigenically homologous H1N1 influenza challenge (Watanabe et al., 2001). More recently, *Katsura et al*. demonstrated a replication-incompetent virus containing an uncleavable HA to completely protect mice against a homologous influenza virus challenge. This HA contained a mutation at the HA cleavage site, where arginine was mutated to threonine, thereby blocking fusion among the membranes of the virus and host within the endosome (Katsura et al., 2012).

Therefore, replication-defective virus vaccines show strong promise as vaccine candidates against influenza viruses due to their ability to combine the advantages of both IIVs and LAIVs. Replication-defective virus vaccines also hold strong promise as vaccine candidates against influenza viruses that continue to pose burdens on public health. One such influenza virus that has recently plagued public health is the new IAV strain, H7N9. This IAV strain has resulted in high morbidity and mortality rates, with 1,568 human cases and 616 deaths as of March 4, 2020 (FAO, 2020). More importantly, the candidate vaccine viruses available are majorly IIVs and are limited to only a few variants of H7N9: A/Shanghai/2/13, A/Anhui/1/13,

A/Guangdong/17SF003/2016, A/Hong Kong/125/2017, and A/Human/02650/2016 (WHO, 2019). Because of IAVs complex evolutionary mechanism of *antigenic drift* and *antigenic shift*, and the disadvantages IIVs and LAIVs possess, my research aims to fill a gap in the H7N9 vaccine development. Specifically, my research aims to develop a replication-defective virus vaccine against a new Canadian isolate, the A/British Columbia/01/2015 (H7N9) [BC15 (H7N9)] that was isolated from two patients in Canada that had recently travelled to China and contracted the disease (Skowronski et al., 2016). The goal is that this replication-defective virus vaccine will provide sufficient protection against H7N9, avoiding the disadvantages of both IIVs and LAIVs.

CHAPTER 2 HYPOTHESIS AND OBJECTIVES

2.1 OVERALL GOALS AND RATIONALE

Influenza A virus (IAV) is a segmented ribonucleic acid (RNA) virus of the *Orthomyxoviridae* family capable of infecting many mammalian species, ranging from birds to sea mammals (Bouvier and Palese, 2011; CDC, 2015). IAV also poses a heavy burden to public health through spillovers, such as avian H7N9 and H5N1 IAV crossing the species barrier from birds to humans (Claas et al., 1998; Gao et al., 2013). Currently, vaccination is the leading method for the prevention and control of influenza viruses. In Canada, the two main commercially available vaccines are the inactivated influenza vaccines (IIV) and the live attenuated influenza vaccines (LAIV). IIVs are most often administered intramuscularly, with correlates of protection directly related to the induction of antibodies against the hemagglutinin (HA) and neuraminidase (NA) viral surface proteins of the vaccine seed strain. Unfortunately, albeit their predominant use in the field settings compared to other vaccine types, they have many limitations. One such limitation is that for an IIV to provide adequate protection, it must closely match the influenza strain that is currently circulating (PHAC, 2017a; Sridhar et al., 2015). However, due to influenza's capability to escape the immune system through mutagenic properties such as *antigenic shift* and *antigenic drift*, this often results in IIVs possessing low efficacy (Acheson, 2011). More importantly, because of these high mutation rates, vaccines need to be frequently updated which can be time-consuming and costly. Conversely, LAIVs are administered intranasally and possess many advantages over IIVs. Some of these advantages include their enhanced protection rates against vaccine mismatches, longer-lasting immunity from both the humoral and cell-mediated responses, as well as the ability to imitate a natural infection, eliciting immune responses comparable to those induced in nature (Isakova-Sivak and Rudenko, 2017; Lorenzo and Fenton, 2013; PHAC, 2017a). LAIVs are also advantageous to IIVs because they do not necessarily depend on the egg-based production system, which can be a limiting factor when large production volumes are required, egg-shortages occur, or if an individual has an egg allergy (Sridhar et al., 2015). However, LAIVs do possess the possibility of virulence reversion, making widespread vaccination programs with LAIVs difficult to implement. Replication-defective virus vaccines are an ideal alternative towards both IIVs and LAIVs because they have been characterized by a high safety profile and the ability to induce strong immune responses (Dudek and Knipe, 2006). Currently, there are no commercial vaccines

available for use against H7N9 influenza infection (PHAC, 2017a). Therefore, *with the severe threat influenza viruses pose through the spillovers into humans, and the inadequate protection IIVs often provide as well as the possibility of reversion for LAIVs, there is an urgent need to develop a replication-defective virus vaccine that is stable, cross protective, and safe to administer to the public against H7N9 influenza infection.*

The development of reverse genetic technology has empowered the generation of any influenza strain desired in minimal time. This technology allows the manipulation of cloned cDNA so that any portion of any viral gene can be altered to suit a research purpose (Hoffmann et al., 2001). Some of these alterations can include the development of replication-defective virus vaccines or LAIVs. This technology not only avoids the use of the egg-based system but also produces efficacious influenza vaccines quickly, making this technology more appealing than the traditional IIV production process (PHAC, 2017a; Sridhar et al., 2015).

IAV possesses a unique feature such that although it can enter cells through the interaction of its viral surface protein, HA, the activation of IAV does not occur until it is cleaved by a host protease. When influenza virus initiates viral infection, HA is present in its precursor form, HA0, which remains non-infectious until HA0 is cleaved into HA1 and HA2. After HA0 is cleaved, the influenza virus becomes activated and continues its replication cycle, which results in the influenza disease (Masic et al., 2008).

Therefore, ***our overall goal is to create a replication-defective H7N9 virus vaccine that has been altered to contain a mutation at the HA cleavage site that renders it inactive during natural infection, but active when provided the appropriate protease in vitro.*** The rationale of this project is that the replication-defective H7N9 virus is replication-defective *in vivo*, due to the lack of the appropriate protease in the host cells capable of cleaving the mutated HA cleavage site, but can prominently grow *in vitro* when provided this appropriate protease. This replication-defective H7N9 virus could serve as a replication-defective virus vaccine, due to the minimal risk of reassortment, as well as the potential to induce immune responses similar to that of a natural infection.

2.2 HYPOTHESIS

A mutant virus containing a modified HA cleavage site is inactive during natural infection due to the lack of an appropriate protease, allowing this mutant virus to serve as a replication-defective virus vaccine in the protection against H7N9 viruses.

2.3 OBJECTIVES

The main objective of my thesis is to generate a replication-defective H7N9 virus that can be used as a replication-defective virus vaccine. The generation of this replication-defective virus vaccine would aid in preventing the spread of the H7N9 virus and its pandemic potential, by inducing strong cell-mediated and humoral immunity.

To achieve my objective three aims need to be fulfilled:

- ***Aim 1* – The establishment of a mouse model of A/British Columbia/01/2015 [BC15 (H7N9)] virus**

  To develop a mouse model to characterize the susceptibility of mice, the replication and pathology induced in the lungs, as well as the immune response mounted against H7N9 as a platform for the development of a vaccine.

- ***Aim 2* – The generation and characterization of the mutant H7N9 virus with its modified HA segment *in vitro* and *in vivo***

  To generate a mutant H7N9 virus in which the HA gene is mutated from a trypsin-sensitive cleavage site (arginine-glycine; Arg-Gly) to an elastase-sensitive cleavage site (valine-glycine; Val-Gly). This mutant virus will also be characterized for its growth properties, genetic stability, and virulence in mice.

- ***Aim 3* – The evaluation of the immunogenicity and protective efficacy of the replication-defective virus vaccine after intranasal administration against A/British Columbia/01/2015 [BC15 (H7N9)] virus**

  To test the potential of the mutant H7N9 virus to be used as a replication-defective virus vaccine.

CHAPTER 3 ESTABLISHMENT OF A MOUSE MODEL OF A/BRITISH COLUMBIA/01/2015 [BC15 (H7N9)] VIRUS

The data presented in this chapter were published as a full-length article in:

In Vivo Characterization of Avian Influenza A (H5N1) and (H7N9) Viruses Isolated from Canadian Travelers

Yao Lu[1,2,†], Shelby Landreth[1,3,†], Amit Gaba[1], Magda Hlasny[1], Guanqun Liu[1,3], Yanyun Huang[4], and Yan Zhou[1,2,3,*]

[1]Vaccine and Infectious Disease Organization - International Vaccine Centre (VIDO-InterVac),
[2]Department of Veterinary Microbiology, Western College of Veterinary Medicine,
[3]Vaccinology & Immunotherapeutics Program, School of Public Health, University of Saskatchewan, Saskatoon, Canada
[4]Prairie Diagnostic Services Inc., Saskatoon, Canada
[†]These authors contributed equally to this work.

Viruses, 11(2), 193, 2019; https://doi.org/10.3390/v11020193.

My contributions to this publication:

For this paper I contributed to the methodology, formal analysis, investigation, original draft preparation, and writing – review and editions. I performed all experiments and analyzed results with respect to BC15 (H7N9). My contributions to this paper were approximately 40%.

3.1 ABSTRACT

Highly pathogenic avian influenza (HPAI) H5N1 and low pathogenic avian influenza (LPAI) H7N9 viruses pose a severe threat to public health through zoonotic infection, causing severe respiratory disease in humans. While HPAI H5N1 human infections have typically been reported in Asian countries, avian H7N9 human infections have been reported mainly in China. However, Canada reported a case of fatal human infection by the HPAI H5N1 virus in 2014, and two cases of human illness associated with avian H7N9 virus infection in 2015. While the genomes of the causative viruses A/Alberta/01/2014 (H5N1) (AB14 (H5N1)) and A/British Columbia/01/2015 (H7N9) (BC15 (H7N9)) are reported, the isolates had not been evaluated for their pathogenicity in animal models. In this study, we characterized the pathogenicity of AB14 (H5N1) and BC15 (H7N9) and found that both strain isolates are highly lethal in mice. AB14 (H5N1) caused systemic viral infection and erratic proinflammatory cytokine gene expression in different organs. In contrast, BC15 (H7N9) replicated efficiently only in the respiratory tract, and was a potent inducer for proinflammatory cytokine genes in the lungs. Our study provides experimental evidence to complement the specific human case reports and animal models for evaluating vaccine and antiviral candidates against potential influenza pandemics.

3.2 INTRODUCTION

Influenza A virus (IAV) is a segmented ribonucleic acid (RNA) virus that infects a wide variety of species including human, avian, swine, equine, and sea mammals. The segmented genome and wide host range enable IAV to undergo antigenic variations through gene reassortment, a mechanism called *antigenic shift*, which is responsible for the emergence of pandemic influenza viruses. The lack of proofreading by the viral RNA-dependent RNA polymerase frequently results in point mutations throughout the viral genome (especially in HA and NA genes), which can lead to *antigenic drift*, a causative mechanism of annual influenza epidemics (Krammer et al., 2018; Webster et al., 1992b). Additionally, IAV also poses a severe threat to public health through zoonotic infection, because avian IAVs can directly cross the species barrier and infect humans, with avian H5N1 and H7N9 viruses being such examples. The first report of human infection by the highly pathogenic avian influenza (HPAI) H5N1 virus was in 1997 in Hong Kong; after a short period of disappearance, the virus re-emerged in 2003 in China (Claas et al., 1998). Since then, sporadic human H5N1 viral infections have been reported in several countries, causing over 400 fatalities (WHO). The low pathogenic avian influenza (LPAI) H7N9 virus circulated exclusively among poultry in China until 2013 when the first human infection was reported (Gao et al., 2013). Similar to the HPAI H5N1 virus, human infection by the H7N9 virus is also associated with a severe and fatal respiratory disease. To date, the H7N9 virus has caused a total of six epidemic waves, having infected over 1600 humans with 623 fatalities (WHO, 2017).

In comparison to the human seasonal H1N1 and H3N2 viruses, the HPAI H5N1 virus induces more proinflammatory cytokines in the human alveolar and bronchial epithelial cells (Chan et al., 2005). H5N1 viral infection also results in the early and excessive infiltration of macrophages and neutrophils in the lungs of infected mice (Perrone et al., 2008b). Animal and human studies have shown that the combinatorial effect of the unrestrained high-level virus infection together with hypercytokinemia is attributable to the increased pathogenesis of H5N1 disease (Abdel-Nasser; et al., 2008; De Jong et al., 2006). Although both H5N1 and H7N9 viral infections lead to fatality, the underlying mechanisms might be different (Meliopoulos et al., 2014). An ex vivo study showed that the human H7N9 virus replicated efficiently in human bronchial epithelial cells, alveolar epithelial cells, and alveolar macrophages, with high titers similar to that of the H5N1 virus (Chan et al., 2013a). However, in animal studies, it has been

reported that the H7N9 virus possesses a greater tropism for the respiratory epithelium than that of the H5N1 virus, and is not capable of inducing hypercytokinemia, which is characteristic of H5N1 viral infection (Meliopoulos et al., 2014). Recently, a risk assessment of the fifth wave of H7N9 viral infection revealed that both the LPAI H7N9 and HPAI H7N9 viruses were isolated from humans. Compared to the LPAI H7N9, the HPAI H7N9 virus was found to possess enhanced virulence, tropism for the brain tissue, as well as the capability to transmit by air droplets, concluding that the HPAI H7N9 virus has gained the ability to cause an H7N9 pandemic (Sun et al., 2018). Thus, both H5N1 and H7N9 viruses are of significant pandemic concerns.

Both HPAI H5N1 and LPAI H7N9 human infections in North America were reported in Canada, in 2014 and 2015 respectively, shortly after the patients returned from China (Maurer-Stroh et al., 2014; Skowronski et al., 2016). The A/Alberta/01/2014 (H5N1) (AB14 (H5N1)) strain isolate caused a fatal infection, whereas the A/British Columbia/01/2015 (H7N9) (BC15 (H7N9)) strain isolate caused an influenza illness from which the patients recovered. Phylogenetic analysis revealed mutations on the receptor binding site of the HA gene in AB14 (H5N1), which facilitated the direct jump from avian to humans (Pabbaraju et al., 2014a). However, for BC15 (H7N9), the analysis showed the genome to be similar to those of previous human H7N9 isolates, carrying clinically relevant markers on HA, PB2, and NA genes (Skowronski et al., 2016). Although H5N1 and H7N9 viruses have been intensively studied, the virulence of these avian-origin influenza strains isolated from these Canadian travelers has been overlooked. The purpose of this study was to experimentally investigate the pathogenicity as well as the cytokine and chemokine gene transcription profile of the AB14 (H5N1) and BC15 (H7N9) strain isolates. We report that both AB14 (H5N1) and BC15 (H7N9) strains are highly lethal in mice. AB14 (H5N1) caused a systemic viral infection as well as an erratic proinflammatory cytokine and chemokine gene response in different organs. In contrast, the BC15 (H7N9) strain replicated efficiently only in the respiratory tract, and was a potent inducer for proinflammatory cytokines in the lungs. Overall, our study not only provides experimental evidence to complement the human case report, but also offers valuable animal models for evaluating vaccine and antiviral candidates against the potential H5 and H7 influenza pandemic viruses.

3.3 MATERIALS AND METHODS

3.3.1 Cells and viruses

Madin-Darby canine kidney (MDCK) (ATCC, #CRL-2936) cells were maintained in minimal essential medium (MEM) (Sigma-Aldrich, St. Louis, MO, USA) supplemented with 10% fetal bovine serum (FBS) (Sigma-Aldrich) and gentamycin (50 µg/mL, Bio Basic, Markham, ON, Canada). MDCK cells were maintained at 37°C in a humidified 5% CO2 incubator. Influenza A/Alberta/01/2014 (H5N1) (AB14 (H5N1)) and A/British Columbia/01/2015 (H7N9) (BC15 (H7N9)) were kind gifts from Dr. Yan Li at the National Microbiology Laboratory, Public Health Agency of Canada. The viruses were propagated in MDCK cells and titrated by plaque assay. Propagated viruses were sequenced, and no mutations were found according to the reference sequences. All infectious experiments were conducted in Biosafety Containment Level 3 at the International Vaccine Centre at the University of Saskatchewan, Canada, under the guidelines of the Public Health Agency of Canada (PHAC) and the Canadian Food Inspection Agency (CFIA).

3.3.2 Ethics statement

All animal procedures were approved by the University Animal Care Committee (UACC) and Animal Research Ethics Board (AREB) of the University of Saskatchewan on 31 August 2017 (Animal Use Protocol #20170087) in accordance with the standards stipulated by the Canadian Council on Animal Care.

3.3.3 Mouse experiments

For this study, 84 six-week-old female BALB/c mice (Charles River Laboratories, Saint-Constant, QC, Canada) were randomly divided into seven groups with 12 mice in each group. These groups were housed in separate cages in Biosafety Containment Level 3 seven days prior to infection. At seven weeks of age, each mouse was intranasally infected with 50 µL of 10^3 PFU, 10^4 PFU, and 10^5 PFU of either the AB14 (H5N1) or BC15 (H7N9) strain isolates. A group of mice was mock infected with PBS. The mice were monitored daily for body weight, and on days 2 and 5 post-infection (d.p.i), three mice from each group were euthanized, after which the lung and spleen tissues were collected for viral titration as well as cytokine and chemokine

profiling. Brain tissues were collected from euthanized mice on either 6 or 7 d.p.i. The rest of the mice were humanely euthanized when they dropped below 20% of their initial body weight.

3.3.4 Virus isolation and titration

Infectious lung, spleen, and brain tissues were processed immediately after collection as previously described (Pyo and Zhou, 2014). Briefly, the tissues were homogenized in MEM supplemented with Penicillin-Streptomycin (Gibco, Thermo Fisher, ON, Canada) in the TissueLyser II (Qiagen, Hilden, Germany) at 25 Hz for 5 min, followed by centrifugation at 5,000 g for 10 min at 4°C. The supernatant was collected in screw-cap tubes and stored at -80°C for further titration.

For virus titration by $TCID_{50}$ assay, MDCK cells were plated in 96-well plates, and the supernatants of homogenized tissues were serially diluted in MEM and incubated with cells for 1 h. The inoculum was removed and supplemented with MEM containing 0.2% BSA and 1 µg/mL TPCK-trypsin (Sigma-Aldrich). The development of cytopathic effects (CPE) was observed and recorded every 24 h until 96 h post-infection. The $TCID_{50}$ titer of each infectious sample was calculated by the Spearman–Kärber algorithm (Kärber, 1931; Spearman, 1908).

3.3.5 RNA extraction and quantitative RT-PCR (qRT-PCR)

Tissue samples of mice collected on 2 or 5 d.p.i. or upon necropsy were submerged into RNA later (Qiagen) and stored overnight at 4°C. The following day, the tissue samples were transferred to screw-cap tubes containing one 5 mm stainless steel bead (Qiagen) and 1 mL of TRIzol Reagent (Invitrogen, Carlsbad, CA, USA). The samples were homogenized using the TissueLyser II (Qiagen) at 25 Hz for 5 min, followed by centrifugation at 5,000 g for 10 min at 4°C. The supernatant was then transferred to new tubes for RNA extraction by the TRIzol method (Invitrogen).

To determine mRNA levels of various cytokines and chemokines induced by AB14 (H5N1) and BC15 (H7N9) viral infection, qRT-PCR was performed on total RNA of the samples collected from mice infected with 10^3 PFU of the respective virus, as previously described (Liu et al., 2018) with the following modifications. Briefly, a 500 µg portion of RNA was reverse transcribed with oligo(dt) and SuperScript III Transcriptase (Invitrogen) to obtain total mRNA. qPCR was performed on a StepOnePlus™ Real-Time PCR system (Applied

Biosystems, CA, USA) with the Power SYBR Green PCR Master Mix (Applied Biosystems). Cytokine mRNA levels were normalized to that of the housekeeping gene hypoxanthine phosphoribosyltransferase (HPRT) and expressed using the ΔΔCT method relative to the PBS group. All sequences of qPCR primers are listed in Table 3.1.

Name	Sequence (5' – 3')
IFN-γ-F	TCAAGTGGCATAGATGTGGAAGAA
IFN-γ-R	TGGCTCTGCAGGATTTTCATG
IFN-α-F	CCTGTGTGATGCAACAGGTC
IFN-α-R	TCACTCCTCCTTGCTCAATC
IFN-β-F	ATCATGAACAACAGGTGGATCCTCC
IFN-β-R	TTCAAGTGGAGAGCAGTTGAG
IP-10-F	ATGACGGGCCAGTGAGAATG
IP-10-R	GAGGCTCTCTGCTGTCCATC
TNFα-F	AGGCACTCCCCCAAAAGATG
TNFα-R	CTGCCACAAGCAGGAATGAG
IL-1β-F	GTGTGGATCCCAAGCAATAC
IL-1β-R	GTCCTGACCACTGTTGTTTC
IL-18-F	TGGTTCCATGCTTTCTGGACTCCT
IL-18-R	TTCCTGGGCCAAGAGGAAGTGATT
IL-6-F	GTGGCTAAGGACCAAGACCA
IL-6-R	TAACGCACTAGGTTTGCCGA
IL-10-F	GCTGCCTGCTCTTACTGACT
IL-10-R	CTGGGAAGTGGGTGCAGTTA
RIG-I-F	CCTCCCATCTCCTTCATGACA
RIG-I-R	CCACCTACATCCTCAGCTACATGA
HPRT-F	GATTAGCGATGATGAACCAGGTT
HPRT-R	CCTCCCATCTCCTTCATGACA

Table 3.1. List of primers used in qRT-PCR studies in mice.
All primers have been validated to have greater than 95% of amplification efficiency. The expression levels of cytokine mRNA were normalized to the expression of the housekeeping gene HPRT. F: forward primer; R: reverse primer.

3.3.6 Histopathology

The left side of the lung was fixed with 10% natural buffered formalin, processed for hematoxylin and eosin (H&E) staining, and assessed in a blind manner by a board-certified veterinary pathologist as previously described (Pyo et al., 2015).

3.4 RESULTS

3.4.1 Survival rate and body weight loss of mice infected with the HPAI H5N1 and LPAI H7N9 strain isolates

To determine the pathogenicity of the AB14 (H5N1) and BC15 (H7N9), BALB/c mice were intranasally inoculated with PBS or either AB14 (H5N1) or BC15 (H7N9) at three different doses (10^3 PFU, 10^4 PFU, and 10^5 PFU). Survival and body weight loss were monitored for 10 days (Figure 3.1). Mice infected with PBS survived the duration of the trial and gained weight as the days progressed. In contrast, mice infected with the different doses of either AB14 (H5N1) or BC15 (H7N9) showed rapid body weight loss and severe mortality rates. Mice infected with 10^4 PFU or 10^5 PFU of AB14 (H5N1) exhibited rapid weight loss greater than 20% of their initial body weight within four days post-infection (d.p.i.). Furthermore, over 60% of mice infected with 10^5 PFU of AB14 (H5N1) had succumbed by 4 d.p.i. (Figure 3.1A,B). By 5 d.p.i., 100% of mice infected with 10^4 PFU and 10^5 PFU were humanely euthanized due to severe body weight loss. Albeit mice infected with 10^3 PFU displayed the slowest rate of body weight loss, they all reached a humane endpoint by 6 d.p.i. With regard to BC15 (H7N9), mice infected with 10^3 PFU displayed the slowest decline of body weight, losing over 20% of their initial body weight by 8 d.p.i. Furthermore, 50% of mice infected with 10^3 PFU reached a humane endpoint by 7 d.p.i., while the other 50% reached this endpoint by 8 d.p.i. (Figure 3.1C,D). In contrast, mice infected with 10^4 PFU and 10^5 PFU had steeper body weight losses and higher mortality rates. In the 10^4 PFU group, 100% of mice reached a humane endpoint by 6 d.p.i., while in the 10^5 PFU group, 50% of the mice by 4 d.p.i. and the other 50% by 5 d.p.i. reached this endpoint. These results demonstrate that both the AB14 (H5N1) and BC15 (H7N9) strain isolates are highly virulent in mice without the need of prior adaptation even at the lowest dose.

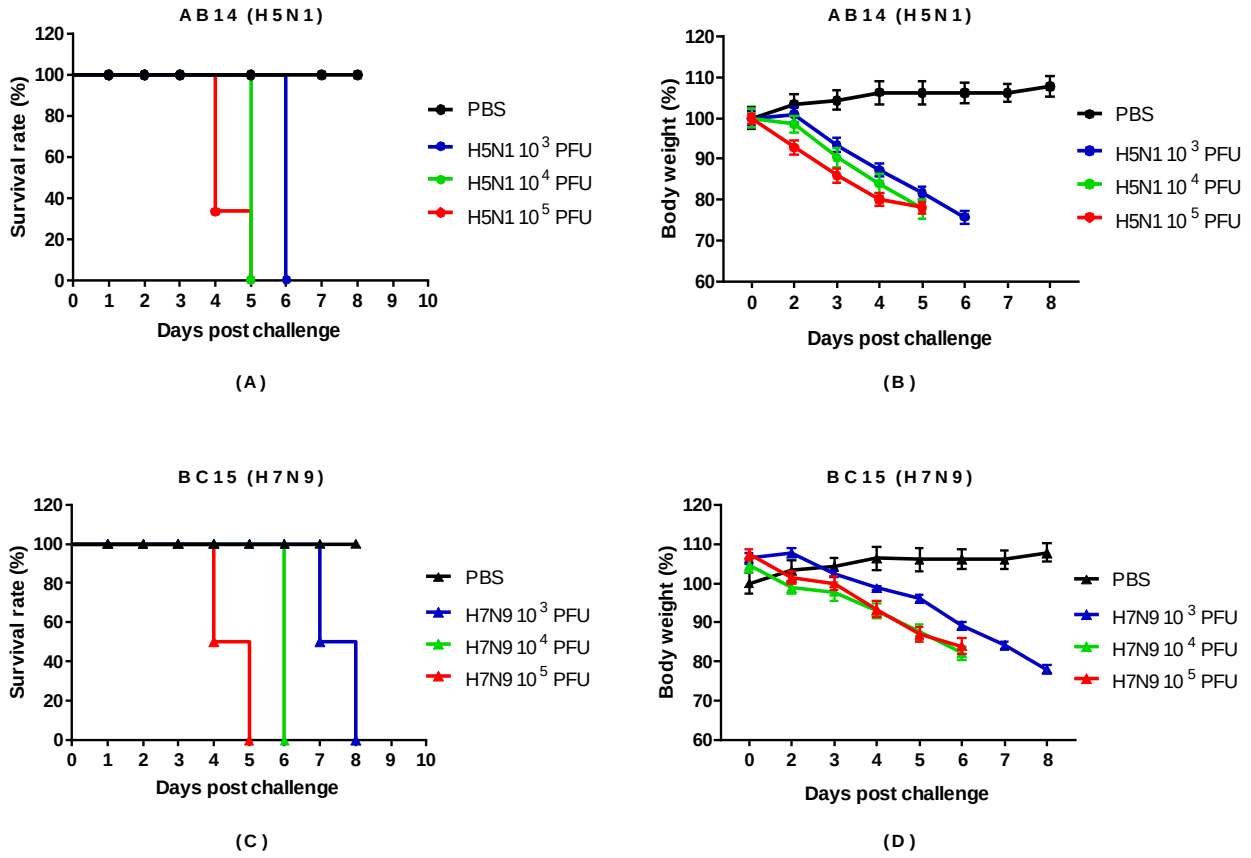

Figure 3.1. Survival rate and body weight loss for the AB14 (H5N1) and BC15 (H7N9) strain isolates.
The survival rates for (**A**) AB14 (H5N1) and (**C**) BC15 (H7N9) as well as body weight changes for (**B**) AB14 (H5N1) and (**D**) BC15 (H7N9) were determined in BALB/c mice (n = 6 per group) infected with 10^3 PFU, 10^4 PFU, and 10^5 PFU of the two different strain isolates.

3.4.2 Histopathology of the mouse lung

To examine the levels of pulmonary pathology from AB14 (H5N1) and BC15 (H7N9) infection, we performed a histopathology study on the lungs of mice infected with 10^3 PFU that reached a humane endpoint on 6 or 7 d.p.i. Mice infected with both AB14 (H5N1) and BC15 (H7N9) strain isolates showed bronchointerstitial pneumonia, with vasculitis (Figure 3.2). Specifically, the walls of the arterioles in infected mice were found to be infiltrated with inflammatory cells, and contained some necrotic debris (Figure 3.2, Panels D and G). In addition, viral infection also led to moderate damage to the mice alveoli and bronchioles. In the alveoli of infected mice, we found moderate thickening of the alveolar walls due to congestion as well as some inflammatory infiltrate (Figure 3.2, Panels E and H). The alveolar space was filled with

edema, and contained small to moderate numbers of mixed neutrophils and macrophages. Occasionally, hyaline membranes lining the alveoli were observed (Figure 3.2, Panel E). Multifocally, the bronchiolar epithelium was necrotic, and the lumen was filled with some necrotic debris and inflammatory cells as seen in the alveolar space (Figure 3.2, Panels F and I).

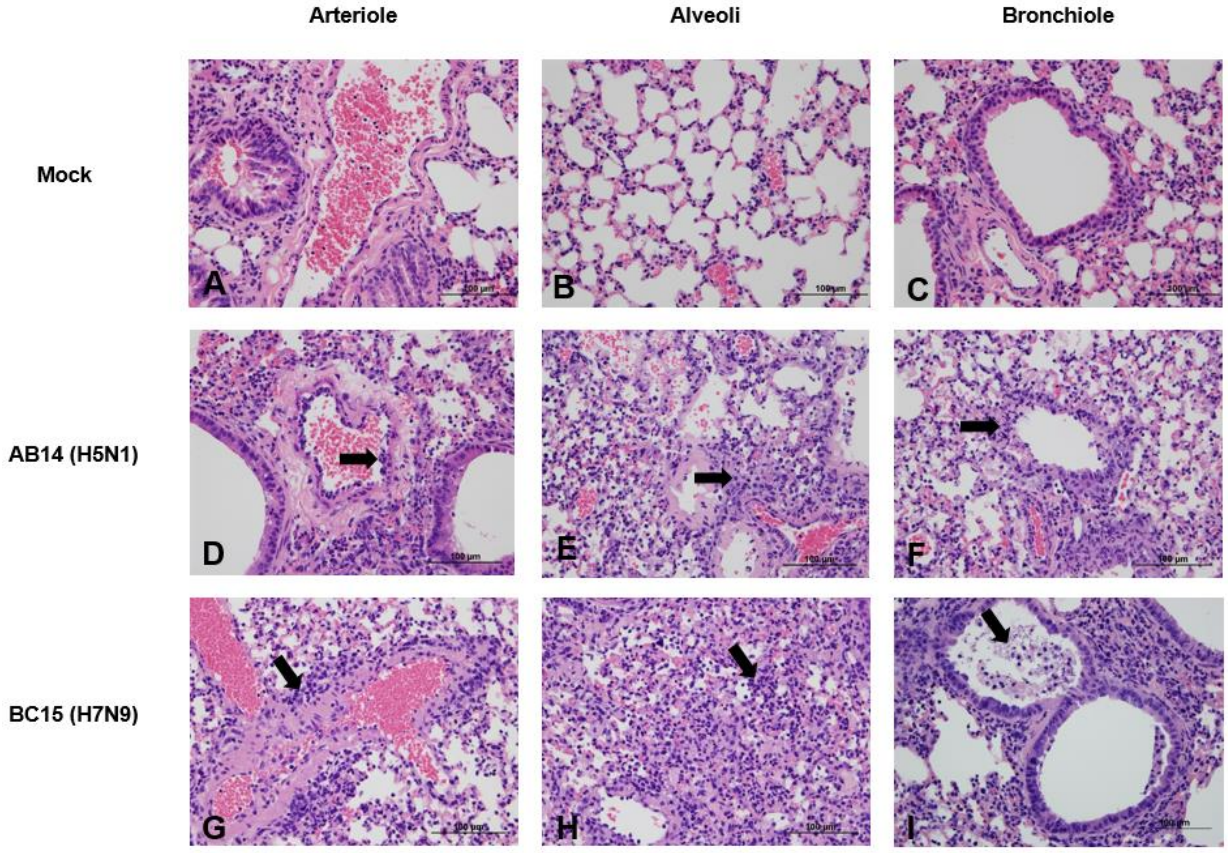

Figure 3.2. Lung histopathology of mice after infection with AB14 (H5N1) and BC15 (H7N9) strain isolates.
Lung samples were fixed, sectioned, and stained with hematoxylin and eosin. (**A**–**C**) Tissues from mock-infected lungs. (**D**–**F**) Tissues from mice infected with AB14 (H5N1) showing infiltration of inflammatory cells into the (**D**) wall of the arteriole, (**E**) alveolar walls, and (**F**) bronchiolar epithelium affected by necrosis. (**G**–**I**) Tissues from mice infected with BC15 (H7N9) showing necrotic debris and inflammatory cells in the (**G**) wall of the arteriole, (**H**) collapsed alveoli, as well as degeneration and necrosis of the (**I**) bronchiolar epithelium. Scale bar represents 100 µm. Black arrows denote the various histopathology features described above.

3.4.3 Replication efficiency of the HPAI H5N1 and LPAI H7N9 strain isolates in different organs of mice

To investigate the replication efficiency and tissue tropism of both strain isolates, mouse lung, spleen, and brain tissues were collected at predetermined days, as well as when the mice reached a critical endpoint (Figure 3.3). In all groups of mice infected with AB14 (H5N1), the peak lung viral titers were reached by 2 d.p.i., which remained at high levels throughout the duration of the trial. The mean titers on 5 d.p.i. were $10^{7.2}$, $10^{6.4}$, and $10^{6.7}$ $TCID_{50}$/g for 10^3 PFU, 10^4 PFU, and 10^5 PFU, respectively (Figure 3.3A). Brain samples taken from the lowest dose group (10^3 PFU) had very high viral titers on 6 d.p.i., with a mean virus titer of 10^7 $TCID_{50}$/g (Figure 3.3C). Note that the brain samples were only harvested at the endpoint. Spleen viral titers remained at an approximate level of $10^{2.5}$ $TCID_{50}$/g from 2 d.p.i. until 5 d.p.i. (day 2: $10^{2.64}$ $TCID_{50}$/g, day 5: $10^{2.46}$ $TCID_{50}$/g) in the mice infected with 10^5 PFU of the AB14 (H5N1) strain isolate (Figure 3.3D). Interestingly, spleen viral titers were not detected for the two lower dose groups (10^3 PFU and 10^4 PFU).

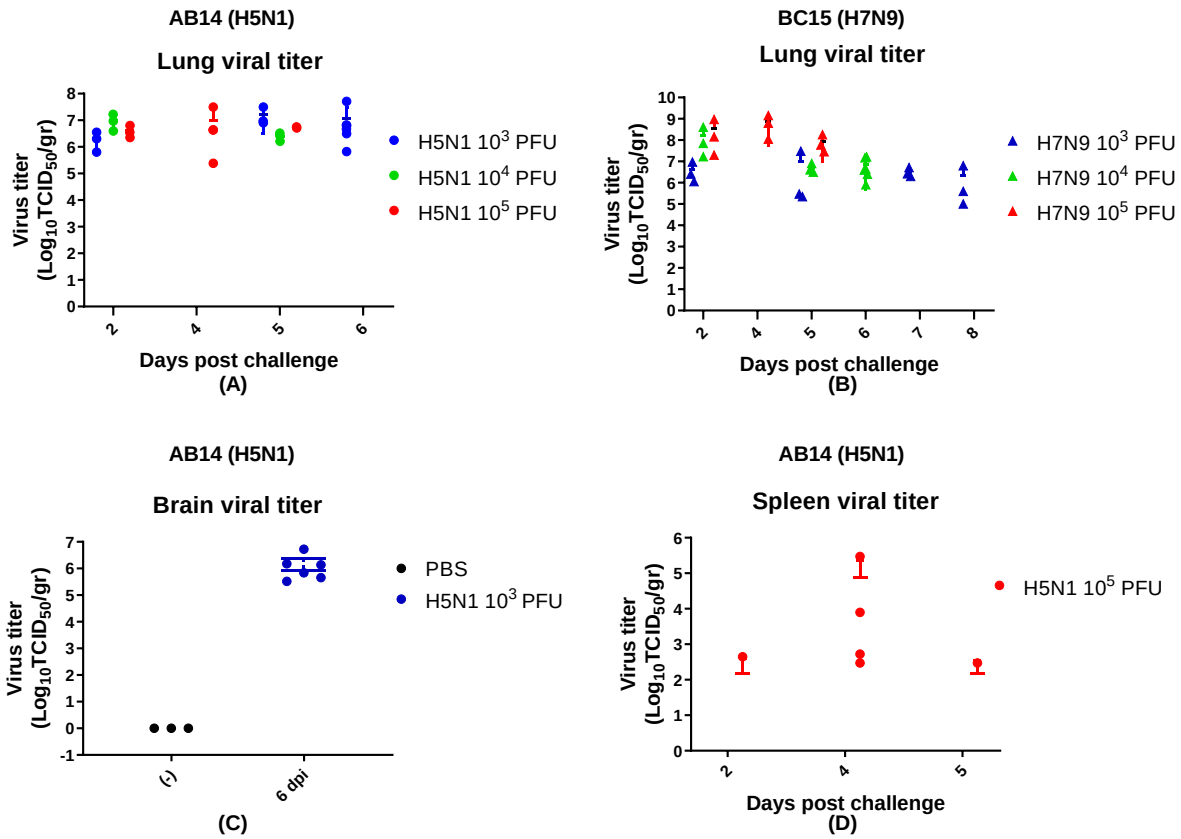

Figure 3.3. Viral titration of the mouse lung, spleen, and brain for the AB14 (H5N1) and BC15 (H7N9) strain isolates.
Mice were intranasally infected with 10^3 PFU, 10^4 PFU, or 10^5 PFU of AB14 (H5N1) or BC15 (H7N9). The lung, spleen, and brain tissues were collected and homogenized for virus titration by $TCID_{50}$ assay. Lung viral titration from (**A**) AB14 (H5N1) and (**B**) BC15 (H7N9) infection for all doses. For AB14 (H5N1), three mice per group were humanely euthanized on 2 d.p.i., four mice infected with 10^5 PFU were euthanized on 4 d.p.i., and two mice on 5 d.p.i. On 5 d.p.i., three mice in the 10^3 and 10^4 PFU group were humanely euthanized. The remaining six mice in the 10^3 PFU group were euthanized on 6 d.p.i. For BC15 (H7N9) three mice per group were humanely euthanized on 2 d.p.i., three mice infected with 10^5 PFU were euthanized on 4 d.p.i., and three mice per group were euthanized on 5 d.p.i. On 6 d.p.i., the remaining six mice in the 10^4 PFU group were humanely euthanized, and for the 10^3 PFU group three mice each on 7 and 8 d.p.i. were humanely euthanized. Brain viral titration from (**C**) AB14 infection (H5N1). Only six mice from the 10^3 PFU group were harvested for analysis. Spleen viral titration from (**D**) AB14 (H5N1) infection. All mice in all groups were harvested for analysis. Please note that BC15 (H7N9) was not detected in the spleen of mice infected by all three doses and brain of mice infected by the 10^3 PFU dose.

In BC15 (H7N9) viral infected lung, the 10^3 PFU group reached a titer of approximately $10^{6.5}$ $TCID_{50}$/g by 2 d.p.i., and remained at this titer throughout the duration of the trial. The 10^4 PFU group displayed a similar trend, with high titers present at 2 d.p.i. (10^8 $TCID_{50}$/g), which decreased by 5 and 6 d.p.i. ($10^{6.5}$ $TCID_{50}$/g). The 10^5 PFU group had the highest titer at 2 d.p.i. (10^8 $TCID_{50}$/g), which remained at this level throughout the duration of the trial (Figure 3.3B). The BC15 (H7N9) strain isolate was not detected in the spleen and brain of mice infected by all three doses by $TCID_{50}$ assay.

3.4.4 Cytokine and chemokine profiling in the mouse lung

To understand the pathogenesis and immune response to AB14 (H5N1) and BC15 (H7N9) viral infection, we assessed the innate immune receptor RIG-I, as well as the cytokine and chemokine gene expression in the lungs and brains of mice infected with the lowest dose (10^3 PFU) of both strain isolates by qRT-PCR. To start, we investigated a group of genes that encode interferons as well as the innate immune sensor RIG-I, a major pattern recognition receptor that recognizes influenza viral infection and activates the interferon response (Loo and Gale, 2011; Opitz et al., 2007). IFN-α and IFN-β are both type I interferons which play important roles in antiviral defense (Taniguchi and Takaoka, 2002). IFN-γ is a type II interferon that is the first cytokine produced in response to foreign invaders, and is an important activator of macrophages and natural killer (NK) cells. IFN-γ also has antiviral activity, and inhibits the proliferation of Th2

cytokines (IL-4, IL-5, and IL-6) (Tau and Rothman, 1999). In the AB14 (H5N1) infected lungs (Figure 3.4A), gene expression of RIG-I peaked on 2 d.p.i., which remained at these levels compared to the negative control. IFN-α gene expression was elevated on 2 d.p.i. IFN-β mRNA levels increased over 60-fold on 2 d.p.i., which remained at high levels on 5 and 7 d.p.i. The type I IFN gene transcription levels showed similar patterns in concordance with that of RIG-I. IFN-γ had the highest induction by 2 d.p.i., which remained at moderately elevated levels compared to the mock. The transcription of the gene encoding interferon-gamma-inducing protein 10 (IP-10), a cytokine produced in response to IFN-γ, was higher (over 2000-fold) on 2 d.p.i., and then remained at equivalent levels, consistent with the IFN-γ mRNA upregulation pattern. Next, we profiled the gene transcription of proinflammatory (TNFα, IL-6, IL-1β, and IL-18) and anti-inflammatory (IL-10) cytokines. TNFα is a proinflammatory cytokine produced in response to foreign invasion, and is often the main cytokine produced by macrophages following infection (Idriss and Naismith, 2000). IL-6 and IL-1β are the main contributors to severe lung inflammation in both humans and poultry infected by influenza virus (Saito et al., 2018). Both TNFα and IL-6 mRNA were markedly enhanced upon AB14 (H5N1) infection and remained at these levels. IL-1β mRNA was upregulated 7-fold on 2 d.p.i. IL-18 mRNA remained at mock levels upon infection. On the contrary, the mRNA level of the anti-inflammatory cytokine IL-10 was enhanced after infection.

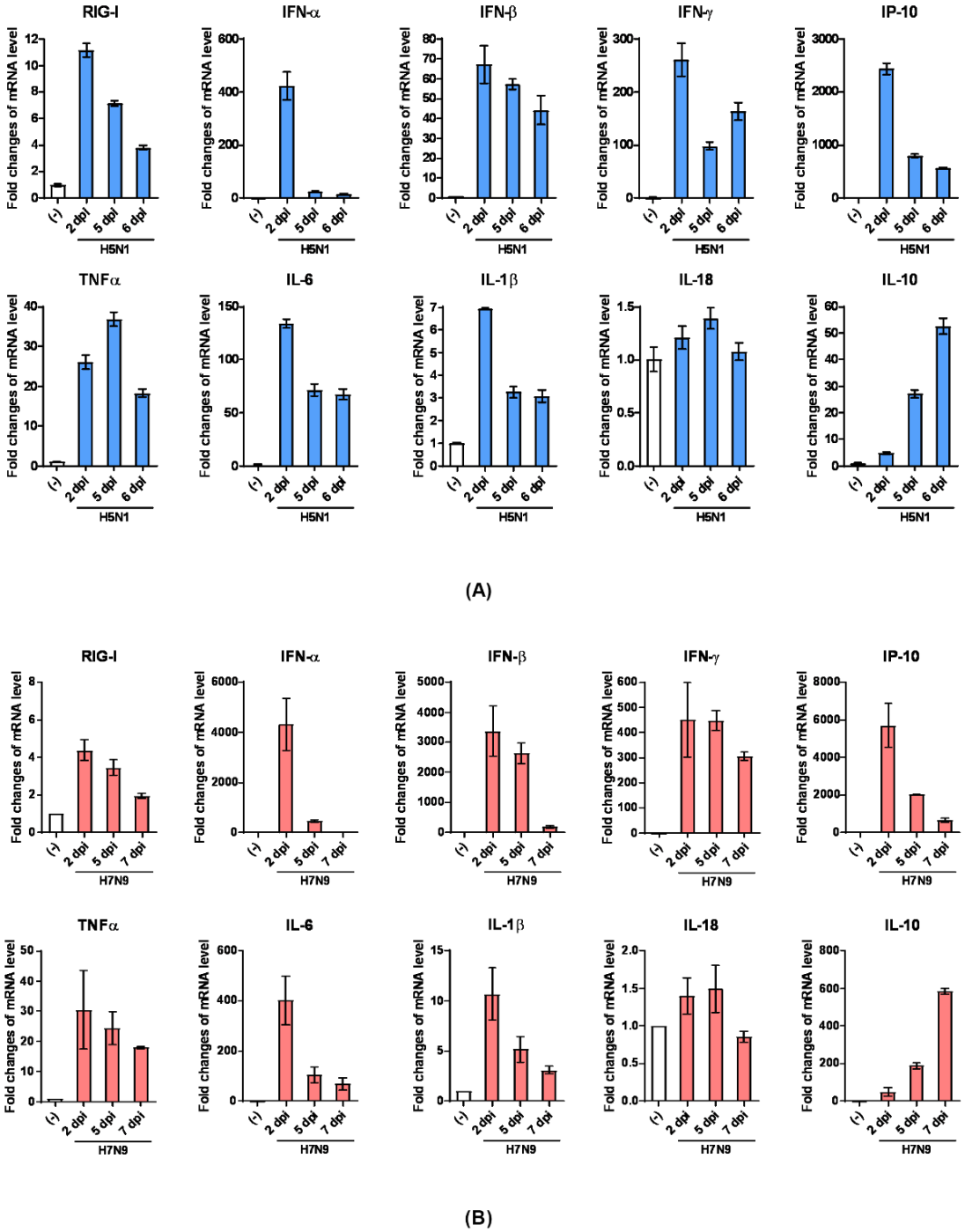

Figure 3.4. Innate immune receptor RIG-I, as well as cytokine and chemokine gene transcription levels in the lungs of mice infected with the AB14 (H5N1) and BC15 (H7N9) strain isolates.

Innate immune receptor as well as cytokine and chemokine mRNA levels of RIG-I, IFN-α, IFN-β, IFN-γ, IP-10, TNFα, IL-6, IL-1β, IL-18, and IL-10 from virus-infected lungs with (**A**) AB14 (H5N1) and (**B**) BC15 (H7N9) (*n* = 3 mice per virus group) were measured by qRT-PCR. Samples were harvested on the indicated d.p.i.; each sample was tested in triplicate.

In the lungs of BC15 (H7N9) infected mice, elevated mRNA levels of interferon genes (IFN-α, IFN-β, and IFN-γ), interferon responsive cytokine gene (IP-10), and proinflammatory cytokine genes (TNFα and IL-6) were obtained on 2 d.p.i. compared to the uninfected control (Figure 3.4B). IFN-α and IFN-β mRNA levels were similar to the negative control by 7 d.p.i., whereas mRNA levels of RIG-I, IFN-γ, and TNFα remained relatively unchanged throughout the duration of the trial. Similar to what we observed for AB14 (H5N1), the IL-18 gene transcript was not upregulated in response to viral infection, whereas the gene transcription of the anti-inflammatory cytokine IL-10 was highest on 7 d.p.i.

Besides cytokine and chemokine gene transcription analysis in the lungs of viral infected mice, we also analyzed select cytokine transcription levels in the brains of mice harvested at the endpoint. In the brains of mice infected with AB14 (H5N1), the transcription of IFN genes (IFN-α and IFN-γ) as well as proinflammatory cytokine genes (TNFα, IL-6, and IL-1β) was higher compared to the uninfected control (Figure 3.5A). Among all genes activated in the brain tissue upon infection, IFN-γ and TNFα were the most transcribed cytokines associated with HPAI AB14 (H5N1) infection. Similar to the cytokine regulation observed in the mouse lung, IL-18 transcripts did not change upon AB14 (H5N1) infection when compared to the uninfected control (Figure 3.5A). In contrast, the brains of mice infected with BC15 (H7N9) had slightly higher levels of IFN-α, IFN-γ, and IL-6 gene transcription, which was marginal compared to the degree of elevation observed in the AB14 (H5N1) viral infected brain. The transcripts of the other inflammatory cytokine genes, TNFα, IL-1β, and IL-18, were similar to the uninfected control (Figure 3.5B).

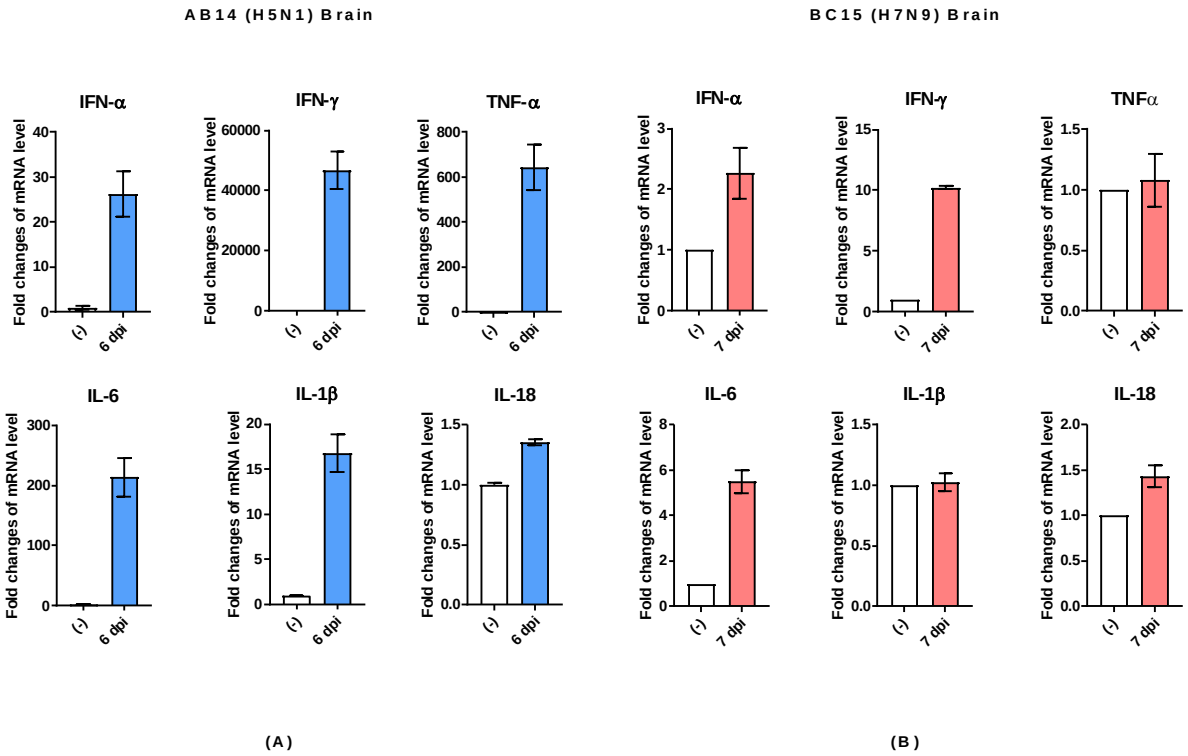

Figure 3.5. Cytokine gene transcription profile in the brains of mice infected with the AB14 (H5N1) and BC15 (H7N9) strain isolates.
Cytokine transcription levels of IFN-α, IFN-γ, TNFα, IL-6, IL-1β, and IL-18 from virus-infected brains with (**A**) AB14 (H5N1) and (**B**) BC15 (H7N9) (*n* = 3 mice per virus group). Samples were harvested on the indicated d.p.i; each sample was tested in triplicate.

3.5 DISCUSSION AND CONCLUSIONS

Following the reporting of the human HPAI (H5N1) and LPAI (H7N9) infection in Canada, the characterization of the causative strain isolates associated with these human infection cases, AB14 (H5N1) and BC15 (H7N9), was reported. *Pabbaraju et al*. analyzed the full genome of AB14 (H5N1) and assessed its molecular markers of pandemic risk (Pabbaraju et al., 2014b). *Skowronski et al*. conducted the serological and phylogenetic analysis of BC15 (H7N9), reporting that this virus belongs to the clade W2-C, which clusters with both the 2014–2015 H7N9 human isolates from the Jiangsu, Zhejiang, and Fujian Provinces of China as well as the 2014 chicken isolate from Jiangsu Province (Skowronski et al., 2016). Despite the analysis of these two Canadian isolates, the infectious and immunological properties as well as the histopathological correlation to disease remained elusive. In this study, we aimed to fill this knowledge gap, and to

provide insightful information on the pathogenesis of the AB14 (H5N1) and BC15 (H7N9) strain isolates in mice.

To ensure that the AB14 (H5N1) and BC15 (H7N9) strain isolates would induce disease in mice, we chose to infect them with three different doses (10^3 PFU, 10^4 PFU, and 10^5 PFU). We found that even at the lowest dose (10^3 PFU), both isolates were lethal to mice. AB14 (H5N1) caused all mice to reach a humane endpoint by 6 d.p.i., whereas BC15 (H7N9) infected mice survived one to two days longer than the mice infected with AB14 (H5N1). This observation is in contrast to the various seasonal or the 2009 pandemic influenza viruses (Groves et al., 2018; Rowe et al., 2010). *Groves et al*. reported that mice infected with 5 X 10^3 PFU of influenza A/England/195/2009 (H1N1) showed mild weight loss over 7 days, whereas mice infected with 10^3 PFU of influenza A/England/691/2010 (H3N2) did not show any signs of disease (Groves et al., 2018). In the study reported by *Rowe et al*., infection of BALB/c mice with 10^4 EID_{50} of the 2009 pandemic virus did not cause any death when using 20% total body weight loss as an endpoint (Rowe et al., 2010). Furthermore, we could detect the AB14 (H5N1) strain in multiple organs, including the lung, spleen, and brain, with consistently high titers in the lung and brain tissues. However, we could only detect the BC15 (H7N9) strain in the mouse lung, with no detectable virus in the spleen and brain by $TCID_{50}$ assay. These results are in agreement with the previous reports that while H5N1 virus has the ability to replicate systemically and spread efficiently to non-respiratory tissues, H7N9 virus replicates well in the upper respiratory tract (URT), covering the nasal passages, nasopharynx-associated lymphoid tissues (Meliopoulos et al., 2014), human bronchus, and the lungs (Chan et al., 2013b). Research has shown that avian IAV strains need to acquire adaptation mutations in order to be infectious in mammals, with one such adaptation being in the polymerase, PB2. This adaptation resides at the amino acid at position 627 of PB2, and determines the viral replication efficiency in different hosts. It is well characterized that avian strains carry a glutamic acid (E) at this position referred to as 627E, whereas mammalian strains carry a lysine (K), namely, 627K (Hatta et al., 2001a). The BC15 (H7N9) strain isolate consists of PB2 encoding 627K, which may explain its ability to replicate well in the human respiratory tract. In contrast, the AB14 (H5N1) strain isolate consists of PB2 possessing the avian signature, namely, 627E. However, our data have shown that while AB14 (H5N1) replicates efficiently without any adaptation in mice, it replicates less efficiently in tissue culture (Lu and Zhou unpublished data). In addition to the PB2 protein, HA protein is also a key viral factor that determines whether an

avian virus can replicate well in mammals. It is reported that AB14 (H5N1) HA contains two novel mutations, R189K and G221R, which are located in the immediate receptor-binding pocket (Pabbaraju et al., 2014b). It was speculated that these mutations arose in an avian H5N1-infected patient, which was also associated with severe illness and spread of the virus to the brain. We observed that the AB14 (H5N1) strain isolate replicated efficiently in the mouse brain, which will provide a model for further investigation of the functional role of G221R in avian influenza HA contributing to viral pathogenesis in mammals.

Research has shown that the dysregulation of the innate immune responses that results in an unusual proinflammatory cytokine production often contributes to the pathogenicity of both the HPAI H5N1 virus and the 1918 Spanish Flu pandemic virus (Cilloniz et al., 2009; Perrone et al., 2008a). Our data show that although at different magnitudes, infection by both AB14 (H5N1) and BC15 (H7N9) induced higher levels of interferon gene and proinflammatory cytokine gene expression in the lungs. Subsequently, both strain isolates, AB14 (H5N1) and BC15 (H7N9) induced increased gene expression of the anti-inflammatory cytokine IL-10. There has been evidence showing IL-10 to inhibit several proinflammatory cytokines and chemokines (Couper et al., 2008), and that it may therefore actually hinder clearance of the virus (Frensing et al., 2016). When comparing the transcription levels of various cytokines, it was found that most cytokine genes had levels in the tens- to hundreds-fold. Interestingly, the two inflammatory cytokines IL-1β and IL-18, whose maturation is regulated by inflammasome activity (Kaplanski, 2018), were not enhanced at the mRNA level; IL-1β mRNA was only moderately enhanced, whereas IL-18 mRNA was not enhanced at all. This finding thus warrants further investigation into the mature IL-1β and IL-18 protein levels, in order to understand their roles in mediating avian IAV-induced pathogenesis. Interestingly, it has been reported that in comparison to other H5N1 strain isolates that are associated with severe human respiratory disease, H7N9 strains isolated from human infections from 2013 to 2015 are poor proinflammatory cytokine and chemokines inducers in mammalian models (Belser et al., 2016). However, our results showed that BC15 (H7N9) is a potent inducer of proinflammatory cytokines in the mouse lung. This finding is consistent with the study of human patients infected with H7N9 virus, where elevated cytokine and chemokine production was observed (Chi et al., 2013). With regard to the cytokine gene expression in the mouse brain, we found that AB14 (H5N1) dramatically enhanced IFN-α, IFN-γ, TNFα, and IL-6 transcription in the brains of mice that reached a humane endpoint. This finding possibly indicates

cytokine hyperinduction in the brains of mice infected with AB14 (H5N1), which may contribute to the pathogenesis. In contrast, only moderate enhancement of both IFN-γ and IL-6 transcripts was observed in the brains of mice infected with BC15 (H7N9). This finding reflects the viral titers found in the infected brains of the mice, such that while mice infected with AB14 (H5N1) had high titers, mice infected with BC15 (H7N9) had no detectable virus in the brain.

Taken together, we showed that the AB14 (H5N1) strain isolate replicates efficiently without prior adaptation not only in the mouse lung, but also in other non-respiratory tissues such as the spleen and brain. The high viral load and hypercytokinemia in multiple organs contributed to the severity of the disease associated with AB14 (H5N1) infection. Similarly, the BC15 (H7N9) strain is also highly pathogenic in mice, but its replication seemed to be more constrained to the respiratory tract. The severity of both AB14 (H5N1) and BC15 (H7N9) disease as well as the significant lung pathology observed may be a result of the unusual enhancement of proinflammatory cytokines including TNFα, IP-10, and IL-6. Our findings not only contribute to a better understanding of the pathogenesis of the strain isolates associated with Canadian human cases of avian H5N1 and H7N9 virus infection, but also provide animal models for testing vaccine and antiviral candidates for viruses that are of significant public health concerns.

3.6 ACKNOWLEDGEMENTS

We are thankful to Yan Li from the National Microbiology Laboratory, PHAC for sharing the AB14 (H5N1) and BC15 (H7N9) strain isolates with us. We are grateful to the animal care staff at VIDO-InterVac for the enormous support in housing, monitoring, infecting, and processing the mice. We also appreciate Tracey Thue in assisting the coordination with both the Canadian Food Inspection Agency (CFIA) and PHAC for the Biosafety regulation of the Containment Level 3 facility. This manuscript was approved for publication by the director of VIDO-InterVac and was assigned the manuscript serial number 857.

TRANSITION BETWEEN CHAPTER 3 AND CHAPTER 4

In the previous chapter we described the successful development of a mouse animal model of A/British Columbia/01/2015 (H7N9) [BC15 (H7N9)], by evaluating the susceptibility, replication abilities, pathology, and immune responses mounted against viral infection. In this next chapter, a recombinant mutant H7N9 virus, BC15-HA/QTV/NA (PR8) was developed and characterized for its growth properties, stability, and virulence in mice as a potential replication-defective virus vaccine candidate.

CHAPTER 4 REVERSE-GENETICS GENERATED ELASTASE-DEPENDENT BC15 (H7N9) INFLUENZA VIRUS IS REPLICATION-DEFECTIVE IN MICE

The data presented in this chapter and chapter 5 will be submitted to Vaccines

4.1 ABSTRACT

Avian influenza H7N9 viruses continue to pose a great threat to public health, evident by their high morbidity and mortality rates. Although H7N9 was first isolated in humans in China in 2013, to date there is no commercial vaccine available against this particular strain. Previous studies have demonstrated that when the hemagglutinin (HA) cleavage site was mutated from a trypsin-sensitive to elastase-sensitive motif, influenza virus became replication-defective *in vivo*, however, this concept has only been presented in mouse-adapted influenza A viruses (IAV) and swine influenza viruses (SIV) (Masic et al., 2008; Stech et al., 2005). In this study, we report the development of a recombinant mutant H7N9 virus, BC15-HA/QTV/NA (PR8) derived from the human isolate A/British Columbia/01/2015 (H7N9) [BC15 (H7N9)] through reverse genetics. The HA cleavage site underwent site-directed mutagenesis to generate a mutant HA plasmid, pHW-BC15/HA-QTV, that possesses three mutations: lysine to glutamine at amino acid (aa) 337 (Lys-Gln), glycine to threonine at aa 338 (Gly-Thr), and arginine to valine at aa 339 (Arg-Val). This mutant HA plasmid was then incorporated into the generation of the recombinant mutant BC15-HA/QTV/NA (PR8) virus. Our results show this virus to rely completely on elastase for its replication, to possess similar growth properties compared to the wild-type virus, and to be genetic stable *in vitro* and replication-defective in mice. Therefore, these results prove the strong potential of this recombinant mutant BC15-HA/QTV/NA (PR8) virus to act as a replication-defective virus vaccine candidate against H7N9 viruses.

4.2 INTRODUCTION

Avian influenza H7N9 viruses are members of the *Orthomyxoviridae* family (Bouvier and Palese, 2011), capable of causing severe respiratory disease in humans, with some of the main symptoms including fever, cough, weakness, muscle soreness, shortness of breath, chest distress, nausea, chills, and pneumonia (Su et al., 2017). Unfortunately, more serious symptoms can occur such as high hospitalization rates or respiratory failure (Zeng et al., 2015). These serious symptoms have led the H7N9 virus to have high morbidity and mortality rates, with 1,568 human cases and 616 deaths as of March 4, 2020 (FAO, 2020). Although cases of H7N9 have been mainly constrained to China, there have been reports in other countries such as Canada (Gao et al., 2013; Skowronski et al., 2016; Zhang et al., 2017). These findings, along with the mutagenic properties influenza retains to escape the immune system through *antigenic shift* and *antigenic drift*, highlight the risk H7N9 poses to public health (Bouvier and Palese, 2011).

Influenza A viruses (IAV) are composed of segmented, negative-sense, single-stranded ribonucleic acid (RNA) genomes (Bouvier and Palese, 2011). One of the main determinants for whether IAV can establish infection and replicate within the host is the binding of the virus to the host cell through the interaction of hemagglutinin (HA) and sialic acid receptors, followed by receptor-mediated endocytosis and fusion of the virus to the endosome. The HA of IAV has three important roles: it enables IAV to bind to the host cell, induces fusion between the viral envelope and endosomal membranes by allowing IAV to infiltrate into the cytoplasm, and is the primary antigen the immune system produces neutralizing antibodies against (Masic et al., 2008). The HA of IAV is initially present in its precursor form, HA0, which must be cleaved into HA1 and HA2 by a host protease. This cleavage is necessary for IAV to become infectious, and can play a role in the pathogenicity and tissue tropism of the influenza virus (Böttcher et al., 2006; Masic et al., 2008; Skehel and Wiley, 2000).

Despite strong efforts to develop a vaccine protective against H7N9, to date, there is no commercial vaccine available for use. Out of the two main types of vaccines available in Canada, inactivated influenza vaccines (IIV) and live attenuated influenza vaccines (LAIV), research has shown LAIVs to have many advantages over IIVs (PHAC, 2017a). Some of these advantages include enhanced protection rates, longer-lasting immune responses, and the ability to mimic a natural infection by stimulating the mucosal immune system. LAIVs do not necessarily depend

on the egg-based system, are easier to administer due to their needle-free properties, are cheaper to manufacture, may only need a single dose, and show a good safety profile (Isakova-Sivak and Rudenko, 2017; Lorenzo and Fenton, 2013; Sridhar et al., 2015). Moreover, one study showed that a single dose of a Len17-H7N9 LAIV stimulated an immune response sufficient to protect against infection and could, therefore, be stockpiled in the event of a pandemic (Isakova-Sivak and Rudenko, 2017). However, albeit the surplus advantages LAIV possess, one disadvantage towards their use is the possibility of virulence reversion, limiting their widespread use (Watanabe et al., 2001). Replication-defective virus vaccines are vaccines composed of viruses that lack one or more vital components to either its replication, synthesis, or assembly of the virion. These viruses, therefore, cannot replicate *in vivo* but can be propagated *in vitro* when provided the appropriate component. These vaccines possess the same advantages both IIVs and LAIVs possess, making them strong IAV vaccine candidates. These advantages include the high safety and efficacy rates, as well as the ability to induce $CD4^+$ T cells, $CD8^+$ T cells, and the humoral immune responses (Dudek and Knipe, 2006). To date, although experimental vaccines are being tested for the H7N9 virus, there is a gap in vaccines against a new Canadian strain isolate from 2015: A/British Columbia/01/2015 (H7N9) [BC15 (H7N9)].

Previous studies have demonstrated the lack of replication of influenza virus *in vivo* when the HA cleavage site was mutated from a trypsin-sensitive motif to an elastase-sensitive motif (Masic et al., 2008; Stech et al., 2005). Unfortunately, there is a gap in knowledge about whether this concept is applicable for human LPAI H7N9 viruses because this concept has only been tested in mouse-adapted IAV or swine influenza viruses (SIV) (Masic et al., 2008; Stech et al., 2005). Therefore, in this chapter, we report the generation of a recombinant mutant H7N9 virus, BC15-HA/QTV/NA (PR8) derived from BC15 (H7N9). This recombinant mutant BC15-HA/QTV/NA (PR8) virus contains mutations at the HA cleavage site to change a trypsin-sensitive motif to an elastase-sensitive motif, specifically, the amino acids (aa) lysine-glycine-arginine (Lys-Gly-Arg) at positions 337, 338, and 339, respectively, were mutated to glutamine-threonine-valine (Gln-Thr-Val). Introduction of these mutations resulted in the recombinant mutant BC15-HA/QTV/NA (PR8) virus being strictly dependent on elastase for its replication, possessed viral kinetics equal to its wild-type counterpart, was genetically stable *in vitro* and was non-virulent and replication-defective in mice. Therefore, these results suggest that this

recombinant mutant BC15-HA/QTV/NA (PR8) virus has high potential to act as a replication-defective virus vaccine candidate against H7N9 virus.

4.3 MATERIALS AND METHODS

4.3.1 Cells and viruses

Madin-Darby canine kidney (MDCK) (ATCC, #CRL-2936) cells and human embryonic kidney (HEK-293T) cells were provided with Minimal Essential Medium (MEM) (Sigma-Aldrich, M4655; St. Louis, MO, USA) and Dulbecco's Modified Eagle Medium (DMEM) (Sigma-Aldrich, D5796; St. Louis, Mo, USA), respectively, supplemented with 10% fetal bovine serum (FBS) (Thermo Fisher; 16000-044) in a humidified 5% CO_2 incubator at 37°C. The A/British Columbia/01/2015 (H7N9) [BC15 (H7N9)] strain isolate was collected from Dr. Yan Li who works at the National Microbiology Laboratory, Public Health Agency of Canada (PHAC). This strain isolate was preserved in Biosafety Containment Level 3 at the Vaccine International Disease Organization, International Vaccine Centre (VIDO-InterVac) at the University of Saskatchewan, Canada. This strain isolate was maintained by following the guidelines implemented from both the Public Health Agency of Canada (PHAC) and the Canadian Food Inspection Agency (CFIA).

4.3.2 Plasmids and primers

Before the mutant HA plasmid could be designed, the wild-type plasmids pHW-BC15-HA and pHW-BC15-NA were developed. To this end, viral RNA from BC15 (H7N9) was isolated from the culture medium of the virus-infected cells using the TRIzol method (Invitrogen). This viral RNA underwent reverse transcription to generate cDNA through the use of the universal Uni12 primer (5' – AGC AAA AGC AGG – 3') (Hoffmann et al., 2001) and the Superscript II Transcriptase (Invitrogen). Once the cDNA was amplified, both HA and NA were cloned into pHW2000 as previously described (Hoffmann et al., 2000), to result in the plasmids pHW-BC15-HA and pHW-BC15-NA, respectively.

For the development of the mutant plasmid, pHW-BC15-HA underwent site-directed mutagenesis to generate an elastase-sensitive motif at the HA cleavage site. Site-directed mutagenesis entailed using PCR to create the mutant plasmid pHW-BC15/HA-QTV, containing three mutations. For this mutant plasmid, lysine, glycine, and arginine (Lys-Gly-Arg) were mutated to glutamine, threonine, and valine (Gln-Thr-Val) at aa positions 337, 338, and 339, respectively. The primers used were 5' – ACA GAC TGT TGG ACT ATT TGG TGC TAT AGC GGG TTT C – 3' and 5' – TCC AAC AGT CTG TGG AAT CTC AGG AAC ATT CTT

CAT C – 3'. The mutant plasmid pHW-BC15/HA-QTV was confirmed by sequencing to ensure only the desired mutations were introduced by PCR.

4.3.3 Generation of viruses by reverse genetics

The recombinant influenza viruses used in this study were generated through the use of the eight-plasmid reverse genetics system, as previously described (Hoffmann et al., 2000). The recombinant H7N9 influenza virus rg-(6+2)-BC15-HA/NA [BC15-HA/NA (PR8)] contains the HA and NA of A/British Columbia/01/2015 [BC15 (H7N9)] and the six internal genes of A/Puerto Rico/8 (H1N1) [PR8 (H1N1)]. The recombinant mutant H7N9 influenza virus rg-(6+2)-BC15/HA-QTV/NA [BC15-HA/QTV/NA (PR8)] contains the mutant HA, HA/QTV, the NA of BC15 (H7N9) and the six internal proteins from PR8 (H1N1). All segments were first cloned into the vector pHW2000 as previously described (Hoffmann et al., 2000). These segments were then used to recover the recombinant BC15-HA/NA (PR8) and recombinant mutant BC15-HA/QTV/NA (PR8) viruses.

Briefly, MDCK cells (2.2 X 10^5 cells) and 293T cells (3.0 X 10^5 cells) were cultured together in a humidified 5% CO_2 incubator at 37°C in 35-mm dishes with DMEM and 10% FBS. 24 hours later and one hour before transfection, the DMEM was removed and replaced with fresh Opti-MEM (Invitrogen). Transfection was performed using the TransIT-LT1 Transfection Reagent (Mirus, MIR 2306; Madison, WI, USA). Six hours post-infection, the transfection mixture was replaced with fresh Opti-MEM. Twenty-four hours after transfection, an additional 1 ml of Opti-MEM containing 0.2% bovine serum albumin (BSA) (Sigma-Aldrich; A7030) and either 2 μg/ml L-[(toluene-4-sulphonamido)-2-phenyl] ethyl chloromethyl ketone (TPCK)-trypsin (recombinant virus) or 1 μg/ml human neutrophil elastase (recombinant mutant virus) (Sigma-Aldrich; E8140) was added. Supernatants were collected 72 h post-transfection (h.p.i.) when cytopathic effects (CPE) were prominent, followed by a passage in MDCK cells to obtain higher titers of the viruses. For this passage, MDCK cells were seeded (4.4 X 10^5 cells) in 35-mm dishes. The next day, the cells were washed with MEM and the harvested supernatant was used to infect MDCK cells (300 μl). After 1 h viral adsorption, the cells were washed with MEM, and then 2 ml of MEM containing 0.2% BSA and either 2 μg/ml TPCK-trypsin (recombinant virus) or 0.5 μg/ml human neutrophil elastase (recombinant mutant virus) was

added. The supernatants were harvested when CPE was present, at either 48 or 72 h.p.i with the titers determined by plaque assay.

4.3.4 Western blot analysis

Cell lysates were separated by sodium dodecyl sulfate-polyacrylamide gel electrophoresis (SDS-PAGE) and transferred to nitrocellulose membranes (Bio-Rad, 0.45 μm). These membranes were blocked for 1 h with 5% skim milk dissolved in TBST (0.1 M Tris, 0.17 M NaCl, 1% Tween 20) and incubated at 4°C overnight with either rabbit anti-NP or rabbit anti-M1 antibodies raised in our lab. The next day, the membranes were incubated with donkey anti-rabbit IgG (IR Dye 680RD, Li-Cor, Lincoln, NE, USA) at room temperature for 1 h, and scanned on an Odyssey infrared imager (Li-Cor Biosciences).

4.3.5 Plaque assay

To determine the viral titers, MDCK cells (5 X 10^5 cells) were plated on a 6-well plate in MEM and 10% FBS. Twenty-four hours later, the cells were infected with the virus at dilutions ranging from 10^{-1} to 10^{-8}. After 1 h of viral adsorption, the cells were washed with MEM, after which an agar overlay was added containing 0.9% agarose, 2X MEM, 0.2% BSA, and either 1 μg/ml TPCK-trypsin (recombinant virus) or 0.5 μg/ml human neutrophil elastase (recombinant mutant virus). The cells were then incubated at 37°C, 5% CO_2 for 48 h. At 48 h, the agar overlay was removed and cells stained with Coomassie Blue Stain. Plaques were counted and the titer was determined as plaque-forming unit (PFU) per ml.

4.3.6 Growth curve

To determine the growth curve, MDCK cells (5 X 10^5 cells) were seeded in 2 ml of MEM containing 10% FBS in a 6-well plate. The next day, the cells were washed with MEM and infected with the virus at an m.o.i. of 0.001. After 1 h viral adsorption, the cells were washed with MEM, and then 2.5 ml of growth medium was added to each well containing MEM, 0.2% BSA, and either 1 μg/ml TPCK-trypsin (recombinant virus) or 0.5 μg/ml human neutrophil elastase (recombinant mutant virus). Aliquots were harvested at 12, 24, 36, 48, 60, and 72 h.p.i. and subjected to plaque assay to determine the viral titer.

4.3.7 Genetic stability of the elastase mutations

To analyze the genetic stability of the elastase mutations, the recombinant mutant BC15-HA/QTV/NA (PR8) virus was passaged five times on MDCK cells at an m.o.i. of 0.001 in the presence of either 1 µg/ml TPCK-trypsin or 0.5 µg/ml human neutrophil elastase. The supernatant of the fifth passage was subjected to plaque assay in either the presence of elastase or TPCK-trypsin. Sequencing of the elastase mutations found on the recombinant mutant BC15-HA/QTV/NA (PR8) virus was also performed to ensure no undesired mutations were introduced.

4.3.8 Virus purification

To generate purified viral stocks of recombinant BC15-HA/NA (PR8) and recombinant mutant BC15-HA/QTV/NA (PR8) viruses, MDCK cells (2.5×10^6 cells) were seeded in 10-cm dishes containing MEM and 10% FBS. The following day, the cells were infected with the respective viruses at an m.o.i. of 0.001. After 1 h of viral adsorption, the cells were washed with MEM and growth medium was then added containing MEM, 0.2% BSA and either 1 µg/ml TPCK-trypsin (recombinant virus) or 0.5 µg/ml human neutrophil elastase (recombinant mutant virus). The cells were incubated at 37°C, 5% CO_2 for 48 h or until CPE was observed. The supernatant was harvested and clarified by centrifugation at 1,621 g for 15 min at 4°C and stored at -80°C until further purification.

The harvested supernatant was subjected to virus purification on a sucrose gradient to remove all residual proteases. First, the supernatant was centrifuged at 132 g for 10 min at 4°C to remove any cellular debris. This clarified supernatant underwent ultracentrifugation to pellet the virus at 82,705 g for 2.5 h at 4°C. The pellet was resuspended in TSE buffer (20 mM Tris pH 7.8, 150 mM NaCl pH 7.8, 2mM EDTA pH 7.8) and left overnight at 4°C to soften the pellet. The next day, pellets were resuspended and layered on a sucrose overlay containing the following layers from bottom to top: 60% sucrose in TSE, 30% sucrose in TSE, and the pooled pellets. The overlay underwent ultracentrifugation at 77,175 g for 2.5 h at 4°C. The virus was harvested from the opalescent band between the 60% and 30% sucrose, put into a new tube, and TSE buffer was added to dilute the sucrose. This underwent ultracentrifugation at 77,175 g for 2 h at 4°C. The pellet was resuspended in 1 ml TSE buffer, left overnight at 4°C, and then aliquoted into 1.5 ml microcentrifuge tubes and stored at -80°C. Viral titers were determined by plaque assay.

4.3.9 Ethics statement

Before proceeding with the animal procedures, approval was required from the University Animal Care Committee (UACC) and Animal Research Ethics Board (AREB) of the University of Saskatchewan. This approval was given on 12 April 2019 (Animal Use Protocol #20190041), under the guidelines given by the Canadian Council on Animal Care (CCAC).

4.3.10 Mouse experiments

For this trial, 36 six-week-old male and female BALB/c mice (18 males and 18 females) (Charles River Laboratories, Saint-Constant, QC, Canada) were randomly divided into three groups with 12 mice in each group (six males and six females). These groups were housed in separate cages and allowed to acclimatize for seven days in Biosafety Containment Level 2. At seven weeks of age, the mice were intranasally inoculated with 50 µl of either MEM or the following recombinant viruses at 1 X 10^3 PFU: BC15-HA/NA (PR8) or BC15-HA/QTV/NA (PR8) (Table 4.1). The mice were monitored daily for body weight and survival rate. On day 3 post-infection (d.p.i.), four mice from each group (two males and two females) were humanely euthanized and their lungs collected for viral titration. The rest of the mice were humanely euthanized when they dropped below 20% of their initial body weight. All animal experiments took place at VIDO-InterVac, University of Saskatchewan following the regulations stipulated by the University of Saskatchewan and the CCAC.

4.3.11 Virus isolation and titration

Upon harvest of the lung tissue, it was immediately placed into 1 ml of MEM supplemented with 1X Penicillin-Streptomycin (100X) (Gibco, Thermo Fisher, ON, Canada). Lung tissue was homogenized using the TissueLyser II (Qiagen, Hilden, Germany) at 25 Hz for 5 min, followed by centrifugation at 5,000 g for 10 min at 4°C. The supernatant containing the homogenized tissue was collected and placed in labelled 1.5 ml screw-cap tubes and stored at -80°C until the plaque assay was performed.

4.4 RESULTS

4.4.1 The production of the mutant plasmid and recombinant mutant BC15-HA/QTV/NA (PR8) virus as a vaccine candidate against BC15 (H7N9)

To generate the recombinant mutant H7N9 virus, BC15-HA/QTV/NA (PR8) which contains the mutations QTV in the HA gene, we exchanged several nucleotides in the HA cleavage site corresponding to positions 1075 to 1086 from AAG GGA AGA GGC to CAG ACT GTT GGA (Figure 4.1), respectively. This exchange resulted in the replacement of amino acid (aa) Lys (L) with Gln (Q) at position 337, Gly (G) with Thr (T) at position 338, and Arg (R) with Val (V) at position 339.

The rationale for mutating these three aa stems from a previous finding where the introduction of a valine into the HA cleavage site resulted in cleavage by leukocyte elastase, and sometimes by porcine pancreatic elastase, rather than by the normal protease trypsin (Masic et al., 2008). According to a previous study in swine, mutagenesis of one aa, Arg (R) to Val (V) at the HA cleavage site should be sufficient to rescue the influenza virus (Masic et al., 2008). However, when only one aa mutation was introduced in the HA of BC15 (H7N9) [Arg (R) to Val (V) at position 339], the recombinant mutant H7N9 virus could not be successfully rescued in the presence of either human neutrophil elastase or porcine pancreatic elastase (data not shown). However, since we were also working on several swine mutant viruses in our laboratory that contained successful elastase mutations (A/swine/Alberta/SD0191/2016 [SD191 (H1N2)]) and (A/swine/Saskatchewan/SD0069/2015 [SD69 (H3N2)]) (Landreth et al. unpublished data), this led us to compare the sequences surrounding the HA cleavage site of the SD191 (H1N2) and SD69 (H3N2) to that of BC15 (H7N9). After comparison, we hypothesized that if we extended our mutagenesis upstream of the HA cleavage site in BC15 (H7N9) to match that of the SD191 (H1N2) and SD69 (H3N2) elastase mutant viruses, we could potentially rescue the recombinant mutant virus (Figure 4.2). This extended mutagenesis led to the successful rescue of both the recombinant mutant virus BC15-HA/QTV/NA (PR8) and recombinant mutant virus BC15-HA/QSV/NA (PR8) (Figure 4.3). The recombinant mutant virus BC15-HA/QSV/NA (PR8) was generated in the same manner as the recombinant mutant virus BC15-HA/QTV/NA (PR8), with the only difference being the aa serine (S) at position 338 instead of threonine (T) (Figure 4.2). Both recombinant mutant H7N9 viruses were successfully rescued in the presence of human neutrophil elastase 72 h after transfection, and could not be rescued in the presence of porcine

pancreatic elastase or trypsin. However, the recombinant mutant virus BC15-HA/QSV/NA (PR8) did not grow to as high a titer (5.57 X 10^6 PFU/ml) as the recombinant mutant virus BC15-HA/QTV/NA (PR8) (1.03 X 10^7 PFU/ml). Thus, the recombinant mutant virus BC15-HA/QTV/NA (PR8) was chosen for future studies. A recombinant wild-type virus, identified as BC15-HA/NA (PR8) was also successfully generated by co-transfection (Figure 4.4) 48 h post-transfection, and could only be rescued in the presence of trypsin. The genotype of the recombinant mutant virus BC15-HA/QTV/NA (PR8) was characterized as well as confirmed by DNA sequencing of the HA gene through RNA extraction followed by RT-PCR (data not shown).

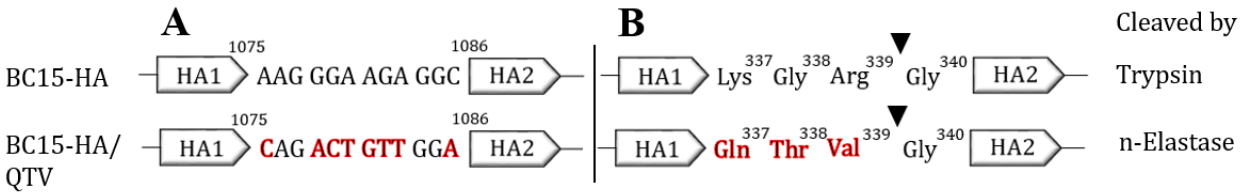

Figure 4.1. Schematic outline of the mutations introduced into the HA cleavage site of BC15 (H7N9).
(**A**) Nucleotide sequences from HA positions 1075 to 1086 and **(B)** Amino acid sequences from HA positions 337 to 340 of BC15-HA (wild-type) and BC15-HA/QTV (mutant). Nucleotide sequences (A) and amino acids (B) in red correspond to the mutations that were introduced. n-Elastase corresponds to the human neutrophil elastase protease.

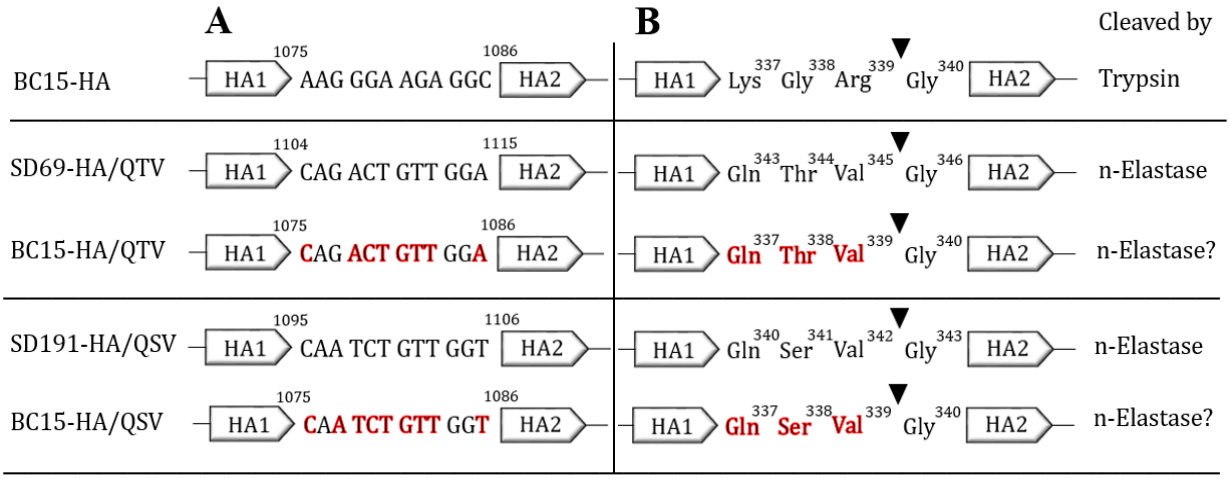

Figure 4.2. Schematic outline displaying the rationale for the mutations introduced into the HA cleavage site of BC15 (H7N9).
(**A**) Nucleotide sequences from HA positions 1075 to 1086 (BC15-HA), 1104 to 1115 (SD69-HA/QTV), 1075 to 1086 (BC15-HA/QTV), 1095 to 1106 (SD191-HA/QSV), and 1075 to 1086 (BC15-HA/QSV). (**B**) Amino acids from HA positions 337 to 340 (BC15-HA), 343 to 346

(SD69-HA/QTV), 337 to 340 (BC15-HA/QTV), 340 to 343 (SD191/HA-QSV), and 337 to 340 (BC15-HA/QSV). Nucleotide sequences (A) and amino acids (B) in red correspond to the mutations that were introduced. n-Elastase corresponds to the human neutrophil elastase protease.

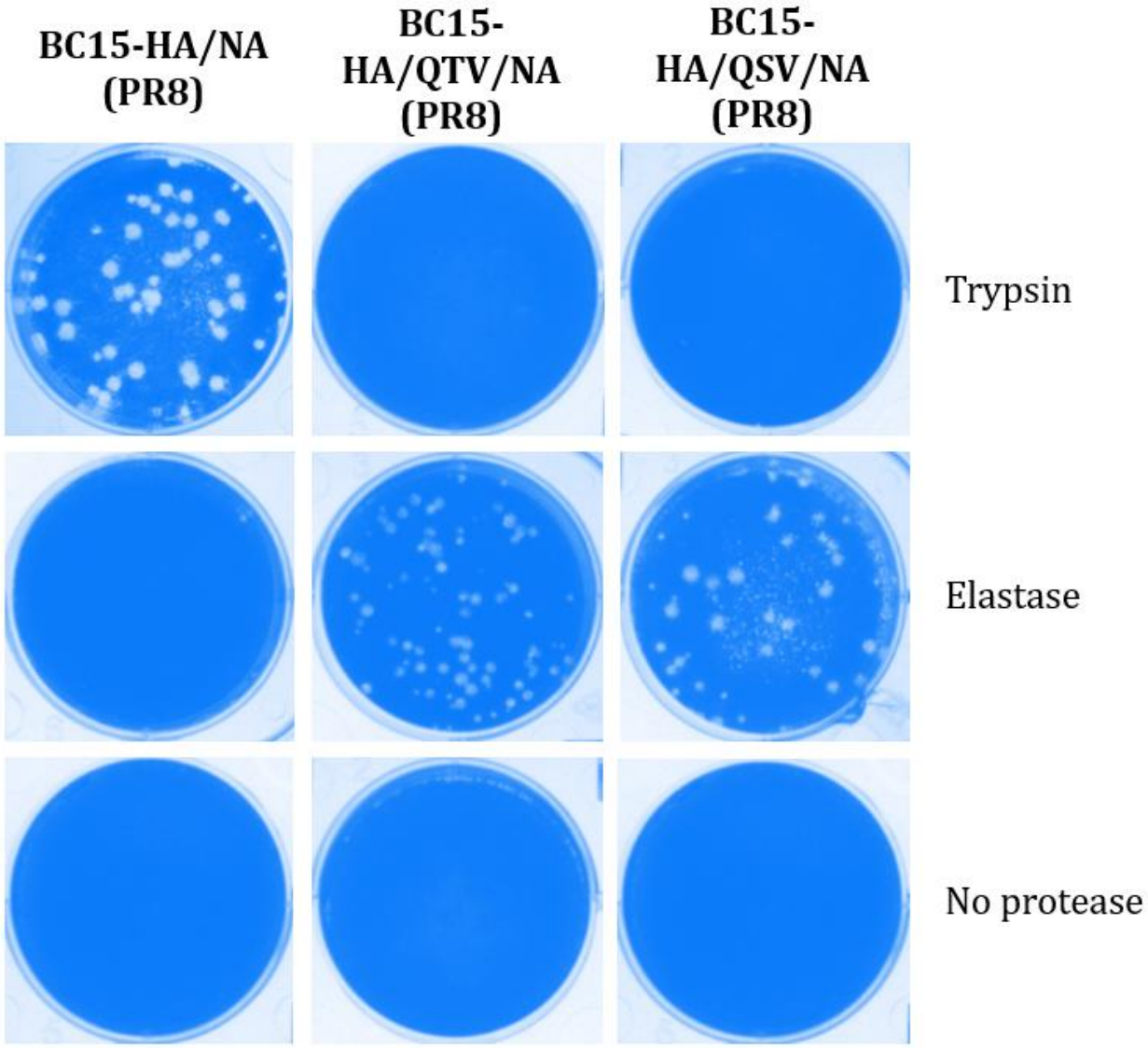

Figure 4.3. Plaque assay illustrating the successful rescue of recombinant BC15-HA/NA (PR8) and recombinant mutant BC15-HA/QTV/NA (PR8) and BC15-HA/QSV/NA (PR8) viruses.

4.4.2 The recombinant mutant BC15-HA/QTV/NA (PR8) virus is strictly dependent on elastase for its replication *in vitro*

To determine the elastase dependency of the recombinant mutant virus BC15-HA/QTV/NA (PR8) *in vitro*, we performed plaque assay and Western blotting. The recombinant

mutant virus, BC15-HA/QTV/NA (PR8), as well as the recombinant virus BC15-HA/NA (PR8) were assayed in the presence of trypsin, human neutrophil elastase, or no protease (Figure 4.4). The recombinant virus BC15-HA/NA (PR8) resulted in the formation of plaques in the presence of trypsin comparable to the plaques formed by the recombinant mutant virus BC15-HA/QTV/NA (PR8) in the presence of elastase (Figure 4.4A). These plaques were clear and large. The recombinant mutant virus BC15-HA/QTV/NA (PR8) was unable to form plaques in the presence of trypsin, or without protease added, highlighting its dependence on elastase. Western blotting also emphasized the same results (Figure 4.4B), in that the viral proteins NP and M1 were only detected when the recombinant mutant virus BC15-HA/QTV/NA (PR8) was provided with elastase. This strict dependence on elastase is essential for this recombinant mutant BC15-HA/QTV/NA (PR8) virus to be considered as a replication-defective virus vaccine because past research has shown elastase-dependent influenza viruses to be completely replication-defective *in vivo* (Masic et al., 2008; Stech et al., 2005).

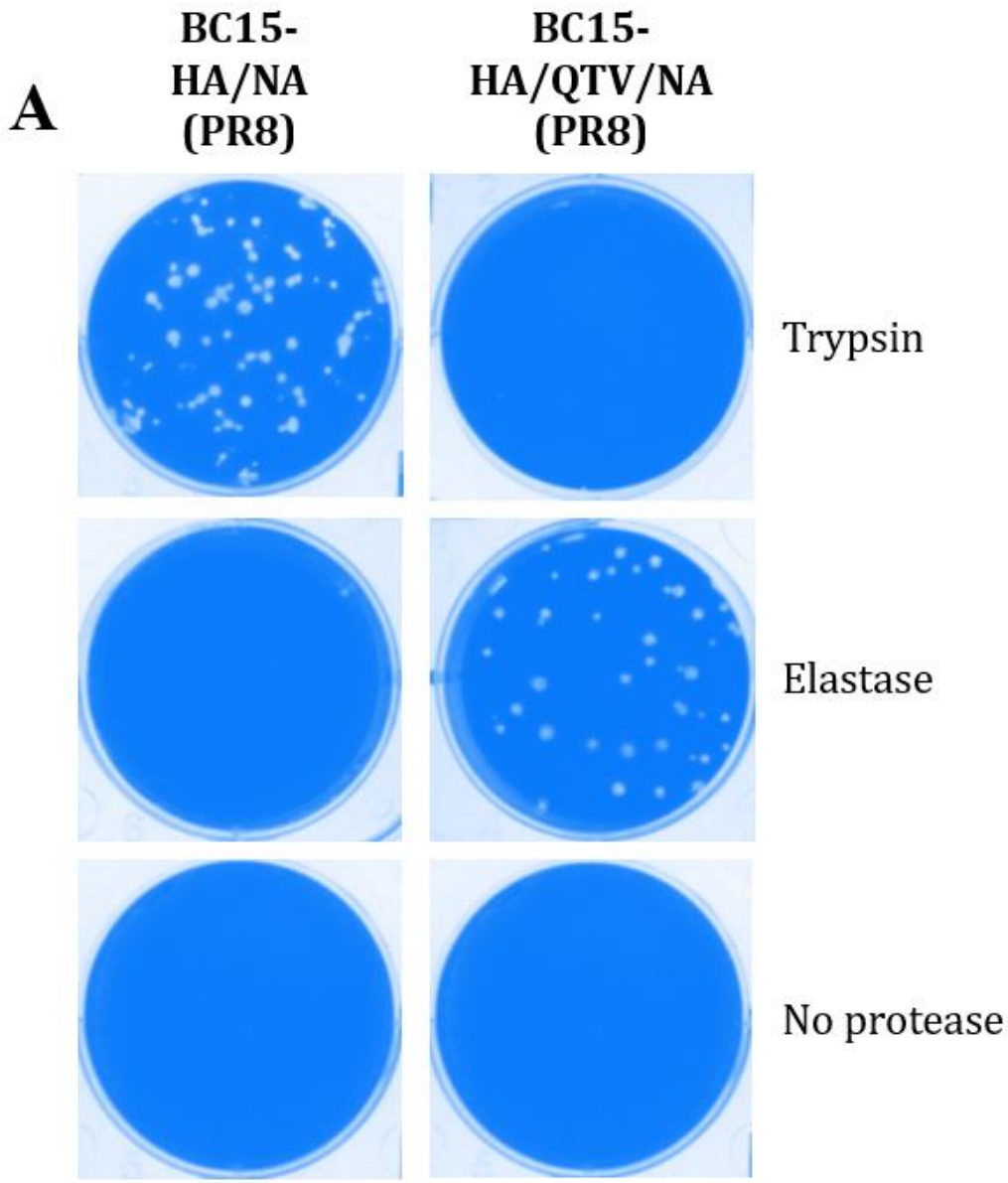
A
BC15-HA/NA (PR8)
BC15-HA/QTV/NA (PR8)
Trypsin
Elastase
No protease

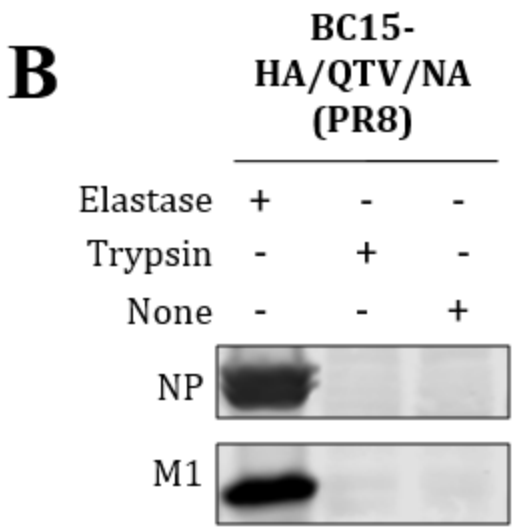

Figure 4.4. The replication dependency of recombinant BC15-HA/NA (PR8) and recombinant mutant BC15-HA/QTV/NA (PR8) viruses.
MDCK cells were infected at an m.o.i. of 0.001 in the presence of trypsin, neutrophil elastase, or in the absence of exogenous protease and subjected to plaque assay (**A**) or Western blotting (**B**). For Western blotting, 48 h.p.i. the cells were lysed to detect the presence of nucleoprotein (NP) and matrix (M1) protein. NP and M1 were detected using rabbit anti-NP or rabbit anti-M1 antibodies raised in our lab, followed by the addition of donkey anti-rabbit IgG for detection on an Odyssey infrared imager.

4.4.3 The recombinant mutant BC15-HA/QTV/NA (PR8) virus possesses equal growth kinetics to its wild-type counterpart *in vitro*

To determine whether the introduction of the mutations in the HA cleavage site could result in altering the replication abilities of the recombinant mutant BC15-HA/QTV/NA (PR8) virus; a multiple cycle growth curve was generated. High replication abilities are one of the requirements for a virus to be considered as a good vaccine candidate; therefore, we did not want the mutations to result in lower replication abilities compared to the wild-type virus. To this end, MDCK cells were infected with the recombinant virus BC15-HA/NA (PR8) or recombinant mutant virus BC15-HA/QTV/NA (PR8) at an m.o.i. of 0.001, with trypsin or elastase added to the medium. The supernatants were harvested at the indicated time points until 72 h.p.i., and the viral titers were determined by plaque assay on MDCK cells (Figure 4.5). The recombinant mutant virus BC15-HA/QTV/NA (PR8) possessed viral kinetics similar to its wild-type counterpart, recombinant virus BC15-HA/NA (PR8), with rapid replication between 12 h and 24 h, which plateaued after 24 h. When trypsin was added to the recombinant mutant virus BC15-

HA/QTV/NA (PR8), no viral replication was detected. Therefore, these results are conclusive in that the introduction of the elastase-sensitive motif to the HA cleavage site of BC15 (H7N9) does not result in the alteration of the viral growth properties in MDCK cells.

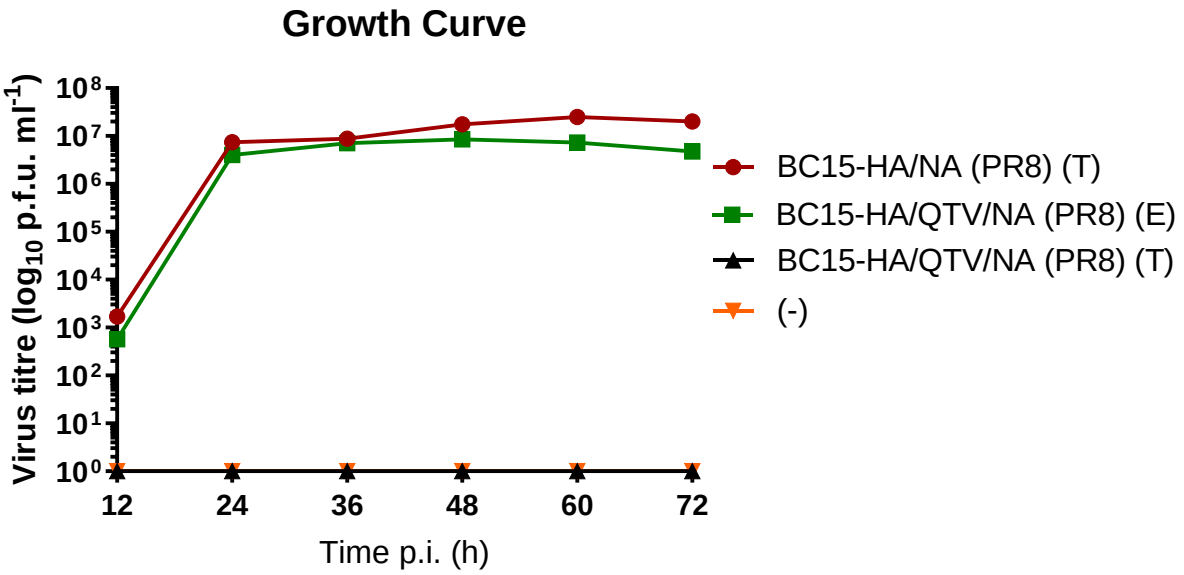

Figure 4.5. Multiple-cycle growth curves of recombinant BC15-HA/NA (PR8) and recombinant mutant BC15-HA/QTV/NA (PR8) viruses.
MDCK cells were infected with the respective viruses at an m.o.i. of 0.001 with either 1 µg/ml trypsin (T) or 0.5 µg/ml human neutrophil elastase (E). The recombinant mutant BC15-HA/QTV/NA (PR8) virus was also tested in the presence of trypsin. The supernatants were collected at specified time points until 72 h.p.i. and then titered by plaque assay on MDCK cells.

4.4.4 The recombinant mutant BC15-HA/QTV/NA (PR8) virus is genetically stable *in vitro*

To determine whether the mutations introduced in the HA cleavage site were stable *in vitro*, the recombinant mutant virus BC15-HA/QTV/NA (PR8) was passaged five times on MDCK cells at an m.o.i. of 0.001 in the presence of trypsin and human neutrophil elastase. The supernatants of the fifth passage were subjected to plaque assay in the presence of trypsin or human neutrophil elastase (Figure 4.6). The recombinant mutant virus BC15-HA/QTV/NA (PR8) was unable to form plaques in the presence of trypsin, highlighting that the mutations introduced were genetically stable after five passages on MDCK cells. Sequencing analysis of the HA cleavage site supported this finding, in that the QTV mutations introduced were retained throughout the five passages (Figure 4.7). Specifically, the nucleotides found from HA positions

1075 to 1086 (CAG ACT GTT) were the same as the nucleotides originally introduced (Figure 4.1). These results show the high level of genetic stability that the recombinant mutant virus BC15-HA/QTV/NA (PR8) possesses in cell culture after five passages. However, further experiments would need to be conducted to confirm this finding, such as using small amounts of elastase and trypsin to select against these genetic mutations. Since replication-defective viruses have demonstrated their safety of preventing virulence reversion through very limited replication within the host, this virus holds an advantage over the traditional LAIVs, whose limited replication poses a higher risk for virulence reversion (Dudek and Knipe, 2006; Watanabe et al., 2001). Therefore, the genetic stability of this recombinant mutant virus BC15-HA/QTV/NA (PR8) demonstrates the strong potential this virus holds as a vaccine candidate against H7N9 viruses.

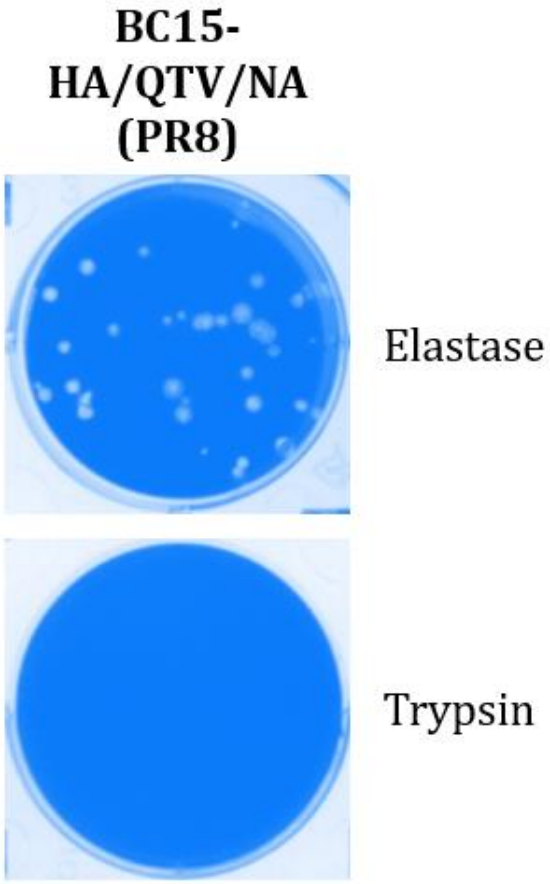

Figure 4.6. The genetic stability of the recombinant mutant BC15-HA/QTV/NA (PR8) virus.
The virus was passaged five times on MDCK cells at an m.o.i. of 0.001 in the presence of either trypsin or human neutrophil elastase. The supernatant of the fifth passage was subjected to plaque assay in the presence of either trypsin or human neutrophil elastase.

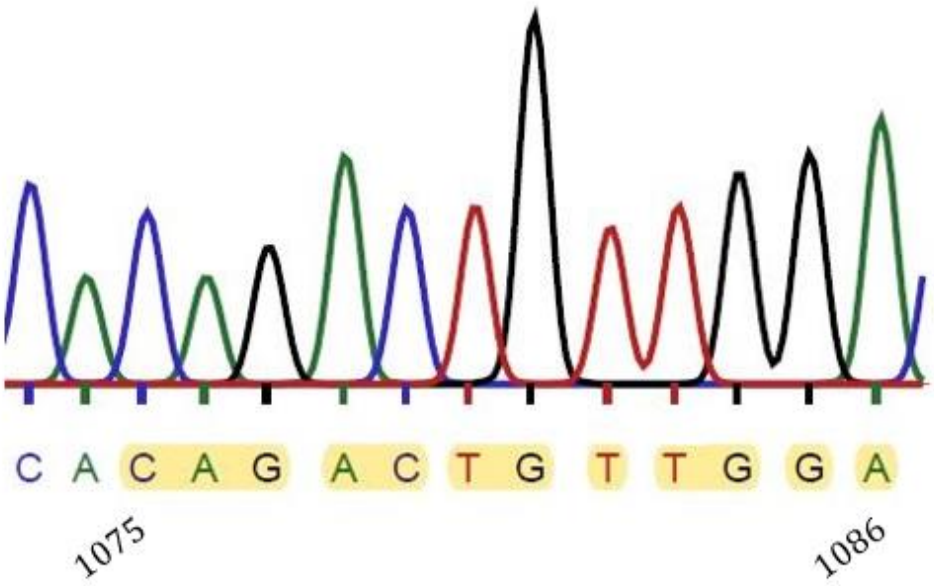

Figure 4.7. Histogram of the sequencing analysis performed on the HA cleavage site of the recombinant mutant BC15-HA/QTV/NA (PR8) virus.
Highlighted in yellow are the nucleotides (CAG ACT GTT) corresponding to the HA nucleotides from positions 1075 to 1086. These nucleotides code for the three amino acid mutations, QTV from HA positions 337 to 340.

4.4.5 The recombinant mutant BC15-HA/QTV/NA (PR8) virus is replication-defective in mice

To assess the virulence of this recombinant mutant BC15-HA/QTV/NA (PR8) virus, 36 six-week-old male and female BALB/c mice (equal males and females) were randomly divided into three groups with 12 mice in each group (six males and six females). Each mouse was intranasally inoculated with 50 µl of either MEM, recombinant virus BC15-HA/NA (PR8) (1 X 10^3 PFU), or recombinant mutant virus BC15-HA/QTV/NA (PR8) (1 X 10^3 PFU) (Table 4.1). The mice were monitored daily for body weight and survival rate (Figure 4.8). The mice that were infected with MEM and the recombinant mutant virus BC15-HA/QTV/NA (PR8) survived the duration of the trial and maintained their initial body weights. The mice that were infected with the recombinant virus BC15-HA/NA (PR8) began to lose weight from 4 d.p.i., with the most weight loss on 7 d.p.i. On 7 d.p.i., the mice exhibited approximately 11% loss of their initial body weight, after which the mice that survived gained weight to mock levels from 7 to 14 d.p.i. In this group, two mice (one female and one male) succumbed to the infection on 7 and 8

d.p.i., respectively. In contrast, mice infected with the recombinant mutant virus BC15-HA/QTV/NA (PR8) did not show any body weight loss for the duration of the trial. On 3 d.p.i., four mice from each group (two males and two females) were humanely euthanized and the lung samples were taken for viral load determination. Lung samples were also taken when the mice succumbed to infection, as well as on 14 d.p.i. On 3 d.p.i., high viral replication was detected in the recombinant BC15-HA/NA (PR8) group (1 X 10^6 PFU/ml/gr), which decreased on 7 and 8 d.p.i., with titers of 1 X 10^4 PFU/ml/gr and 1 X 10^3 PFU/ml/gr, respectively (Figure 4.9). On 14 d.p.i., no virus was detected in all lung samples from the recombinant BC15-HA/NA (PR8) group, illustrating that the mice cleared the influenza infection. In the recombinant mutant BC15-HA/QTV/NA (PR8) group, no viral replication was detected in any of the days sampled. Therefore, since no body weight loss or viral replication in the lungs was observed for the recombinant mutant BC15-HA/QTV/NA (PR8) virus, it was concluded that this virus is replication-defective in mice. Since being replication-defective is one of the requirements for this recombinant mutant BC15-HA/QTV/NA (PR8) virus to be considered as a replication-defective virus vaccine (Masic et al., 2008; Stech et al., 2005), we were able to move on to test this recombinant mutant BC15-HA/QTV/NA (PR8) virus in an immunoprotection study, which is explained in detail in chapter 5 of my thesis.

Groups (*n* = 12)	**Inoculum**	**Concentration**	**Dose volume**	**Route**
1	MEM	-	50 µl / 25 µl nostril	Intranasal
2	BC15-HA/NA (PR8)	1 X 10^3 PFU	50 µl / 25 µl nostril	Intranasal
3	BC15-HA/QTV/NA (PR8)	1 X 10^3 PFU	50 µl / 25 µl nostril	Intranasal

Table 4.1. Outline of mouse trial to evaluate the virulence of the recombinant mutant BC15-HA/QTV/NA (PR8) virus.
n = number of mice

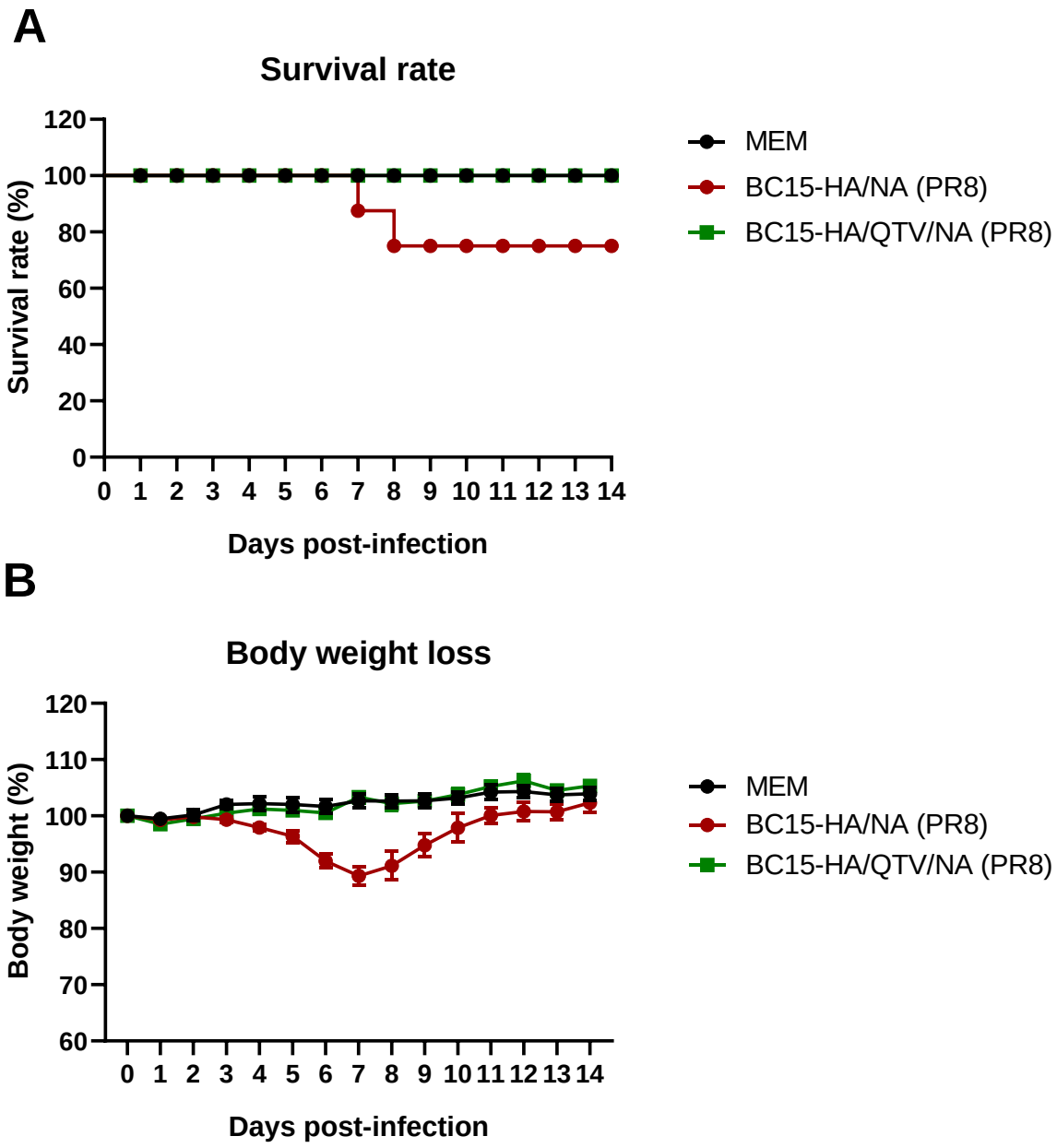

Figure 4.8. The survival rate and body weight loss of mice infected with the recombinant BC15-HA/NA (PR8) and the recombinant mutant BC15-HA/QTV/NA (PR8) viruses. The survival rates (**A**) and body weight loss (**B**) of the mice infected with MEM (control) or 1 X 10^3 PFU of recombinant BC15-HA/NA (PR8) or the recombinant mutant BC15-HA/QTV/NA (PR8) viruses (n = 12 per group).

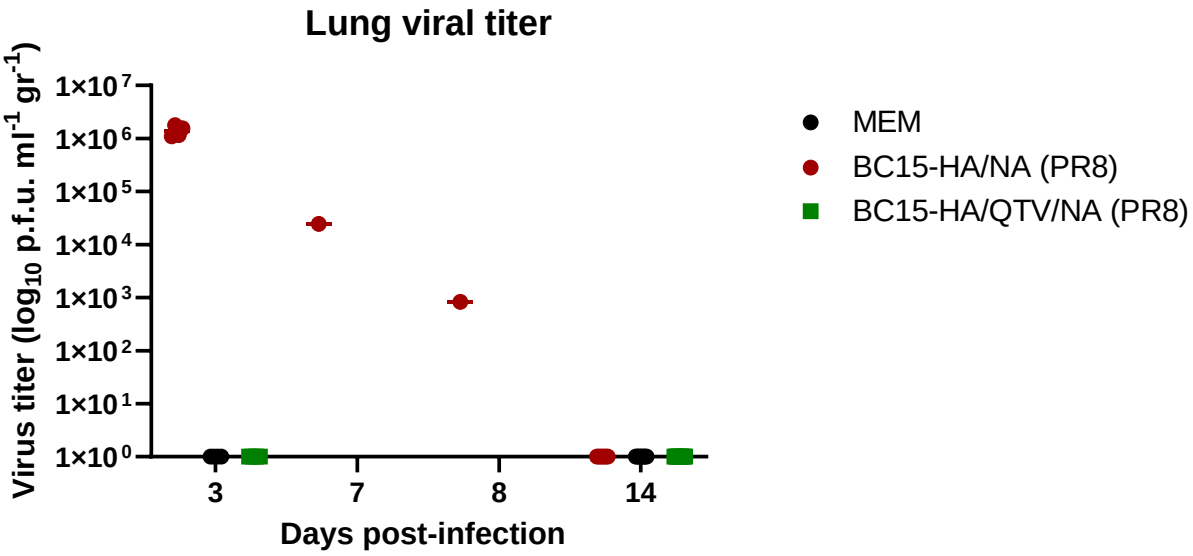

Figure 4.9. Viral titration of lungs from mice infected with the recombinant BC15-HA/NA (PR8) and the recombinant mutant BC15-HA/QTV/NA (PR8) viruses.
Mice were intranasally infected with MEM (control) or the BC15-HA/NA (PR8) or the BC15-HA/QTV/NA (PR8) viruses at a dose of 1 X 10^3 PFU. The lung samples were collected, homogenized, and titrated by plaque assay; the samples were analyzed in duplicate. Viral titers are expressed as PFU per milliliter per gram (PFU/ml/gr).

4.5 DISCUSSION AND CONCLUSIONS

Currently, H7N9 IAV continues to pose a great threat to society, apparent by the high morbidity and mortality rates it induces. Although much research has been focused on the development of a vaccine, at present, there is no commercial vaccine available. Out of the two main types of vaccines against influenza virus, IIV and LAIV, LAIVs have demonstrated much promise due to their superiority over IIVs. However, due to LAIVs possibility of virulence reversion, they have not yet become widespread throughout the world (Jang and Seong, 2012; Watanabe et al., 2001). Replication-defective virus vaccines are characteristically known to be defective in one or more essential functions of the virus replication, protein synthesis, or assembly (Dudek and Knipe, 2006). These vaccines possess the combined advantages of IIVs and LAIVs, with regards to their high safety and efficacy rates, low possibility of reversion, and ability to stimulate a balanced immune response (Dudek and Knipe, 2006; Watanabe et al., 2001). In addition, previous studies have demonstrated their high protection and efficacy rates against homologous challenges. In one study, mice vaccinated with replication-incompetent influenza virus-like particle (VLP) composed of cDNA from all influenza segments except the

NS2 gene were 94% protected against a homologous influenza challenge (Watanabe et al., 2001). Therefore, these replication-defective virus vaccines hold potential as influenza vaccine candidates.

In previous studies, a LAIV was generated through the introduction of specific mutations at the HA cleavage site; which is different from the commonly known temperature-sensitive LAIV (Masic et al., 2008; Sridhar et al., 2015; Stech et al., 2005). More specifically, these mutations at the HA cleavage site resulted in cleavage that was strictly dependent on the protease elastase. In this study, a mouse-adapted HA mutant virus was generated, which was dependent on elastase, grew similarly to the wild-type strain, and was completely replication-defective in mice at a dosage of 1 X 10^6 PFU (Stech et al., 2005). Similarly, *Masic et al.* came to the same conclusions in that a pig HA mutant virus was dependent on elastase, grew similarly to the wild-type strain, and completely replication-defective in pigs at a dose of 4 X 10^6 PFU, a natural host for influenza virus (Masic et al., 2009). These findings impelled us to determine whether this concept could be applied to an H7N9 virus capable of infecting humans.

In this chapter, we generated a recombinant mutant BC15-HA/QTV/NA (PR8) virus completely dependent on elastase *in vitro*. To generate this virus, we first generated a mutant plasmid, pHW-BC15/HA-QTV, which contained three mutations on the HA gene with the HA cleavage site to result in an elastase-sensitive motif. We then used reverse genetics to rescue the recombinant mutant virus rg-(6+2)-BC15/HA-QTV/NA [BC15-HA/QTV/NA (PR8)], composed of six segments from A/Puerto Rico/8 [PR8 (H1N1)], and two segments (HA, NA) from A/British Columbia/01/2015 [BC15 (H7N9)]. This recombinant mutant BC15-HA/QTV/NA (PR8) virus could only be rescued in the presence of human neutrophil elastase and grew to titers similar to its wild-type counterpart.

After generating this recombinant mutant BC15-HA/QTV/NA (PR8) virus, we proceeded to characterize the virus *in vitro*. Our results showed this recombinant mutant BC15-HA/QTV/NA (PR8) virus to be completely dependent on human neutrophil elastase for its activation, have identical growth kinetics to its wild-type counterpart and be genetically stable after five passages in MDCK cells (Figures 4.4-4.7). These results suggest that this recombinant mutant BC15-HA/QTV/NA (PR8) virus holds strong promise as a replication-defective virus vaccine candidate, as the mutations introduced did not result in alteration of the replication abilities of the virus, and the mutations did not revert to wild-type form, one common

disadvantage of the use of LAIVs. This recombinant mutant BC15-HA/QTV/NA (PR8) virus is characterized as a replication-defective virus vaccine, and not a LAIV because the mutations introduced resulted in halting the virus replication cycle. This halt leads to the restriction of influenza virus to a single-cycle of replication, unable to infect neighbouring cells.

Since our *in vitro* characterization demonstrated the potential of this recombinant mutant BC15-HA/QTV/NA (PR8) virus as a replication-defective virus vaccine candidate, we proceeded to investigate whether these replication-defective properties would hold *in vivo*. Specifically, we infected BALB/c mice with the recombinant virus rg-(6+2)-BC15-HA/NA [BC15-HA/NA (PR8)] and the recombinant mutant virus BC15-HA/QTV/NA (PR8) and monitored the mice daily for 14 days. Data collected from the daily body weights and viral load determination in their lungs demonstrated complete replication-defective properties of the recombinant mutant BC15-HA/QTV/NA (PR8) virus in mice. Their body weights remained equal to those of the uninfected group (Figure 4.8B), and no viral replication was detected by plaque assay (Figure 4.9). Thus, this recombinant mutant BC15-HA/QTV/NA (PR8) virus was completely replication-defective in mice.

Taken together, our results support the findings reported in *Masic et al.* and *Stech et al*., and demonstrate the potential of using this recombinant mutant BC15-HA/QTV/NA (PR8) virus for protection against H7N9 viruses capable of infecting humans (Masic et al., 2009; Stech et al., 2005). Since this recombinant mutant BC15-HA/QTV/NA (PR8) virus displays strong promise as a replication-defective virus vaccine candidate, the next step was to test whether this recombinant mutant BC15-HA/QTV/NA (PR8) virus could provide protection against A/British Columbia/01/2015 [BC15 (H7N9)] in mice.

TRANSITION BETWEEN CHAPTER 4 AND CHAPTER 5

In the previous chapter, a recombinant mutant BC15-HA/QTV/NA (PR8) virus was successfully generated and characterized with respect to its growth properties, stability, and virulence in mice. Since this recombinant mutant BC15-HA/QTV/NA (PR8) virus showed promise as a vaccine due to its non-virulence and non-replication nature *in vivo* and comparable virological characteristics to its wild-type counterpart *in vitro*, in this next chapter, the potential of this recombinant mutant BC15-HA/QTV/NA (PR8) virus as a replication-defective virus vaccine candidate was evaluated.

CHAPTER 5 THE REPLICATION-DEFECTIVE H7N9 VIRUS ELICITED COMPLETE PROTECTION AGAINST BC15 (H7N9) VIRAL CHALLENGE IN MICE

The data presented in this chapter and chapter 4 will be submitted to Vaccines

5.1 ABSTRACT

Avian influenza H7N9 virus infections in humans are common and pose substantial burdens to public health through their high morbidity and mortality rates. In the previous chapter, we demonstrated a recombinant mutant BC15-HA/QTV/NA (PR8) virus to be dependent on elastase for its replication and be genetically stable, possess comparable growth kinetics to its wild-type counterpart *in vitro*, as well as possess complete replication-defective properties in mice. Because vaccination is still the primary means for protecting the public against influenza viruses, in this chapter the immunogenicity and protective efficacy of the recombinant mutant BC15-HA/QTV/NA (PR8) virus against a lethal dose of A/British Columbia/01/2015 (H7N9) [BC15 (H7N9)] was evaluated in mice. We report that this recombinant mutant BC15-HA/QTV/NA (PR8) virus completely protects mice against a lethal challenge of BC15 (H7N9). This protection was demonstrated through the lack of body weight loss, 100% survival rate, and the induction of significantly elevated levels of antigen-specific IFN-γ and IL-5 secreting cells in the splenocytes, which is evidence of a strong cell-mediated response. In addition, this protection was demonstrated by the increased the levels of neutralizing antibodies in the mouse serum, tested by both the hemagglutinin inhibition (HAI) and serum virus neutralization (SVN) assays, as well as heightened the levels of antigen-specific IgG, IgG1, and IgG2a in the mouse serum. This protection was also confirmed through the inhibition of BC15 (H7N9) virus replication, and the reduction of various proinflammatory cytokine levels induced in the mouse lung that are associated with the influenza disease. Therefore, these results provide strong evidence for the use of this recombinant mutant BC15-HA/QTV/NA (PR8) virus as a replication-defective virus vaccine candidate against BC15 (H7N9).

5.2 INTRODUCTION

Influenza A viruses (IAV) are part of the *Orthomyxoviridae* family and consist of ribonucleic acid (RNA) genomes that are segmented, negative-sense, and single-stranded (Bouvier and Palese, 2011). IAVs initiates infection by entering the host respiratory tract through either aerosol inoculation or by fomites (Racaniello, 2009). Once IAV is inside the respiratory tract, it enters the host cell through the attachment of its hemagglutinin (HA) protein to the sialic acid receptors found on the host epithelial cells (Skehel and Wiley, 2000). The incubation period of IAV can last anywhere from 1 – 5 days and is usually asymptomatic. During this time, IAV initiates its replication and can be excreted and transmitted to other hosts through respiratory routes, such as coughing or sneezing. Once IAV enters the host, the host cells use their pattern recognition receptors (PRR) to sense pathogen-associated molecular patterns (PAMPS) found on the pathogen. Sensing of a foreign pathogen results in the innate immune signalling pathway activation, triggering the production of antiviral cytokines and interferons (IFNs). Meanwhile, dendritic cells (DCs) travel to the lymph node, where they present the foreign antigens to T cells, which leads to the activation of an antigen-specific or adaptive immune response. This immune response is characterized by the production of T cells and B cells, with the T cells aiding in infection elimination and the B cells producing antibodies that aid in immunological memory. Upon clearance of the IAV infection, the host is then protected against the particular strain it was infected with through the secretion of antibodies that can bind to and neutralize the virus (Murray et al., 2013). However, due to the complex evolutionary mechanisms IAV possesses, such as *antigenic drift* and *antigenic shift*, the same host can be repeatedly infected with different variants of the same IAV subtype (Bouvier and Palese, 2011). These complex evolutionary mechanisms can also facilitate IAV jumping from one species into another, adding to the intricacy of this disease (Su et al., 2017). Therefore, IAV poses a great challenge for researchers to develop a vaccine because the continuous evolution and ability to escape the immune system results in vaccines not always being protective against the particular strain it was intended for.

Avian influenza H7N9 viruses pose a significant threat to public health due to their recently acquired ability to infect humans and cause extraordinary morbidity and mortality rates. As of March 4, 2020, H7N9 had infected 1,568 humans and resulted in 616 deaths (FAO, 2020). Prior to 2013, avian influenza H7N9 virus circulated solely within the poultry population. Unfortunately, 2013 was the year when the low pathogenic avian influenza (LPAI) H7N9 virus

jumped species from birds into humans (Gao et al., 2013). Luckily, human LPAI H7N9 infections have not yet spread worldwide, being restricted to China due to its diverse and connected environment. China is known for its live-poultry markets here poultry are kept in close-quarters and contact with humans. This close contact between poultry and humans has been the primary reason for human infections with LPAI H7N9 for six epidemic waves from 2013 to 2017 (Su et al., 2017). Due to influenza's complex evolutionary mechanisms, the fifth epidemic wave brought about the evolution of the highly pathogenic avian influenza (HPAI) H7N9 virus. Since the emergence of the HPAI H7N9 virus, it has resulted in a total of 33 laboratory-confirmed human infections and has been detected in both poultry and ducks (Tang et al., 2019). This HPAI H7N9 virus has had such high morbidity and mortality rates among humans that it has resulted in more infections and deaths than the first four epidemic waves combined (Su et al., 2017; Yang et al., 2019). Throughout these epidemic waves, case fatality rates (CFR's) ranged from 33% to 45% for LPAI H7N9 and HPAI H7N9, respectively (Su et al., 2017). Although avian influenza H7N9 virus has not yet acquired the ability of sustained human-to-human transmission, the high morbidity and mortality rates as well as the evolution of the HPAI H7N9 virus highlights the importance of an effective vaccine against this avian influenza virus (Zheng et al., 2019).

Before IAV can become infectious, cleavage of the HA precursor form, HA0, must occur by various host proteases, most often by the protease trypsin. This cleavage results in the generation of HA1 and HA2, allowing IAV to become infectious and continue its replication cycle (Masic et al., 2008). Several studies have demonstrated the replication-defective properties IAV can possess through the mutation of the trypsin-sensitive HA cleavage site to an elastase-sensitive HA cleavage site. These studies have been demonstrated in the swine influenza virus (SIV) H1N1, in a human-derived H7N7 HPAI, in a mouse-adapted human-derived H1N1 virus, as well as in influenza B virus (IBV) (Babiuk et al., 2011; Gabriel et al., 2008; Mamerow et al., 2019; Masic et al., 2009; Masic et al., 2010; Masic et al., 2013; Stech et al., 2011; Stech et al., 2005). These replication-defective properties have been known to be a result of the respiratory tract lacking the protease elastase, thus, blocking the cleavage of HA and the continuation of the replication cycle *in vivo* (Mamerow et al., 2019). Therefore, these replication-defective viruses can be readily propagated *in vitro* when provided the protease elastase, but are unable to replicate *in vivo* where there is no elastase available (Stech et al., 2005). However, although in these

studies the various elastase mutant viruses were proven to confer high protective efficacy and immunogenicity against several homologous and heterologous viruses, this concept has not been tested for the H7N9 virus. Moreover, the few candidate virus vaccines available for H7N9, including A/Shanghai/2/13, A/Anhui/1/13, A/Guangdong/17SF003/2016, A/Hong Kong/125/2017, and A/Human/02650/2016, do not cover all variants of H7N9 influenza virus and are mainly inactivated influenza vaccines (IIV), which have disadvantages limiting their use (WHO, 2019). In the previous chapter of my thesis a recombinant mutant BC15-HA/QTV/NA (PR8) virus derived from a new Canadian isolate, A/British Columbia/01/2015 (H7N9) [BC15 (H7N9)] was developed, that was isolated from two patients that had recently visited China (Skowronski et al., 2016). This recombinant mutant BC15-HA/QTV/NA (PR8) virus was dependent on elastase and genetically stable *in vitro*, and entirely replication-defective in mice. Therefore, in this chapter, the immunogenicity and protective efficacy of this recombinant mutant BC15-HA/QTV/NA (PR8) virus against BC15 (H7N9) was evaluated. We found this recombinant mutant BC15-HA/QTV/NA (PR8) virus to completely protect mice from a lethal challenge of BC15 (H7N9), and possesses evidence of a strong cell-mediated and humoral immune response that may contribute to the high protection efficacy. This recombinant mutant BC15-HA/QTV/NA (PR8) virus was found to eliminate BC15 (H7N9) viral replication and significantly reduce the induction of proinflammatory cytokines associated with the influenza disease in the mouse lung. Therefore, as an approach to control the spread of the H7N9 virus, this recombinant mutant BC15-HA/QTV/NA (PR8) virus holds strong promise as a replication-defective virus vaccine candidate not only against BC15 (H7N9) but also against other subtypes of H7N9 influenza virus.

5.3 MATERIALS AND METHODS

5.3.1 Cells and viruses

Madin-Darby canine kidney (MDCK) (ATCC, #CRL-2936) cells were cultured in Minimal Essential Medium (MEM) (Sigma-Aldrich; M4655, St. Louis, MO, USA) supplemented with 10% fetal bovine serum (FBS) (Thermo Fisher; 16000-044) in a humidified 5% CO_2 incubator at 37°C. The recombinant mutant H7N9 virus rg-(6+2)-BC15/HA-QTV/NA [BC15-HA/QTV/NA (PR8)], as well as recombinant H7N9 virus rg-(6+2)-BC15-HA/NA [BC15-HA/NA (PR8)], used in this study were generated as described in chapter 4. The recombinant mutant H7N9 virus, BC15-HA/QTV/NA (PR8) was grown in MDCK cells supplemented with 0.2% bovine serum albumin (BSA) (Sigma-Aldrich; A7030) and 0.5 µg/ml human neutrophil elastase (Sigma-Aldrich; E8140). The recombinant H7N9 virus BC15-HA/NA (PR8) was grown in the presence of 0.2% BSA and 1 µg/ml L-[(toluene-4-sulphonamido)-2-phenyl] ethyl chloromethyl ketone (TPCK)-trypsin and purified by sucrose gradient purification. After sucrose gradient purification, the titers of the recombinant mutant BC15-HA/QTV/NA (PR8) virus and the recombinant BC15-HA/NA (PR8) virus was 2.08 X 10^7 PFU/ml and 3.19 X 10^7 PFU/ml, respectively. The A/British Columbia/01/2015 (H7N9) [BC15 (H7N9)] strain isolate was obtained from Dr. Yan Li, National Microbiology Laboratory, Public Health Agency of Canada. This strain isolate was maintained in Biosafety Containment Level 3 at the Vaccine International Disease Organization, International Vaccine Centre (VIDO-InterVac) at the University of Saskatchewan. All infectious experiments were conducted in Biosafety Containment Level 3 at the International Vaccine Centre at the University of Saskatchewan, Canada, under the guidelines of the Public Health Agency of Canada (PHAC) and the Canadian Food Inspection Agency (CFIA). All titers in this chapter were determined by either $TCID_{50}$ assay or plaque assay as described in chapter 3 and 4, respectively.

5.3.2 Ethics statement

Before commencing the animal experiments, we obtained approval from both the University Animal Care Committee (UACC) and Animal Research Ethics Board (AREB) of the University of Saskatchewan. This approval was given on 18 June 2019 (Animal Use Protocol

#20190079), guided by the stipulations implemented by the Canadian Council on Animal Care (CCAC).

5.3.3 Mouse experiments and sampling

For this trial, 38 six-week-old male and female BALB/c mice (19 males and 19 females) (Charles River Laboratories, Saint-Constant, QC, Canada) were randomly divided into three groups with either 12 or 14 mice in each group (six or seven males and females, respectively). These groups were housed in separate cages and allowed to acclimatize for seven days in Biosafety Containment Level 2. The males and females were housed in separate cages within the groups. At seven weeks of age, the mice were intranasally vaccinated with 50 µl of either MEM or BC15-HA/QTV/NA (PR8) at a dose of 1 X 10^3 PFU. At 10 weeks of age (21 days later), the mice received a second vaccination in the same manner as the first vaccination. On day 30, four mice from each group were euthanized (two males and two females) and their spleens collected for isolation to detect IFN-γ and IL-5 secreting cells by the enzyme-linked immunospot (ELISPOT) assay. The remaining eight or ten mice per group (four or five males and females, respectively) were transferred to Biosafety Containment Level 3. The following day (day 31), these transferred mice were challenged with a lethal dose 100 (LD100) of A/British Columbia/01/2015 [BC15 (H7N9)] (1 X 10^3 PFU). After the challenge, the mice were monitored daily for 14 days for both body weight loss and clinical scores. On day 3 post-challenge, four mice per group (two males and two females) were humanely euthanized and their lungs and serum were collected. Any mouse that lost over 20% of its total initial body weight throughout the trial was humanely euthanized. In addition, the serum of all mice was collected on days 0, 21, 30, as well as on 3 and 14 days post-challenge and when a mouse was humanely euthanized.

5.3.4 Isolation of splenocytes from mouse spleen

To isolate the splenocytes, after harvesting the spleens they were immediately placed into 40 µM BD falcon cell strainers (Corning; 352340) in a 6-well plate containing wash medium composed of MEM (Sigma-Aldrich) supplemented with Penicillin-Streptomycin (10,000 U/mL) (Gibco, ThermoFisher), 50 µg/ml gentamycin (Bio Basic, Canada), and HEPES (1M) (Gibco, ThermoFisher). After the excess fat was removed, the spleens were cut into 6-8 small pieces, and then gently pushed through the 40 µM cell strainer using the plunger of a 5 ml plastic syringe.

The wash medium now filled with cells was then pipetted through the cell strainer three times to break up the cells, and then added to a 15 ml tube and topped up with wash medium. The tubes underwent centrifugation at 200 g for 10 min at 4°C, after which 1 ml of Red Blood Cell Lysing Buffer Hybri-Max^{TM} (Sigma-Aldrich) was added to the cell pellet and gently mixed to lyse the cells. Exactly 30 seconds later wash medium was added to stop the lysis and the tubes underwent centrifugation at 200 g for 10 min at 4°C. The supernatant was discarded, and this step was repeated. After the second centrifugation, the supernatant was discarded and the cells were resuspended in culture medium composed of AIM-V^{TM} Medium (ThermoFisher; 12055091) supplemented with Non-Essential Amino Acids (NEAA) Solution (1X) (Gibco, ThermoFisher), Sodium Pyruvate (1X) (Gibco, ThermoFisher), HEPES buffer (1X), and 50 mM 2-mercaptoethanol (Sigma-Aldrich). The cell density was determined with a coulter counter and adjusted to 5 X 10^6 cells/ml for the ELISPOT assay.

5.3.5 Detection of IFN-γ and IL-5 secreting cells by enzyme-linked immunospot (ELISPOT) assay

For the enzyme-linked immunospot (ELISPOT) assay, multiscreen-HA plates, 0.45 µM, sterile (Millipore; MAHAS4510) were coated with either purified rat anti-mouse IFN-γ (BD; 551216) or purified rat anti-mouse IL-5 (BD; 554393) at a concentration of 2 µg/ml diluted in sterile coating buffer and incubated overnight at 4°C. The next day the plates were washed with sterile PBS four times, and then blocked overnight at 4°C with 1% BSA diluted in PBS. The following day, the plates were rinsed with 200 µl/well of culture medium and the splenocytes seeded at 5 X 10^5 cells/well in a final volume of 200 µl/well. The cells were stimulated for 20 h at 37°C with 50 µg/ml of the purified β-propiolactone-inactivated recombinant virus [BC15-HA/NA (PR8)], 5 µg/ml concanavalin A (Sigma-Aldrich), or medium only in triplicate. The purified virus [BC15-HA/NA (PR8)] was inactivated with β-propiolactone (Sigma-Aldrich) at a 1:2000 dilution for 24 h with rocking incubation at 4°C. This inactivation was confirmed through the absence of plaques by a plaque assay. After stimulation, the plates were washed once with PBST (PBS + 0.1% Tween 20) and twice with ddH_2O to lyse the cells. During the second wash with ddH_2O, the cells were incubated for 5 min. The plates were washed three times with PBST and two times with ddH_2O, after which either biotinylated rat anti-mouse IFN-γ (BD; 554410) or biotinylated rat anti-mouse IL-5 (BD; 554397) at a concentration of 2 µg/ml in PBS containing

1% BSA (1% PBS/BSA) was added. Subsequently, the plates were incubated at room temperature for 2 h. After the wells were washed four times with PBST and twice with ddH_2O, alkaline phosphatase (AP)-conjugated streptavidin (Jackson ImmunoResearch; 016-050-084) diluted 1/2000 in 1% PBS/BSA was added to each well, and the plates were incubated at room temperature for 1.5 h. The plates were then washed four times with PBST and twice with ddH_2O, after which BCIP/NBT substrate (Sigma-Aldrich; B5655) was added. The plates were incubated for 5 min, after which they were washed eight times with ddH_2O and left to dry overnight. The spots were counted with the ELISPOT reader (AID, Strassberg, Germany). The data reported are presented as the number of IFN-γ and IL-5-secreting cells per 5 X 10^5 cells with the number of spots in the medium only wells subtracted as background.

5.3.6 Hemagglutination inhibition (HAI) and serum virus neutralization (SVN) assay

To measure the HAI titers, the HAI assay was performed. Mouse serum was pretreated with receptor destroying enzyme (RDE) (Cholera filtrate; C8772) (Sigma-Aldrich) at a 1:4 ratio in calcium saline pH 7.2 (0.1% calcium chloride, dihydrate; 0.9% sodium chloride, anhydrous; 0.12% boric acid, anhydrous; 0.0052% sodium borate, decahydrate) overnight at 37°C. After incubation, the RDE was inactivated through the addition of 1.5% sodium citrate solution, pH 7.2 at a 1:10 ratio followed by a 30 min incubation at 56°C to inactivate any remaining RDE. The treated serum samples were then serially diluted in duplicate two-fold in PBS in V-bottom 96-well plates (Corning), to which four hemagglutination units of BC15 (H7N9) were added and incubated at room temperature for 1 h. After this incubation, 0.5% chicken red blood cells (RBC) were added to all wells, and the plates incubated for 30 min. At this time, the HAI titers of the serum were determined as the reciprocal of the highest dilution that completely inhibits hemagglutination.

To measure the serum virus neutralization (SVN) titers, MDCK cells (2 X 10^4 cells/well) were seeded in flat-bottom 96-well cell culture plates (Corning) and incubated overnight at 37°C in 5% CO_2. Serum collected from mice on days 0, 21, and 30 were heat-inactivated for 30 min at 56°C. This inactivated serum was then tested in quadruplicate, with 12 µl per replicate subjected to two-fold serial dilutions in MEM containing 1 µg/ml of TPCK-trypsin within sterile U-bottom 96-well plates (Corning). A negative control composed of only MEM and TPCK-trypsin was

included among the replicates. After the serum was serially diluted, 100 $TCID_{50}$/50 µl BC15 (H7N9) influenza virus diluted in MEM containing 1 µg/ml TPCK-trypsin was added to each well, minus the negative control wells which only received MEM and TPCK-trypsin, and the plates incubated at 37°C in 5% CO_2 for 1 h. These serially diluted plates are referred to as the serum-virus mixture plates. After the MDCK cells were washed with MEM, 100 µl of the serum-virus mixture was added to each well and allowed to incubate for 1 h at 37°C in 5% CO_2. After incubation, the serum-virus mixture was removed, MDCK cells were washed with MEM, and 200 µl of MEM containing 1 µg/ml TPCK-trypsin and 50 µg/ml gentamicin was added to each well. The plates were incubated at 37°C in 5% CO_2 for 72 h, after which the presence or absence of cytopathic effects (CPE) was observed and recorded. The SVN titer was determined as the highest dilution of serum that completely protected the cells from CPE in 50% of the wells.

5.3.7 Enzyme-linked immunosorbent assay (ELISA) to detect antigen-specific IgG, IgG1, and IgG2

To measure the influenza-specific IgG levels induced by vaccination, an enzyme-linked immunosorbent assay (ELISA) was performed using mouse serum samples taken before vaccination, after the first vaccination, and after the second vaccination. Purified β-propiolactone-inactivated recombinant virus BC15-HA/NA (PR8) (2.5 µg/ml) was coated onto 96-well Immulon-2 plates (Dynex Technology Inc., Chantilly, VA) and incubated overnight at 4°C. This purified virus was confirmed to be inactivated by the absence of plaques in a plaque assay. After incubation, the plates were blocked for 1 h at room temperature with 100 µl of 1% skim milk in TBST (0.1 M Tris, 0.17 M NaCl, and 0.1% Tween 20) and washed four times with TBST (TBS + 0.1% Tween 20). Serially diluted mouse sera were added and left to incubate at room temperature for 1.5 h, and then washed four times with TBST. Goat anti-mouse IgG (H+L) (Invitrogen; B2763), goat anti-mouse IgG1 (Southern Biotech; 1070-08), or goat anti-mouse IgG2a (Southern Biotech; 1080-08) was added for 1 h at room temperature to detect IgG, IgG1, or IgG2a, respectively, and then washed four times with TBST. Color development was initiated by the addition of AP-conjugated streptavidin (Jackson ImmunoResearch) and p-nitrophenyl phosphate (PNPP) substrate [10 mg/ml p-nitrophenyl phosphate di(tris) salt crystalline (Sigma-Aldrich), 1% diethanolamine (Sigma-Aldrich), 0.5 mg/ml $MgCl_2$, pH 9.8]. Detection of the optical density (OD) occurred at 405 nm (using a reference filter of 490 nm) on a microplate

reader (Molecular Devices SpectraMax Plus 384). The titers of each sample were determined as the highest dilution at which the OD of the sample was larger than the defined cut-off. The cut-off was defined as the mean OD of a known negative sample plus twice the standard deviation.

5.3.8 Virus isolation and titration

Upon harvest of the mouse lung, the tissues were submerged in 1 mL MEM supplemented with (1X) Penicillin-Streptomycin (100X) (Gibco, Thermo Fisher, ON, Canada) in a 2 mL pre-labelled and pre-weighed tube. Upon submersion, the tissues were placed on ice and transferred from the animal containment room to the laboratory containment room. Subsequently, the tubes were weighed and the tissues homogenized in the TissueLyser II (Qiagen, Hilden, Germany) at 25 Hz for 5 min, followed by centrifugation at 5,000 g for 10 min at 4°C. The homogenized supernatant was transferred to new pre-labelled 1.5 ml screw-cap tubes and stored at -80°C until analysis.

For analysis, a $TCID_{50}$ assay was performed for which MDCK cells (2×10^4 cells) were seeded in Biosafety Containment Level 2 in flat-bottom 96-well cell culture plates (Corning). The plates were transferred to Biosafety Containment Level 3, where the cells were washed with basal MEM without FBS, and then serial dilutions of the homogenized supernatants were added to the cells and left to incubate at 37°C for 1 h. After this incubation, growth medium composed of MEM supplemented with 0.2% BSA and 1 µg/ml TPCK-trypsin was added to the cells. The cells were observed daily for 96 hours post-infection (h.p.i.) for the presence or absence of cytopathic effects (CPE). The $TCID_{50}$ titer was calculated by the Spearman-Kärber algorithm (Kärber, 1931; Spearman, 1908).

5.3.9 RNA extraction and quantitative RT-PCR (qRT-PCR)

The lung tissue harvested on 3 days post-challenge was immediately placed into RNAlater (Qiagen) and stored overnight at 4°C. The next day, the lung tissues were transferred into 1.5 ml screw-cap tubes and stored at -80°C until further processing was performed. For processing, RNA was extracted using the TRIzol method with minor modifications. Briefly, the tissues were thawed on ice, and 1 mL of TRIzol Reagent (Invitrogen, Carlsbad, CA, USA) was added along with one 5-mm stainless steel bead (Qiagen). The tissues underwent homogenization using the TissueLyser II (Qiagen, Hilden, Germany) at 25 Hz for 5 min, followed by centrifugation at

5,000 g for 10 min at 4°C. After centrifugation, the homogenized supernatants were transferred to 1.5 ml tubes, which were kept upright on ice while they were transferred from Biosafety Containment Level 3 to Biosafety Containment Level 2.

In Biosafety Containment Level 2, the tubes were inverted and left to incubate at room temperature for 2 min. After this incubation, 200 µl of chloroform (Sigma-Aldrich, St. Louis, MO, USA) per 1 mL TRIzol was added, shaken vigorously for 15 seconds, and then incubated at room temperature for 3 min. The tubes then underwent centrifugation at 12,000 g for 15 min at 4°C. Centrifugation resulted in the liquid separating into three distinct layers; the aqueous phase was harvested and put into a new tube containing 500 µl isopropanol. These tubes were inverted, left to incubate for 10 min at room temperature, and then centrifuged at 12,000 g for 10 min at 4°C. Supernatants were discarded and replaced with 75% ethanol, the tubes were briefly vortexed and then centrifuged at 7,500 g for 5 min at 4°C. The supernatants were discarded, and the pellets left to air-dry for 12 min, after which they were resuspended in RNase-free DEPC H_2O. This mixture incubated at 55°C for 12 min, and the concentration of RNA was determined using the Thermo Scientific Nanodrop 2000 Spectrophotometer (ND-200).

To use the RNA for quantitative PCR (qPCR), we first used 1 µg of RNA as a template to generate complementary DNA (cDNA) by RT-PCR. For this, the RNA was treated with 100 U of DNase I (Invitrogen; 18068-015) and left to incubate at room temperature for 15 min. After the incubation, the DNase I was inactivated through the addition of 25 mM ethylenediaminetetraacetic acid (EDTA) (Invitrogen; Y02353) and incubation at 65°C for 10 min. Next, 10 mM dNTP (Invitrogen; 18427-088) and 50 uM oligo(dt) primers were added and incubated for 5 min at 65°C. Subsequently, the tubes were put on ice for 2 min, and then the final reverse transcription step was performed through the addition of 5X First-Strand buffer (Invitrogen; Y02321), 0.1 M dithiothreitol (DTT) (Invitrogen; Y00147), RNase-out (Invitrogen; 10777-019), and the superscript III reverse transcriptase enzyme (Invitrogen; 18080-044). This final step occurred at 50°C for 1 h followed by 15 min at 70°C.

The qPCR procedure began with the dilution of the cDNA either 10-fold or 50-fold in H_2O. In addition, a master-mix for each cytokine tested was generated through the addition of a forward (10 µM) and reverse (10 µM) primer, 2X SYBR green master-mix (Thermo Scientific) and H_2O. This master-mix was added to the diluted cDNA inside a MicroAmp Fast 96-well Reaction Plate (0.1 ml) (Applied Biosystems). An adhesive film was added to cover the plates,

which underwent centrifugation at 1,000 g for 3 min at room temperature. The plates underwent qPCR in the StepOnePlus™ Real-Time PCR system (Applied Biosystems, CA, USA) with the Power SYBR Green PCR Master Mix (Applied Biosystems). The hypoxanthine phosphoribosyltransferase (HPRT) housekeeping gene was used to standardize the cytokine mRNA levels. All results are reported according to the ΔΔCT method (Rao et al., 2013) using the MEM group as a reference. All qPCR primer sequences are listed in Table 3.1.

5.3.10 Statistical analysis

The statistical analysis was executed using GraphPad Prism 8. For this analysis, a one-way ANOVA was performed followed by the Tukey posthoc test to determine the P-value. For the ELISPOT, ELISA, and qPCR the samples were analyzed in triplicate. For the SVN assay, the samples were performed in quadruplicate. For the HAI assay, the samples were tested in duplicate. Significant differences among groups are signified by * ($p < 0.05$), ** ($p < 0.01$), *** ($p < 0.001$) or **** ($p < 0.0001$). ns = not significant.

5.4 RESULTS

5.4.1 Vaccination with the replication-defective BC15-HA/QTV/NA (PR8) virus provides evidence of a strong cell-mediated response

To determine portions of the cell-mediated immune response induced after intranasal vaccination with MEM (control) or BC15-HA/QTV/NA (PR8), male and female BALB/c mice were intranasally immunized on days 0 and 21 with MEM (control, 'mock-vaccinated') or 1 X 10^3 PFU of BC15-HA/QTV/NA (PR8) ('vaccinated'). The mouse spleens were harvested on day 30 from both the mock-vaccinated and vaccinated mice (two males and two females per group) (Figure 5.1 and Table 5.1). The splenocytes were isolated and the antigen-specific responses were measured by both IFN-γ and IL-5 ELISPOT assay. As shown in Figure 5.2A, intranasal vaccination with BC15-HA/QTV/NA (PR8) induced significantly higher numbers of antigen-specific IFN-γ secreting cells compared to the mock-vaccinated MEM control group ($p = < 0.0001$). Concomitantly, the number of antigen-specific IL-5 secreting cells induced by BC15-HA/QTV/NA (PR8) vaccination, although not as high as IFN-γ, was still significantly higher compared to the mock-vaccinated MEM control group ($p = < 0.0001$) (Figure 5.2B).

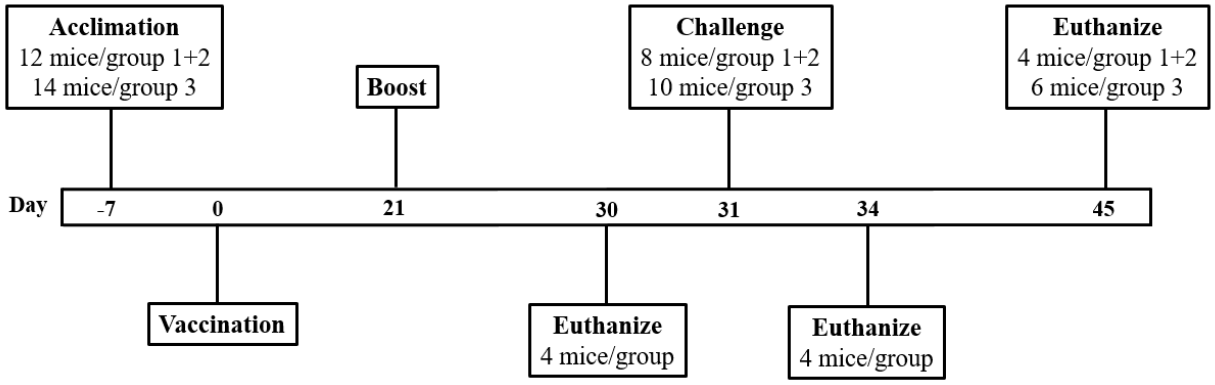

Figure 5.1. Outline of the mouse trial to evaluate the immunoprotection induced by the replication-defective recombinant mutant BC15-HA/QTV/NA (PR8) virus.
BALB/c mice (*n* = 12 or 14; equal males and females) were intranasally vaccinated on days 0 and 21 with 50 µl of MEM (control) or BC15-HA/QTV/NA (PR8) (1 X 10^3 PFU). On day 30, four mice per group (two males and two females) were euthanized for isolation. On day 31, the remaining mice were intranasally challenged with MEM (control) or a lethal dose of BC15 (H7N9) (1 X 10^3 PFU). On day 34 (3 days post-challenge), four mice per group (two males and two females), were euthanized for sampling. The trial concluded on day 45 (14 days post-challenge), where the remaining mice were euthanized and sampled. Sampling included serum and lung tissue. Refer to table 5.1 for the grouping of the mice.

Groups	Vaccination		Challenge (Day 31)
	1st (Day 0)	2nd (Day 21)	
1 (*n* = 12)	MEM	MEM	MEM
2 (*n* = 12)	MEM	MEM	BC15 (H7N9) (1 X 10^3 PFU)
3 (*n* = 14)	BC15-HA/QTV/NA (PR8) (1 X 10^3 PFU)	BC15-HA/QTV/NA (PR8) (1 X 10^3 PFU)	BC15 (H7N9) (1 X 10^3 PFU)

Table 5.1. Grouping within the mouse trial to evaluate the immunoprotection of the replication-defective recombinant mutant BC15-HA/QTV/NA (PR8) virus.
BALB/c mice (*n* = 12 or 14; equal males and females) were intranasally vaccinated on days 0 and 21 with 50 µl of MEM (control) or BC15-HA/QTV/NA (PR8) (1 X 10^3 PFU). On day 31, the remaining mice (eight or 10 mice; equal males and females) were intranasally challenged with MEM (control) or a lethal dose of BC15 (H7N9) (1 X 10^3 PFU).

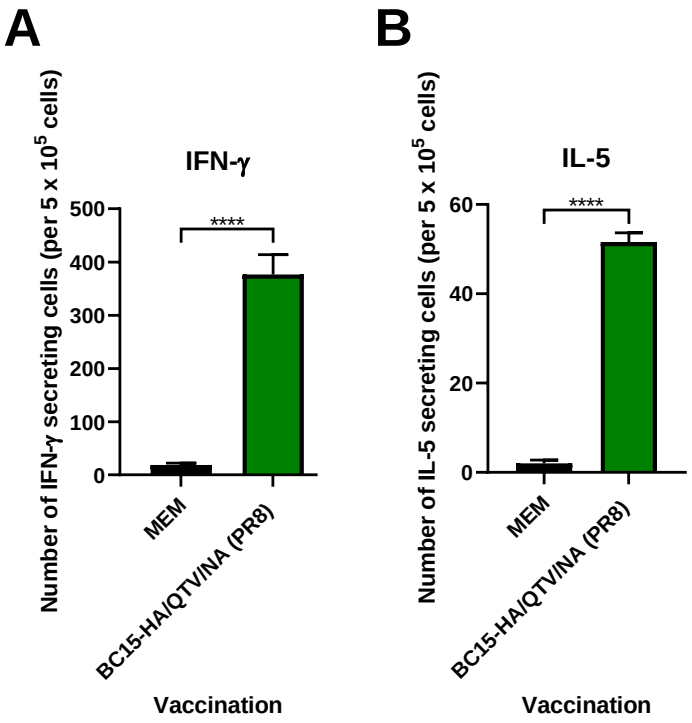

Figure 5.2. Antigen-specific IFN-γ and IL-5 secreting cells induced by BC15-HA/QTV/NA (PR8) vaccination in mice.

BALB/c mice were vaccinated with two doses of MEM (control) or BC15-HA/QTV/NA (PR8) (1 X 10^3 PFU). Nine days after the second vaccination (day 30) BALB/c mice (four mice per group; two males and two females) were euthanized and their splenocytes isolated. The numbers of IFN-γ **(A)** and IL-5 **(B)** secreting T cells per 5 X 10^5 splenocytes were determined by ELISPOT; each sample was tested in triplicate. The antigen-induced counts were determined by subtracting the number of IFN-γ or IL-5 secreting cells with the medium-treated control cells. The bars represent the mean value obtained from all mice in the respective groups, and the error bar represents the standard deviation. Significant differences among groups are signified by * ($p < 0.05$), ** ($p < 0.01$), *** ($p < 0.001$) or **** ($p < 0.0001$). ns = not significant.

5.4.2 The replication-defective BC15-HA/QTV/NA (PR8) virus induces a robust humoral response

To determine the humoral immune response induced by BC15-HA/QTV/NA (PR8) vaccination, mouse serum was collected before vaccination (day 0), after the first vaccination (day 21), and after the second vaccination (day 30) (Figure 5.1). This serum was screened for BC15 (H7N9) specific antibodies by the hemagglutinin inhibition (HAI) assay as well as the serum virus neutralization (SVN) assay. Concerning the HAI assay, all mice were negative on day 0 for BC15 (H7N9) antibodies (HAI ≤ 1:16), and the mice that were mock-vaccinated with MEM remained negative on days 21 and 30 for BC15 (H7N9) antibodies (HAI ≤ 1:16) (Figure 5.3A). After the first intranasal vaccination (day 21) with the BC15-HA/QTV/NA (PR8), all the mice seroconverted to the BC15 (H7N9) antigen with an average HAI level of 115. This level of seroconversion was much higher than the gold standard HAI cut-off of 40 that is associated with a 50% reduction in the risk of contracting influenza. Following the second vaccination (day 30), the level of seroconversion in the BC15-HA/QTV/NA (PR8) vaccinated mice increased significantly reaching an average HAI titer of 309. With regards to the SVN assay, all mice in the mock-vaccinated MEM control group and the BC15-HA/QTV/NA (PR8) vaccinated group possessed low SVN titers on day 0 (SVN ≤ 1:16) (Figure 5.3B). After the mice received their first intranasal vaccination (day 21), SVN titers increased dramatically in the BC15-HA/QTV/NA (PR8) vaccinated group, reaching an average SVN titer of 369. Moreover, after these mice received their second vaccination (day 30), the SVN titers further increased reaching an average SVN titer of 1547. Therefore, these high SVN and HAI titers reflect the protection that was conferred against BC15 (H7N9) challenge.

Influenza-specific IgG, IgG1, and IgG2a in the mouse serum were determined for days 0, 21, and 30 by ELISA using purified β-propiolactone-inactivated recombinant virus BC15-HA/NA

(PR8) as the capture antigen. As seen in Figure 5.4A, moderate upregulation of IgG was observed after the first BC15-HA/QTV/NA (PR8) vaccination (day 21 titer = 98,101), and significant upregulation was observed after the second vaccination (day 30 titer = 1,502,010). Similarly, the level of IgG1 after the first BC15-HA/QTV/NA (PR8) vaccination was only moderately upregulated ($p = 0.0464$) in comparison to the day 0 levels (day 0 titer = 225; day 21 titer = 65,428) (Figure 5.4B). However, after the second BC15-HA/QTV/NA (PR8) vaccination, the level of IgG1 was significantly elevated (day 30 titer = 335,175) in comparison to day 21 ($p = < 0.0001$) and day 0 ($p = < 0.0001$). In comparison, the level of IgG2a after the first BC15-HA/QTV/NA (PR8) vaccination was significantly elevated ($p = < 0.0001$) when compared to the day 0 levels (day 0 titer = 290; day 21 titer = 677,648) (Figure 5.4 C). Moreover, the level of IgG2a was significantly elevated (day 30 titer = 3,601,440) in comparison to day 21.

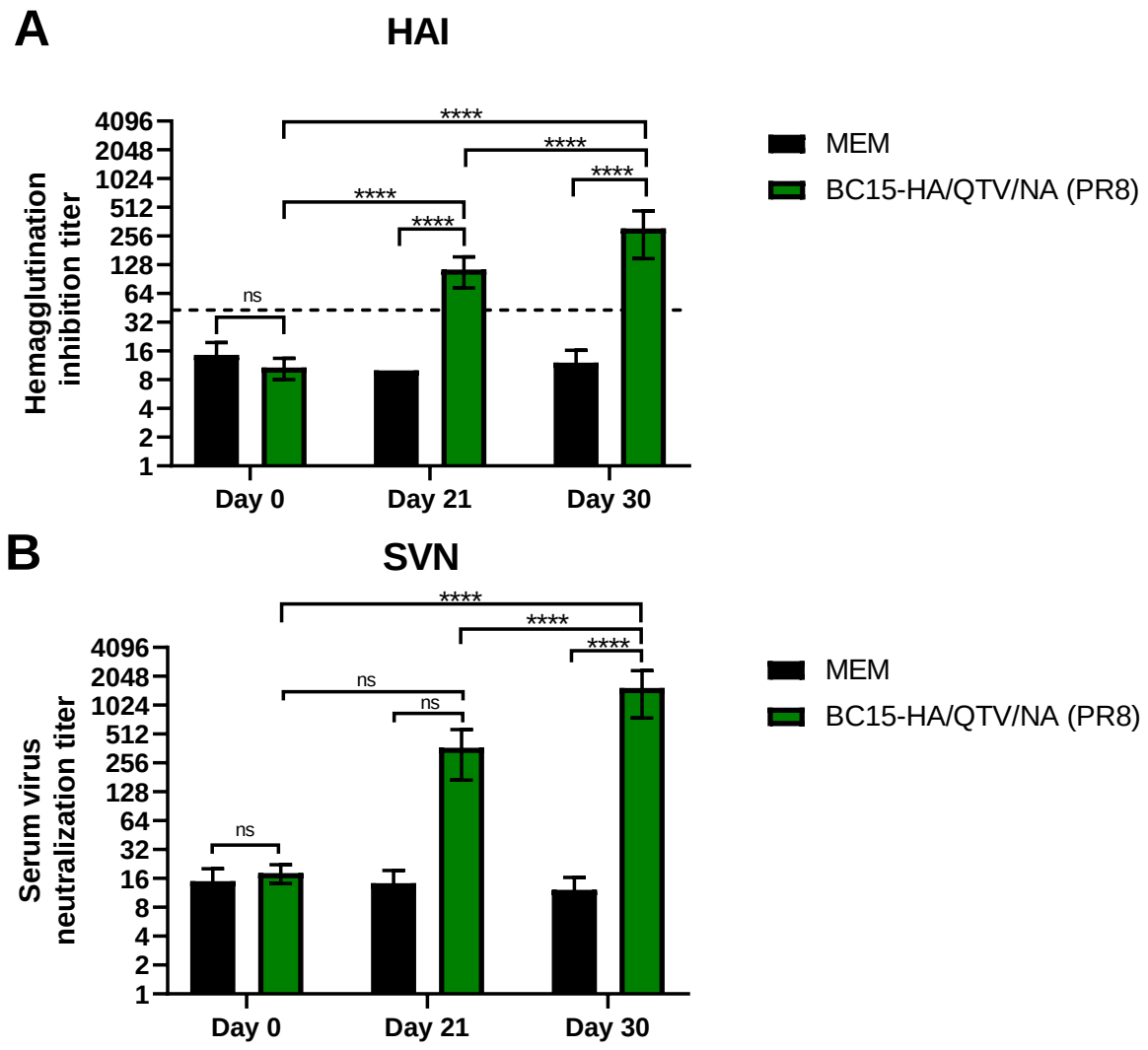

Figure 5.3. Humoral immune responses mounted after BC15-HA/QTV/NA (PR8) vaccination.

BALB/c mice were vaccinated on days 0 and 21 with MEM (control) or BC15-HA/QTV/NA (PR8) (1 X 10^3 PFU). Serum was collected on days 0, 21, and 30 to be titered using the HAI assay and the SVN assay against the BC15 (H7N9) virus. **(A)** Serum HAI titers were determined using 0.5% RBCs against the BC15 (H7N9) virus; samples were analyzed in duplicate. The dotted line corresponds to the negative cut-off of 40, which is associated with a 50% reduction in the chance of contracting influenza virus. **(B)** SVN titers were determined using 100 $TCID_{50}$/50 µl of BC15 (H7N9) influenza virus; samples were analyzed in quadruplicate. The bars represent the mean value obtained from all mice in the respective groups, and the error bar represents the standard deviation. Significant differences among groups are signified by * ($p < 0.05$), ** ($p < 0.01$), *** ($p < 0.001$) or **** ($p < 0.0001$). ns = not significant.

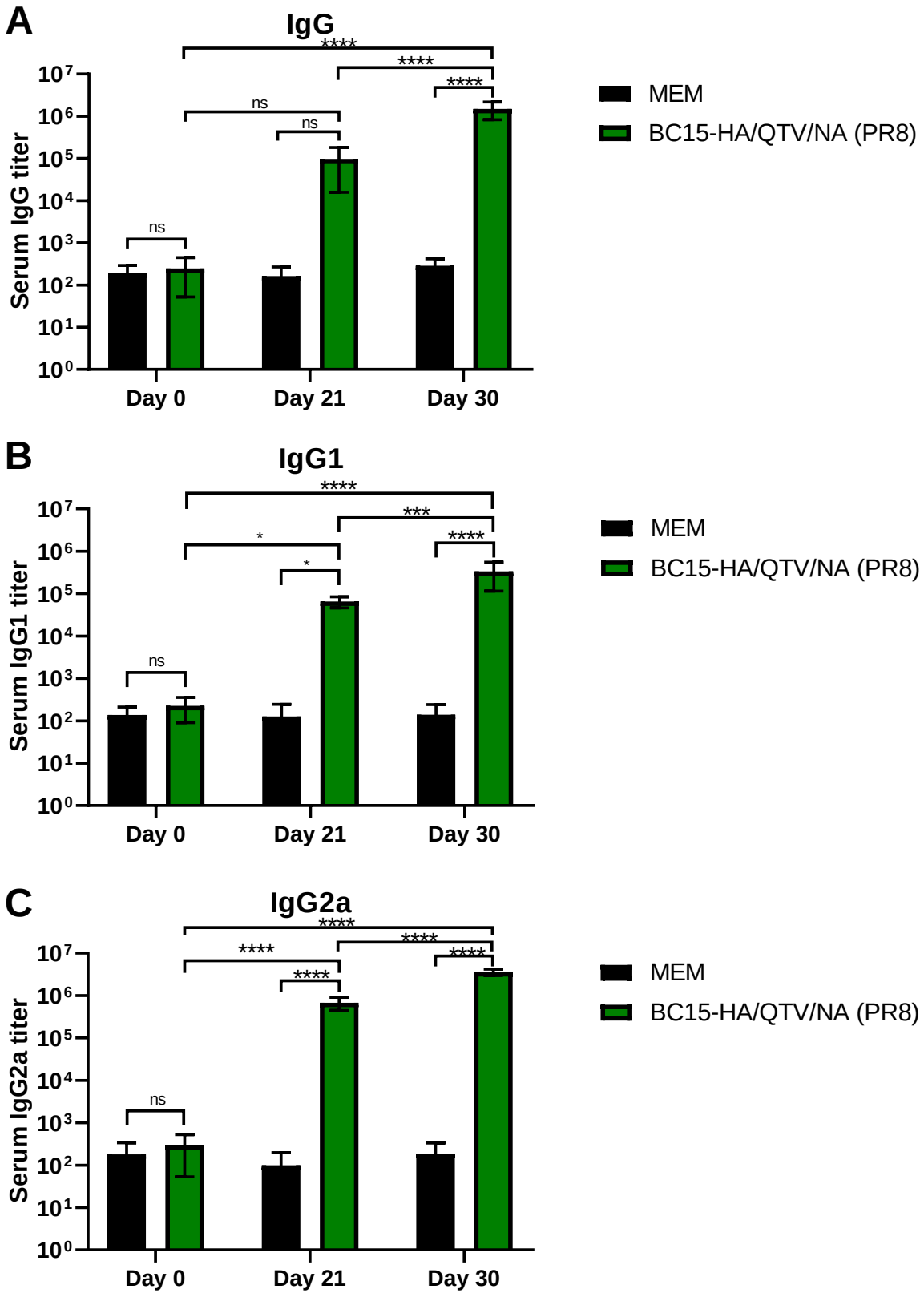
A
IgG
Serum IgG titer
10^7
10^6
10^5
10^4
10^3
10^2
10^1
10^0
****
****
****
ns
ns
ns
Day 0
Day 21
Day 30
MEM
BC15-HA/QTV/NA (PR8)
B
IgG1
Serum IgG1 titer
****
***
*
****
*
ns
Day 0
Day 21
Day 30
MEM
BC15-HA/QTV/NA (PR8)
C
IgG2a
Serum IgG2a titer
****
****
****
****
****
ns
Day 0
Day 21
Day 30
MEM
BC15-HA/QTV/NA (PR8)

Figure 5.4. Antibody responses induced by BC15-HA/QTV/NA (PR8) vaccination. BALB/c mice were vaccinated on days 0 and 21 with MEM (control) or BC15-HA/QTV/NA (PR8) (1 X 10^3 PFU). Serum was collected on days 0, 21, and 30 to be titered using an ELISA to detect influenza-specific IgG, IgG1, and IgG2a; samples were analyzed in triplicate. **(A)** IgG. **(B)** IgG1. **(C)** IgG2a. The bars represent the mean value obtained from all mice in the respective groups, and the error bar represents the standard deviation. Significant differences among groups are signified by * ($p < 0.05$), ** ($p < 0.01$), *** ($p < 0.001$) or **** ($p < 0.0001$). ns = not significant.

5.4.3 The replication-defective BC15-HA/QTV/NA (PR8) virus completely protects mice from a lethal challenge of BC15 (H7N9)

To evaluate the protective efficacy of the recombinant mutant BC15-HA/QTV/NA (PR8) virus against BC15 (H7N9), male and female BALB/c mice were intranasally immunized on days 0 and 21 with MEM (control, 'mock-vaccinated') or 1 X 10^3 PFU of BC15-HA/QTV/NA (PR8) (vaccinated). On day 31 (10 days after the second vaccination), the mice were challenged with either MEM (control, 'mock-challenged') or a lethal dose of BC15 (H7N9) (1 X 10^3 PFU) (vaccinated) (Lu et al., 2019). These mice were monitored for 14 days post-challenge for body weight loss and survival rates (Figure 5.1 and Table 5.1). Mice that were mock-vaccinated and mock-challenged with MEM survived the duration of the trial, slightly gaining weight as the days progressed. Likewise, the mice that were vaccinated with BC15-HA/QTV/NA (PR8) and challenged with BC15 (H7N9) survived the duration of the trial, also gaining weight as the days progressed. Conversely, the mice that were mock-vaccinated with MEM and challenged with BC15 (H7N9) demonstrated rapid weight loss, reaching a humane endpoint of weight loss greater than 20% of their initial body weight within 6 and 7 days post-challenge (Figure 5.5A-B). Therefore, these results demonstrated that the recombinant mutant BC15-HA/QTV/NA (PR8) virus completely protected the mice against a lethal homologous challenge of BC15 (H7N9) virus, evident by a lack of body weight loss and a 100% survival rate.

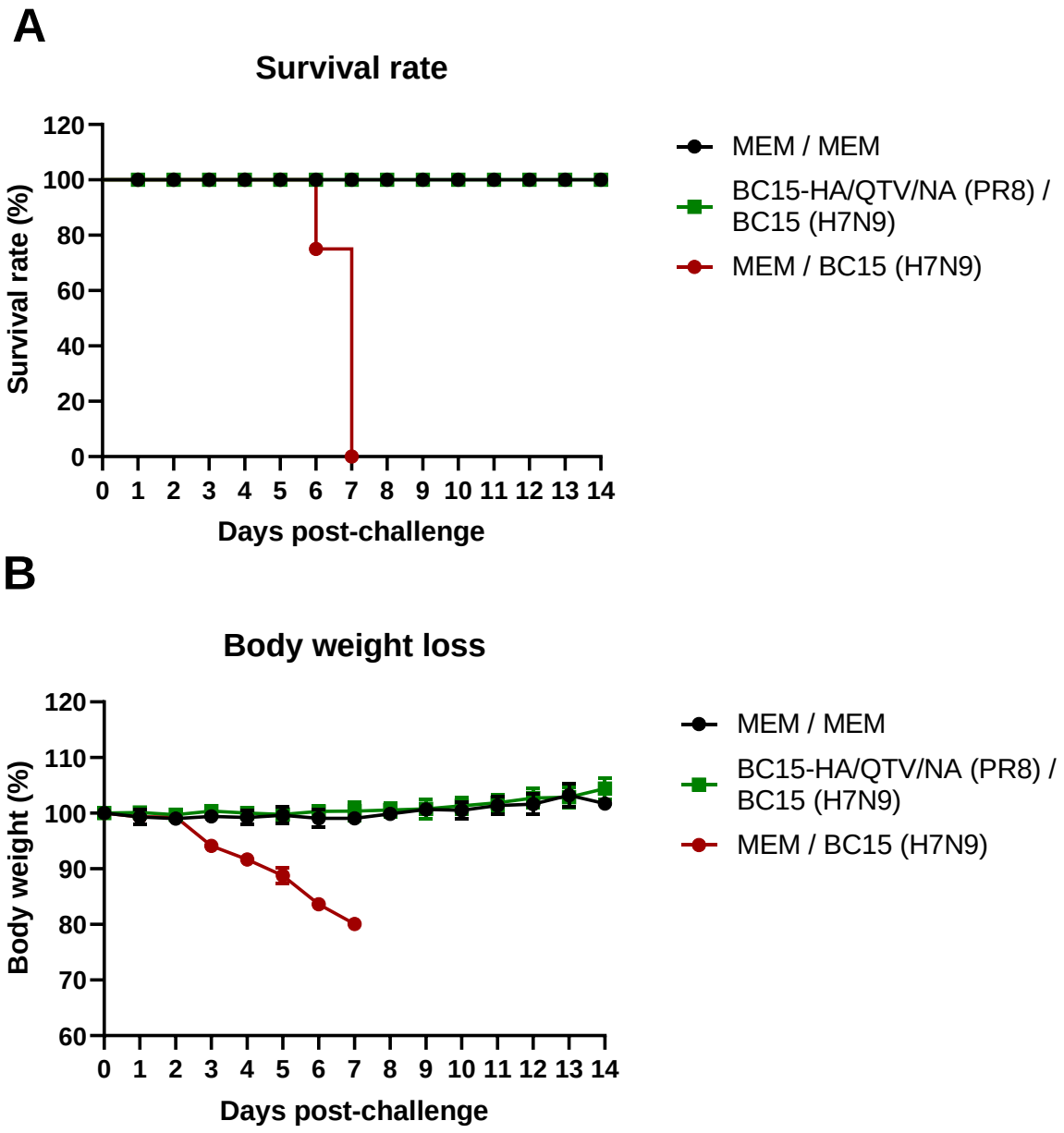

Figure 5.5. The survival rate and body weight loss of vaccinated mice after homologous viral challenge with BC15 (H7N9).
BALB/c mice (*n* = 8 or 10 per group; equal males and females) were vaccinated with two doses of MEM (control) or BC15-HA/QTV/NA (PR8) (1 X 10^3 PFU) followed by an intranasal challenge of a lethal dose of BC15 (H7N9) (1 X 10^3 PFU). **(A)** The survival rates. **(B)** The body weight loss.

5.4.4 Vaccination with BC15-HA/QTV/NA (PR8) eliminated virus replication in the mouse lung

To further investigate the protective efficacy of the recombinant mutant BC15-HA/QTV/NA (PR8) virus, lung tissue was collected from mice that received two intranasal vaccinations of either MEM (control, 'mock-vaccinated') or BC15-HA/QTV/NA (PR8) virus (1 X 10^3 PFU) (vaccinated) followed by a challenge with either MEM (control, 'mock-challenged') or a lethal dose of BC15 (H7N9) (1 X 10^3 PFU), homogenized, and titrated by the $TCID_{50}$ assay (Figure 5.6). The mice mock-vaccinated and mock-challenged with MEM displayed no viral replication. In contrast, the mice mock-vaccinated with MEM and challenged with BC15 (H7N9) displayed high lung mean viral loads on 3 days post-challenge ($10^{7.65}$ $TCID_{50}$/gr), 6 days post-challenge ($10^{6.65}$ $TCID_{50}$/gr), and 7 days post-challenge ($10^{6.36}$ $TCID_{50}$/gr), with all the mice succumbing to infection by 7 days post-challenge (Figure 5.5). In the BC15-HA/QTV/NA (PR8) vaccinated group, no viral replication in the mouse lung was detected by $TCID_{50}$ assay at 3 and 14 days post-challenge These findings are consistent with the lack of body weight loss and 100% survival rate in this BC15-HA/QTV/NA (PR8) vaccinated group (Figure 5.5).

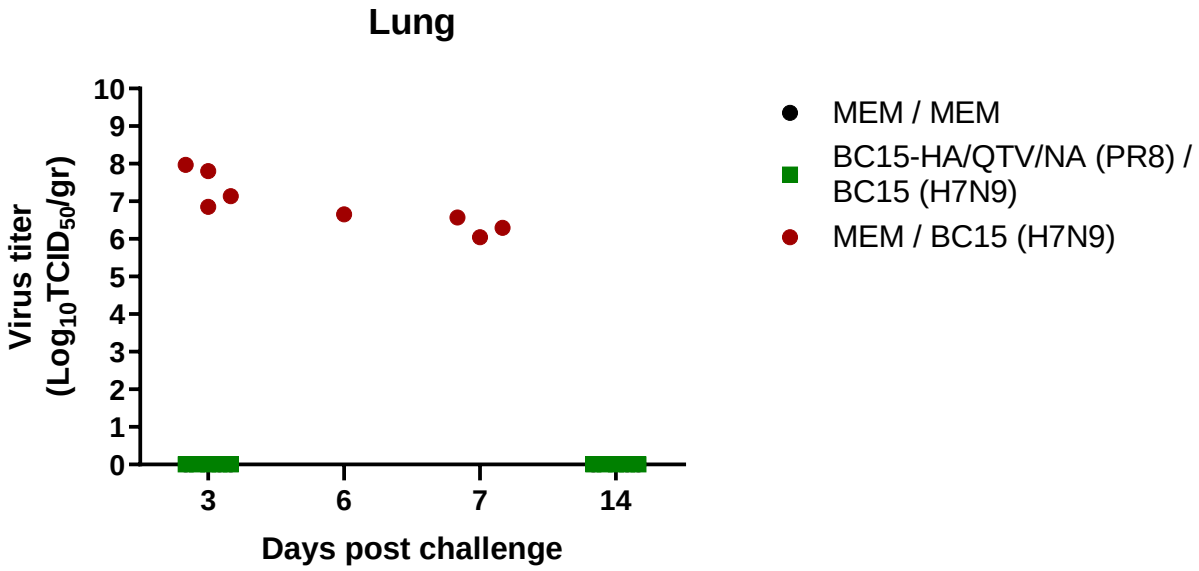

Figure 5.6. Viral titration of the mouse lung from BC15-HA/QTV/NA (PR8) vaccinated mice after homologous viral challenge with BC15 (H7N9).
BALB/c mice were intranasally vaccinated with two doses of MEM (control) or BC15-HA/QTV/NA (PR8) (1 X 10^3 PFU). These mice were then intranasally challenged with BC15 (H7N9) at a lethal dose of 1 X 10^3 PFU. [*n* = eight per group; four males and four females for MEM and MEM / BC15 (H7N9)]; [*n* = 10 per group; five males and five females for BC15-

HA/QTV/NA (PR8) / BC15 (H7N9)]. Viral titration of the homogenized lung tissue was conducted by the $TCID_{50}$ assay; samples were analyzed in quadruplicate. Four mice per group were humanely euthanized on 3 days post-challenge, while the remaining mice were euthanized on 14 days post-challenge Dots correspond to the individual murine lung titers; the four dots on 3 days post-challenge corresponding to four mice that were humanely euthanized; the one dot on 6 days post-challenge corresponding to one mouse that succumbed to infection; three dots on 7 days post-challenge correspond to three mice that succumbed to infection.

5.4.5 Vaccination with BC15-HA/QTV/NA (PR8) reduced the production of proinflammatory cytokines in the mouse lung associated with the influenza infection

To confirm that vaccination with the replication-defective virus vaccine provided complete protection against the viral challenge, the gene expression of various cytokines and chemokines after BC15 (H7N9) virus challenge was evaluated by qPCR. Retinoic acid-inducible gene-I (RIG-I) is an important pattern recognition receptor (PRR) that recognizes foreign RNA from IAV. This recognition leads to the initiation of the antiviral state which helps to restrict IAV replication through the production of various type I IFNs and IFN-stimulated genes (ISGs) (Liu et al., 2018). As shown in Figure 5.7, while the mRNA levels of RIG-I were significantly upregulated in the mice mock-vaccinated with MEM and challenged with BC15 (H7N9) (over 15-fold), mRNA levels in the mice vaccinated with BC15-HA/QTV/NA (PR8) and challenged with BC15 (H7N9) were comparable to the mice mock-vaccinated and mock-challenged with MEM. IFN-α, IFN-β, and IFN-γ are essential IFNs for the activation of the innate immune response due to their antiviral properties. These IFNs have also been shown to possess immunomodulatory effects, enhance the expression of major histocompatibility complex (MHC) class I and II molecules, as well as be an important activator of natural killer (NK) cells (Price et al., 2000). These IFNs were significantly upregulated in the mice mock-vaccinated with MEM and challenged with BC15 (H7N9) (IFN-α around 1000-fold, IFN-β around 6000-fold, and IFN-γ around 200-fold), but remained unchanged in the mice vaccinated with BC15-HA/QTV/NA (PR8) and challenged with BC15 (H7N9) when compared to the mice mock-vaccinated and mock-challenged with MEM. The mRNA levels of IFN-γ-inducing protein 10 (IP-10), a cytokine produced as a by-product of IFN-γ production also displayed significant upregulation in the mice mock-vaccinated with MEM and challenged with BC15 (H7N9) (over 300-fold). However, there was no significant change in the BC15-HA/QTV/NA (PR8) vaccinated and mock-vaccinated and

mock-challenged MEM control groups (Dufour et al., 2002). Conversely, the mRNA levels of proinflammatory cytokines TNFα, IL-6, and IL-1β, as well as anti-inflammatory cytokine IL-10, displayed similar trends, in that significant upregulation was observed in the mice mock-vaccinated with MEM and challenged with BC15 (H7N9) (TNFα around 80-fold, IL-6 around 150-fold, IL-1β around 10-fold and IL-10 around 30-fold). However, there was no significant change in the mice vaccinated with BC15-HA/QTV/NA (PR8) and challenged with BC15 (H7N9) when compared to the mock-vaccinated and mock-challenged MEM control group. There was no significant change for IL-18 for all groups tested.

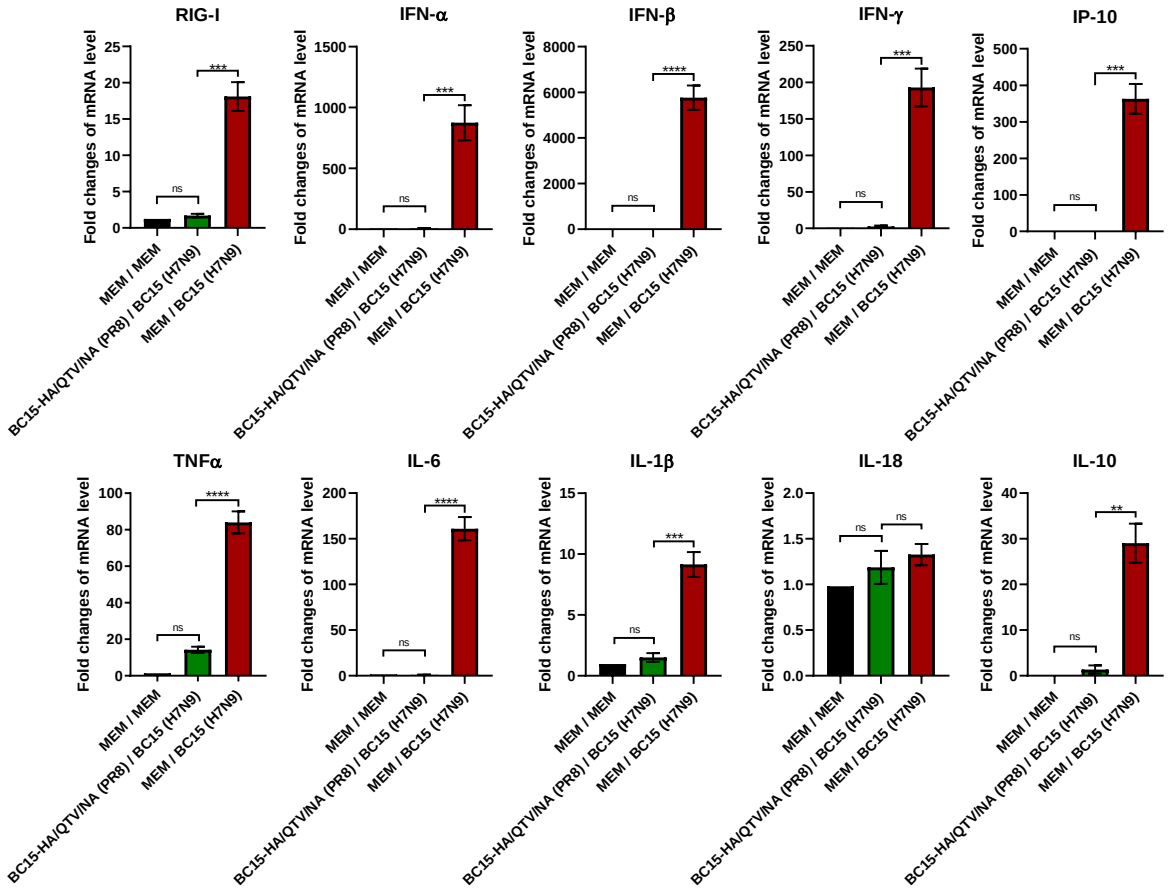

Figure 5.7. Cytokine production after homologous viral challenge with BC15 (H7N9). The mRNA levels of RIG-I, IFN-α, IFN-β, IFN-γ, IP-10, TNFα, IL-6, IL-1β, IL-18, and IL-10 were determined from the mouse lung on 3 days post-challenge (*n* = four mice per group; two males and two females). These levels were assessed by qPCR, where each sample was tested in triplicate. The bars represent the mean value obtained from all mice in the respective group, and the error bar represents the standard deviation. Significant differences among groups are signified by * ($p < 0.05$), ** ($p < 0.01$), *** ($p < 0.001$) or **** ($p < 0.0001$). ns = not significant.

5.5 DISCUSSION AND CONCLUSIONS

In previous studies, the efficacy of an elastase-dependent mutant virus vaccine candidate defective through the introduction of an elastase-sensitive motif to the HA cleavage site was demonstrated. This virus was generated through the mutation of the original trypsin-sensitive motif (Arg-Gly) to Val-Gly or Ala-Gly. These studies have shown that these mutant viruses are inactive during infection due to the inability of host proteases to cleave the elastase-sensitive HA cleavage site, which results in HA remaining in its precursor form. Remaining in this precursor form inhibits the exposure of the fusion peptide within HA2, which prevents fusion of the virus to the endosomal membrane and the continuation of the replication cycle (Masic et al., 2008). In the previous chapter, we generated a recombinant mutant H7N9 virus, BC15-HA/QTV/NA (PR8) and demonstrated this virus to be strictly elastase-dependent and genetically stable *in vitro*, as well as be replication-defective in male and female BALB/c mice. This is similar to a study performed by *Masic et al.*, in that two reverse-genetics generated swine mutant viruses, SIV/SK-R345V and SIV/SK-R345A were elastase-dependent, genetically stable, and replication-defective in pigs at doses of 1 X 10^5 PFU/ml and 1 X 10^6 PFU/ml, respectively (Masic et al., 2008). In this chapter, we found two intranasal vaccinations with BC15-HA/QTV/NA (PR8) to be sufficient in providing 100% protection against a homologous lethal challenge of BC15 (H7N9) in mice. These vaccinated and challenged mice experienced no body weight loss throughout the duration of the trial, with levels comparable to the mock-vaccinated and mock-challenged with MEM (Figure 5.5). These BC15-HA/QTV/NA (PR8) vaccinated and BC15 (H7N9) challenged mice also possessed a 100% survival rate. In comparison, the mice mock-vaccinated with MEM and challenged with BC15 (H7N9) displayed rapid body weight loss, with all mice in this group succumbing to infection by 7 days post-challenge. The BC15 (H7N9) virus was undetected in the lungs of mice vaccinated with BC15-HA/QTV/NA (PR8) and challenged with BC15 (H7N9), whereas high viral loads were detected in the mock-vaccinated and mock-challenged MEM control group (Figure 5.6). Similarly, a study performed by *Masic et al.* for his prior research demonstrated that the SIV/SK-R345V mutant virus administered intratracheally at a 4 X 10^6 PFU dose completely protected pigs against a homologous challenge (Masic et al., 2009). These results aid in the conclusion that the BC15-HA/QTV/NA (PR8) virus can sufficiently protect mice from a lethal dose of BC15 (H7N9).

It has long been believed that both the cell-mediated immunity and humoral immunity play essential, yet distinct roles in the control of influenza viruses. Humoral immunity has been known to entirely block and prevent influenza infection through the production of antibodies against various influenza antigens (Bahadoran et al., 2016; Thomas et al., 2006). More specifically, it has been shown that the most important antibody for the neutralization of influenza is the HA-specific antibody, one that is induced after influenza vaccination. This antibody functions by mainly binding to the trimeric globular head of HA on the influenza virus to block attachment and entry of the virus into the host cell. Antibodies are also generated against the HA stem of influenza virus, although to a lesser extent (Bahadoran et al., 2016). On the contrary, cell-mediated immunity does not prevent viral entry but instead promotes the viral clearance through the activation of T cells, specifically $CD4^+$ and $CD8^+$ T cells. $CD8^+$ T cells are known to differentiate into cytotoxic T lymphocytes (CTLs), with their primary function being to aid in the host defence by killing virus-infected cells. The production of IFN-γ has been shown to aid in the differentiation of $CD8^+$ T cells into CTLs. Conversely, $CD4^+$ T cells possess a more complex role, differentiating into Th1 or Th2 cells upon influenza infection, to activate B cells, stimulate antibody production, as well as express antiviral cytokines such as IFN-γ. $CD4^+$ T cells are also known to produce cytokines such as IL-5 and IL-4, known to promote antibody responses (Chen et al., 2018). The production of IFN-γ, therefore, is essential for the control of influenza virus within the host cell. IFN-γ is also known to possess antiviral activity and is one of the first cytokines produced in response to pathogen invasion which leads to the activation of macrophages and NK cells to aid in controlling infection (Tau and Rothman, 1999). Moreover, the induction of cell-mediated immunity has been correlated with the protection against the highly pathogenic avian influenza (HPAI) viruses, such as the H5N1 influenza virus. Several studies have demonstrated that the protection against the HPAI viruses can be entirely mediated by cellular immunity, even in the complete absence of humoral immunity (Thomas et al., 2006). In our study, two intranasal vaccinations with BC15-HA/QTV/NA (PR8) was adequate to induce significant levels of IFN-γ secreting-cells in the mouse spleen (Figure 5.2A). In a previous study, significant elevation of IFN-γ secreting-cells was also induced following two intranasal vaccinations of the swine mutant virus SIV/SK-R345V in pigs, which conferred protection against homologous challenge (Masic et al., 2010). Simultaneously, two intranasal vaccinations of BC15-HA/QTV/NA (PR8) was also sufficient to induce significant levels of IL-5 secreting-

cells, although to a lower extent compared to IFN-γ (Figure 5.2B). These results, therefore, demonstrate that this recombinant mutant BC15-HA/QTV/NA (PR8) virus is capable of inducing T cell activation.

Antibody responses to the BC15-HA/QTV/NA (PR8) virus were determined in the mouse serum after the first and second immunization. Analysis by the HAI assay demonstrated the production of neutralization antibodies above the gold standard HAI cut-off of 40 after both the first (HAI titer of 115) and second immunizations (HAI titer of 309). Analysis by the SVN assay also demonstrated the high production of neutralization antibodies that could correlate with protection after the first (SVN titer of 369) and second immunizations (SVN titer of 1547) (Figure 5.3). In addition, the levels of antigen-specific IgG, IgG1, and IgG2a were significantly elevated after both the first and second immunizations (Figure 5.4). IgG2a and IgG1 are known to be immunoglobulin indicators for Th1 and Th2 responses, respectively (Mountford et al., 1994). A Th1 response is known to produce cytokines such as IFN-γ and IL-2, aiding in the production of the cell-mediated response. Conversely, a Th2 response aids in the production of IL-4, IL-5, and IL-10 and antibody production. Since IgG1 and IgG2a were both elevated after the first and second immunizations, this could potentially point to both Th1 and Th2 responses being important for the protection against BC15 (H7N9) virus. This dual induction could also be due to the genetic background of the mice we used (BALB/c), which are Th2 prone, and could possess a large effect on the immune responses we observed (Geeraedts et al., 2008). This theory could be tested by performing the same study in Th1 prone mice, such as C57BL/6 mice, and comparing the results. Therefore, these findings could potentially indicate that one vaccination could be sufficient to induce protection in the mice against BC15 (H7N9), although further research would be required to test this theory.

Influenza viruses, such as H7N9, are known to be potent inducers of proinflammatory cytokines, which can lead to inflammation and damage of the lung epithelial cells (Lu et al., 2019). One of the host's first line of defence against influenza virus is inflammation, a process responsible for the activation of both the innate and adaptive immune responses in an effort to control the disease. If not regulated properly, the inflammatory response can induce a cytokine storm, which can often result in substantial pathology and occasional death of the host. This cytokine storm can be characterized by the production of proinflammatory cytokines such as TNFα, IL-6, and IL-1 (D'Elia et al., 2013). In chapter 3 of my thesis, during the establishment of

a mouse model of British Columbia/2015 (H7N9) virus, BC15 (H7N9) was found to be a potent inducer of proinflammatory cytokines and chemokines in the mouse lung (Lu et al., 2019). Several studies have demonstrated that the success of a vaccine is correlated to the levels of proinflammatory cytokines induced; the reduction of proinflammatory cytokines such as IFN-α, TNFα or IL-6 can reduce the pathogenesis of the influenza disease (Van Reeth et al., 2002). In this study, the levels of proinflammatory cytokines and chemokines IFN-α, IFN-β, IFN-γ, IP-10, TNFα, IL-6, IL-1β, and IL-10 were all significantly reduced when compared to the mice mock-vaccinated with MEM and challenged with BC15 (H7N9) (Figure 5.7). Similarly, a previous study also demonstrated the reduction of proinflammatory cytokine induction through vaccination with an elastase mutant virus in pigs (Masic et al., 2009). The levels of RIG-I, one of the major receptors that recognize the influenza virus and activates type I IFN production was also significantly reduced (Loo and Gale, 2011). In addition, the level of the anti-inflammatory cytokine, IL-10, was significantly lower than that in the mice mock-vaccinated with MEM and challenged with BC15 (H7N9). Therefore, this significant reduction of proinflammatory and anti-inflammatory cytokines and chemokines clearly show that the administration of two intranasal vaccinations of BC15-HA/QTV/NA (PR8) virus elicits complete protection against a homologous lethal challenge of BC15 (H7N9).

The two main types of vaccines against influenza virus are the inactivated influenza vaccines (IIV) and the live attenuated influenza vaccines (LAIV). IIVs have been broadly obtainable since the 1940s, and are most commonly propagated in an egg-based system, although they can also be propagated in a cell-culture based system (Blanco-Lobo et al., 2019). In Canada, the only approved influenza vaccines are those that are inactivated and produced in eggs (PHAC, 2019). Unfortunately, IIVs have been known to possess a variety of disadvantages, some of which include their poor efficacy against homologous and heterologous variants (Sridhar et al., 2015). Conversely, LAIVs are a newer type of vaccine that can be completely generated and propagated in a cell-culture based system, avoiding the egg-based system. This avoidance of the egg-based system can be advantageous when egg-storages occur, large volumes are required, or for the use in individuals with an egg allergy (Sridhar et al., 2015). To date, there is only one LAIV authorized for commercial use, FluMist®; however, its use in Canada has been not permitted for the 2019-2020 season (PHAC, 2019). Albeit the strong potential LAIVs have as a vaccine candidate to influenza viruses, one common disadvantage towards their use is the risk of

reversion by secondary mutations or reassortment between the current circulating field strains and the vaccine virus (Jang and Seong, 2012; Mamerow et al., 2019). Replication-defective virus vaccines are composed of viruses defective in either their replication, synthesis, or viral assembly. These viruses by default possess extremely limited replication within their host, making them safer and more advantageous than LAIVs due to their lower likelihood of virulence reversion (Dudek and Knipe, 2006). The recombinant mutant BC15-HA/QTV/NA (PR8) virus contains a mutation at the HA cleavage site such that the host proteases can no longer cleave HA *in vivo* to create an infectious virus. This lack of HA cleavage, therefore, only permits a single-cycle of replication to occur inside the host cell, and thus, decreases the risk of reversion or reassortment of the recombinant mutant BC15-HA/QTV/NA (PR8) virus with a natural influenza virus found in the wild (Masic et al., 2008). The work in this chapter demonstrated that two intranasal vaccinations of BC15-HA/QTV/NA (PR8) were sufficient to generate protection against a homologous challenge of BC15 (H7N9). The immune response generated after vaccination induced both arms of the immune system, the humoral and evidence of the cell-mediated immunity. This dual stimulation ability is advantageous in comparison to IIVs, which mainly stimulate the humoral immunity (Sridhar et al., 2015). More importantly, intranasal vaccination with BC15-HA/QTV/NA (PR8) completely prevented influenza replication in the mouse lung, as influenza is known to be a potent agent of proinflammatory cytokine induction and pathology in the host cells (D'Elia et al., 2013). This recombinant mutant BC15-HA/QTV/NA (PR8) virus, therefore, could have a significant impact on preventing the spread of BC15 (H7N9) virus in the human populations. Further research of this BC15-HA/QTV (PR8) virus vaccine should be conducted in other animal models, such as the ferret model, to establish the safety, immunogenicity, and protective efficacy. Further research should also be conducted to evaluate whether one vaccination is sufficient to induce protection, as well as whether this BC15-HA/QTV/NA (PR8) virus vaccine is protective against viral infection with other H7N9 strains given its evidence to stimulate the cell-mediated immunity.

CHAPTER 6 GENERAL DISCUSSION

Replication-defective virus vaccines are generated through the use of viruses that are defective in replication, synthesis, or viral assembly, resulting in extremely limited viral replication in the host cell (Dudek and Knipe, 2006). Replication-defective virus vaccines are advantageous compared to both IIVs and LAIVs because they possess the combined advantages of both types of vaccines, without possessing the disadvantages. More specifically, replication-defective vaccines, like IIVs, are extremely safe due to their limited replication within the host (Dudek and Knipe, 2006). This limited replication avoids the possibility of virulence reversion, a common concern of LAIVs (Watanabe et al., 2001). Replication-defective virus vaccines are also capable of inducing the same immune responses LAIVs induce, specifically, $CD4^+$ T cells, $CD8^+$ T cells, and the humoral immune response, which is in contrast to IIVs, which induce a limited primarily humoral immune response (Dudek and Knipe, 2006). Therefore, the goal of this study was to develop a replication-defective virus vaccine that could confer protection against the H7N9 influenza virus. In order to achieve this goal, my Master's project included three aims; (1) the establishment of a mouse animal model of A/British Columbia/01/2015 (H7N9) [BC15 (H7N9)]; (2) The generation and characterization of a replication-defective H7N9 virus vaccine; and (3) The evaluation of the immunogenicity and protective efficacy of this replication-defective virus vaccine in mice.

6.1.1 The establishment of a mouse model of A/British Columbia/01/2015 [BC15 (H7N9)] virus

When studying IAV, animal models are important for elucidating mechanisms, the roles various viral and host factors play in the severity of the disease, as well as aiding in the development of interventions to either prevent or reduce the severity of the disease. Depending on the research conducted, different animal models are available; some of them being mice, cotton rats, Syrian hamsters, dogs, domestic swine, cynomolgus macaques, marmosets, ferret, and guinea pigs (Thangavel and Bouvier, 2014). Mice are considered the most common influenza animal model due to their moderately low cost, availability, small size and thus ease of handling and availability of reagents. In addition, several different inbred strains and outbred stocks of mice, as well as transgenic, knockout, and knock-in strains are available (Rodriguez et al., 2017; Thangavel and Bouvier, 2014). Albeit these advantages of the use of the mouse model

for influenza virus, their response to influenza infection is not identical to that of humans. For one, mice display different clinical signs of infection compared to humans, including anorexia, lethargy, hunching and a rough coat (Bouvier and Lowen, 2010). Influenza infection in mice is also clinically characterized as primary viral pneumonia, which can be marked with heavy breathing and severe pulmonary histopathology upon euthanization (Fukushi et al., 2011; Tripp and Tompkins, 2009). Secondly, many subtypes of influenza virus directly isolated from humans are not directly infectious or pathogenic in inbred mouse strains such as BALB/c and C57BL/6 (Bouvier and Lowen, 2010). For these isolates to become infectious, they characteristically need to be serially passaged in mice (Tripp and Tompkins, 2009). However, some influenza viruses isolated from humans can directly infect and cause disease in mice, some of these strains include the 1918 H1N1 pandemic strain, most of the HPAI H5N1 strains, and some of the H7 strains, including the H7N9 virus that arose in 2013 in China (Bouvier and Lowen, 2010; Hai et al., 2013). For my first aim, we developed a mouse model of British Columbia/01/2015 (H7N9) [BC15 (H7N9)] virus. This model development entailed intranasally infecting BALB/c mice with three different doses of BC15 (H7N9) (10^3 PFU, 10^4 PFU, and 10^5 PFU) and then monitoring the mice for clinical signs and body weight changes. This model development also entailed analyzing viral load, various cytokines and chemokines, and pathology in the mouse lung. Our study demonstrated that this human isolate could directly infect mice to result in the influenza disease, similar to other studies (Hai et al., 2013). This disease was prevalent among all three doses tested, with high viral replication detected in the respiratory tract, as well as substantial production of various proinflammatory cytokines and chemokines in the mouse lung. Moreover, since all doses tested were lethal in mice, we chose the lowest dose (10^3 PFU) to be the optimal dose for future studies.

6.1.2 The generation and characterization of the mutant H7N9 virus with its modified HA segment *in vitro* and *in vivo*

During the IAV replication cycle, the HA precursor form, HA0, undergoes cleavage into HA1 and HA2 by trypsin-proteases found within the host. This cleavage is essential for IAVs infectivity, pathogenicity, and the ability to spread to different hosts (Stech et al., 2005). Several studies have demonstrated that the alteration of the HA cleavage site from a trypsin-sensitive motif to an elastase-sensitive motif generates a replication-defective IAV *in vivo* (Masic et al.,

2008; Stech et al., 2005). These viruses have been shown to be replication-defective due to the lack of the appropriate protease at the infection site inhibiting cleavage of HA which concomitantly prevents fusion of the virus to the host endosome, and thus, blocks further replication of the virus (Masic et al., 2008). Correspondingly, we tested this replication-defective concept for the development of a replication-defective virus vaccine candidate for BC15 (H7N9) in mice.

To test this strategy we generated a recombinant mutant BC15-HA/QTV/NA (PR8) virus using the reverse genetics system, composed of the six internal genes of A/Puerto Rico/8 (H1N1) [PR8 (H1N1)], the mutated HA, as well as the wild-type NA from BC15 (H7N9). This HA was mutated such that it was strictly susceptible to cleavage by the protease elastase. Characterization of this recombinant mutant BC15-HA/QTV/NA (PR8) virus resulted in the discovery that this virus to not only grows similar to its wild-type counterpart, BC15-HA/NA (PR8) but also is genetically stable after five passages in MDCK cells *in vitro*. More importantly, this recombinant mutant BC15-HA/QTV/NA (PR8) virus was found to be non-virulent in mice, with no detectable clinical signs and viral replication in the lungs of infected mice. These findings suggested that the BC15-HA/QTV/NA (PR8) virus was replication-defective in mice and could potentially serve as a replication-defective virus vaccine candidate in mice.

6.1.3 The evaluation of the immunogenicity and protective efficacy after intranasal administration of the replication-defective virus vaccine against A/British Columbia/01/2015 [BC15 (H7N9)] virus

Since the goal of this study was to develop a replication-defective virus vaccine for H7N9 IAV, the next aim of this study was to test the immunogenic and protective efficacy of this recombinant mutant BC15-HA/QTV/NA (PR8) virus in mice. To evaluate portions of the cell-mediated response, we performed the ELISPOT assay to detect IFN-γ and IL-5 secreting cells. IFN-γ, a type II IFN, and part of the type 1 immune response is produced when NK cells detect foreign invaders and become activated (Lee et al., 2017a). This production of IFN-γ has been shown to play an essential role in antiviral immunity by linking the innate immune response to the stimulation of the adaptive immune response (Vivier et al., 2008). On the other hand, IL-5, a cytokine part of the type 2 immune response, is one of the vital cytokines responsible for eosinophil persistence in humans and B cell growth in mice (Takatsu, 2011). Although the

majority of viral infections are characterized by production of the typical type 1 immune responses, the production of type 2 immune responses is often accompanied by a pre-existing allergy disease (Bendelja et al., 2000). However, there is increasing evidence to support the idea that the production of a type 2 immune response may actually be involved in protecting the infected tissue from damage inflicted from infection (Allen and Wynn, 2011). As shown in section five (Figure 5.2), BC15-HA/QTV/NA (PR8) is capable of inducing significantly elevated numbers of both IFN-γ and IL-5 secreting cells after the second vaccination, although the IFN-γ levels were substantially higher compared to IL-5. These levels could suggest that although IFN-γ secreting cells play a predominant role, the production of IL-5 could also aid in the protection against BC15 (H7N9).

To assess the humoral response, we performed the HAI assay, SVN assay, and ELISA on the mouse serum taken before the first vaccination, after the first vaccination, and after the second vaccination. The results from these assays were all somewhat similar as shown in section five (Figure 5.3-5.4), in that elevated levels of HAI titers, SVN titers, IgG and IgG1 titers were prominent after the first vaccination. The IgG2a levels were significantly elevated after the first vaccination. However, after the second vaccination, the HAI assay, SVN assay, and ELISA had significantly elevated titers compared to before and after the first vaccination. These significantly elevated titers point to the requirement of two vaccinations of this BC15-HA/QTV/NA (PR8) virus in mice to elicit sufficient protection against BC15 (H7N9), although the protection efficacy was not measured after a single vaccination. However, these results demonstrated that the BC15-HA/QTV/NA (PR8) virus is capable of inducing a strong humoral immune response after two intranasal vaccinations in mice.

In order to evaluate the protective efficacy of the recombinant mutant BC15-HA/QTV/NA (PR8) virus in mice, after two intranasal vaccinations, we challenged the mice with a lethal dose of BC15 (H7N9). As demonstrated in section five, two vaccinations were sufficient to completely protect mice against a homologous challenge. This conferred protection was evident by the lack of clinical signs and body weight loss observed in the BC15-HA/QTV/NA (PR8) vaccinated group (Figure 5.5). These vaccinated mice also showed no evidence of viral load by the $TCID_{50}$ assay, as well as no proinflammatory cytokine induction when compared to the mice mock-vaccinated with MEM and challenged with BC15 (H7N9)

(Figure 5.6-5.7). These results demonstrated that this recombinant mutant BC15-HA/QTV/NA (PR8) virus completely protected the mice from a viral infection with BC15 (H7N9).

Altogether, our data demonstrated that two intranasal administrations of BC15-HA/QTV/NA (PR8) induced significantly elevated immune responses that could explain the protection observed after homologous challenge with BC15 (H7N9). In addition, the possibility of the BC15-HA/QTV/NA (PR8) virus causing disease in mice was substantially reduced due to its replication-defective phenotype, generating a desirable vaccine candidate for the H7N9 IAV. Due to the lack of a commercially available vaccine for H7N9 infection in humans, this recombinant mutant BC15-HA/QTV/NA (PR8) virus possesses strong potential as a preventive measure for a potential H7N9 pandemic.

6.1.4 Future directions

Although this recombinant mutant BC15-HA/QTV/NA (PR8) virus can be considered a desirable vaccine candidate against H7N9 infection, much more research should be performed to ensure its candidacy. For one, although this recombinant mutant BC15-HA/QTV/NA (PR8) virus has been proven stable *in vitro* after a small number of passages, one should perform a similar experiment *in vivo* to ensure this stability accurately represents what could occur in nature. In addition, one should measure the protective efficacy after a single vaccination, as well as optimize the dosage of the vaccine. These factors play a major role in the vaccination industry concerning compliance rates, cost, manufacturing time, required volume, etc. Other important research that could be conducted would be to measure the protective and cross-protective efficacy against other H7 subtypes, and other subtypes in general, such as HPAI H5N1. Influenza vaccines are known for their low cross-protective efficacy, so this should be determined for the recombinant mutant BC15-HA/QTV/NA (PR8) virus for its vaccine candidacy. If this recombinant mutant BC15-HA/QTV/NA (PR8) virus demonstrated acceptable results concerning the above research, then I believe it could be considered as a strong vaccine candidate for the world in which we live in.

REFERENCES

Abdel-Nasser;, Abdel-Ghafar;, Tawee, C., Zhancheng, G., al;, e., 2008. Update on Avian Influenza A H5N1 Virus Infection in Humans. N. Engl. J. Med. 358, 261-273.

Acheson, N.H., 2011. Fundamentals of Molecular Virology. 2nd edition, 210.

Allen, J.E., Wynn, T.A., 2011. Evolution of Th2 immunity: a rapid repair response to tissue destructive pathogens. PLoS Pathog 7, e1002003.

Appel, W., 1974. Elastase: General Information. Methods of Enzymatic Analysis 2, 1041-1045.

Babiuk, S., Masic, A., Graham, J., Neufeld, J., van der Loop, M., Copps, J., Berhane, Y., Pasick, J., Potter, A., Babiuk, L.A., Weingartl, H., Zhou, Y., 2011. An elastase-dependent attenuated heterologous swine influenza virus protects against pandemic H1N1 2009 influenza challenge in swine. Vaccine 29, 3118-3123.

Badham, M.D., Rossman, J.S., 2016. Filamentous Influenza Viruses. Curr Clin Microbiol Rep 3, 155-161.

Bahadoran, A., Lee, S.H., Wang, S.M., Manikam, R., Rajarajeswaran, J., Raju, C.S., Sekaran, S.D., 2016. Immune Responses to Influenza Virus and Its Correlation to Age and Inherited Factors. Front Microbiol 7.

Baudin, F., Bach, C., Cusack, S., Ruigrok, R.W., 1994. Structure of influenza virus RNP. I. Influenze virus nucleoprotein melts secondary structure in panhandle RNA and exposes the bases to the solvent. EMBO J 13, 3158-3165.

Belser, J.A., Creager, H.M., Sun, X., Gustin, K.M., Jones, T., Shieh, W.J., Maines, T.R., Tumpey, T.M., 2016. Mammalian Pathogenesis and Transmission of H7N9 Influenza Viruses from Three Waves, 2013-2015. J Virol 90, 4647-4657.

Belser, J.A., Gustin, K.M., Pearce, M.B., Maines, T.R., Zeng, H., Pappas, C., Sun, X., Carney, P.J., Villanueva, J.M., Stevens, J., Katz, J.M., Tumpey, T.M., 2013. Pathogenesis and transmission of avian influenza A (H7N9) virus in ferrets and mice. Nature 501, 556-559.

Belshe, R., Lee, M.S., Walker, R.E., Stoddard, J., Mendelman, P.M., 2004. Safety, immunogenicity and efficacy of intranasal, live attenuated influenza vaccine. Expert Rev Vaccines 3, 643-654.

Bendelja, K., Gagro, A., Bace, A., Lokar-Kolbas, R., Krsulovic-Hresic, V., Drazenovic, V., Milinaric-Galinovic, G., Rabatic, S., 2000. Predominant type-2 response in infants with respiratory syncytial virus (RSV) infection demonstrated by cytokine flow cytometry. Clin Exp Immunol 121, 332-338.

Berg, J.M., Tymoczko, J.L., Stryer, L., 2007. Biochemistry. 6.

Black, L.D., Allen, P.G., Morris, S.M., Stone, P.J., Suki, B., 2008. Mechanical and Failure Properties of Extracellular Matrix Sheets as a Function of Structural Protein Composition. Biophysical Journal 94, 1916-1929.

Blanco-Lobo, P., Nogales, A., Rodriguez, L., Martínez-Sobrido, L., 2019. Novel Approaches for The Development of Live Attenuated Influenza Vaccines. Viruses 11, 190.

Böttcher-Friebertshäuser, E., Hans-Dieter, K., Garten, W., 2013. Activation of influenza viruses by proteases from host cells and bacteria in the human airway epithelium. Pathogens and Disease 69, 87-100.

Böttcher, E., Matrosovich, T., Beyerle, M., Klenk, H., Garten, W., Matrosovich, M., 2006. Proteolytic Activation of Influenza Viruses by Serine Proteases TMPRSS2 and HAT from Human Airway Epithelium. J Virol 80, 9896-9898.

Bouvier, N.M., Lowen, A.C., 2010. Animal Models for Influenza Virus Pathogenesis and Transmission. Viruses 2, 1530-1563.
Bouvier, N.M., Palese, P., 2011. The Biology of Influenza Viruses. Vaccine 26, D49-D53.
Cady, S.D., Luo, W., Hu, F., Hong, M., 2009. Structure and Function of the Influenza A M2 Proton Channel. Biochemistry 48, 7356-7364.
CDC, 2015. Spread of Bird Flu Viruses Between Animals and People.
CDC, 2017. Types of Influenza Viruses.
Cha, T.A., Kao, K., Zhao, J., Fast, P.E., Mendelman, P.M., Arvin, A., 2000. Genotypic stability of cold-adapted influenza virus vaccine in an efficacy clinical trial. J Clin Microbiol 38, 839-845.
Chan, M.C., Chan, R.W., Chan, L.L., Mok, C.K., Hui, K.P., Fong, J.H., Tao, K.P., Poon, L.L., Nicholls, J.M., Guan, Y., Peiris, J.S., 2013a. Tropism and innate host responses of a novel avian influenza A H7N9 virus: an analysis of ex-vivo and in-vitro cultures of the human respiratory tract. Lancet Respir Med 1, 534-542.
Chan, M.C., Cheung, C.Y., Chui, W.H., Tsao, S.W., Nicholls, J.M., Chan, Y.O., Chan, R.W., Long, H.T., Poon, L.L., Guan, Y., al., e., 2005. Proinflammatory cytokine responses induced by influenza A (H5N1) viruses in primary human alveolar and bronchial epithelial cells. Respir. Res 6.
Chan, M.C.W., Chan, R.W.Y., Chan, L.L.Y., Mok, C.K.P., Hui, K.P.Y., Fong, J.H.M., Tao, K.P., Poon, L.L.M., Nicholls, J.M., Guan, Y., Peiris, J.S.M., 2013b. Tropism and innate host responses of a novel avian influenza A H7N9 virus: an analysis of ex-vivo and in-vitro cultures of the human respiratory tract. The Lancet Respiratory Medicine 1, 534-542.
Chen, J., Lee, K.H., Steinhauer, D.A., Stevens, D.J., Skehel, J.J., Wiley, D.C., 1998. Structure of the Hemagglutinin Precursor Cleavage Site, a Determinant of Influenza Pathogenicity and the Origin of the Labile Conformation. Cell 95, 409-417.
Chen, L., Sun, L., Li, R., Chen, Y., Zhang, Z., Xiong, C., Zhao, G., Jiang, Q., 2016. Is a highly pathogenic avian influenza virus H5N1 fragment recombined in PB1 the key for the epidemic of the novel AIV H7N9 in China, 2013? Int. J. Infect. Dis. 43, 85-89.
Chen, X., Liu, S., Goraya, M.U., Maarouf, M., Huang, S., Chen, J.L., 2018. Host Immune Response to Influenza A Virus Infection. Front Immunol 9.
Cheng, W., Wang, X., Shen, Y., Yu, Z., Liu, S., Cai, J., Chen, E., 2017. Comparison of the three waves of avian influenza A(H7N9) virus circulation since live poultry markets were permanently closed in the main urban areas in Zhejiang Province, July 2014 - June 2017. Wiley Online Library 12.
Chi, Y., Zhu, Y., Wen, T., Cui, L., Ge, Y., Jiao, Y., Wu, T., Ge, A., Ji, H., Xu, K., Bao, C., Zhu, Z., Qi, X., Wu, B., Shi, Z., Tang, F., Xing, Z., Zhou, M., 2013. Cytokine and chemokine levels in patients infected with the novel avian influenza A (H7N9) virus in China. J Infect Dis 208, 1962-1967.
Chlanda, P., Schraidt, O., Kummer, S., Riches, J., Oberwinkler, H., Prinz, S., Krausslich, H.G., Briggs, J.A.G., 2015. Structural Analysis of the Roles of Influenza A Virus Membrane-Associated Proteins in Assembly and Morphology. JVI 89.
Cilloniz, C., Shinya, K., Peng, X., Korth, M.J., Proll, S.C., Aicher, L.D., Carter, V.S., Chang, J.H., Kobasa, D., Feldmann, F., Strong, J.E., Feldmann, H., Kawaoka, Y., Katze, M.G., 2009. Lethal influenza virus infection in macaques is associated with early dysregulation of inflammatory related genes. Plos Pathog 5, e1000604.

Claas, E.C.J., Osterhaus, A.D.M.E., van Beek, R., De Jong, J.C., Rimmelzwaan, G.F., Senne, D.A., Krauss, S., Shortridge, K.F., Webster, R.G., 1998. Human influenza A H5N1 virus related to a highly pathogenic avian influenza virus. Lancet 351, 472-477.
Couch, R.B., 1996. Medical Microbiology. 4th edition., Chapter 58.
Couper, K.N., Blount, D.G., Riley, E.M., 2008. IL-10: The Master Regulator of Immunity to Infection. The Journal of Immunology 180, 5771-5777.
Cox, N.J., Kitame, F., Kendal, A.P., Maassab, H.F., Naeve, C., 1998. Identification of sequence changes in the cold-adapted, live attenuated influenza vaccine strain, A/Ann Arbor/6/60 (H2N2). Virology 167, 554-567.
D'Elia, R.V., Harrison, K., Oyston, P.C., Lukaszewski, R.A., Clark, G.C., 2013. Targeting the "Cytokine Storm" for Therapeutic Benefit. Clinical and Vaccine Immunology 20, 319-327.
Darani, H.Y., Doenhoff, M.J., 2009. Anomalous Immunogenic Properties of Serine Proteases. Scandinavian Journal of Immunology 70.
Dawood, F.S., Jain, S., Finelli, L., Shaw, M.W., Lindstrom, S., Garten, R.J., Gubareva, L.V., Xu, X., Bridges, C.B., Uyeki, T.M., 2009. Emergence of a Novel Swine-Origin Influenza A (H1N1) Virus in Humans. N. Engl. J. Med. 360, 2605-2615.
De, C., F;, S;, C., Arcangeletti, M.C., Orlandini, G., Gatti, R., Dettori, G., Chezzi, C., 2011. Differential infectious entry of human influenza A/NWS/33 virus (H1N1) in mammalian kidney cells. Virus Res 155, 221-230.
De Jong, M.D., Simmons, C.P., Thanh, T.T., Hien, V.M., Smith, G.J.D., Chau, T.N.B., Hoang, D.M., Van Vinh Chau, N., Khanh, T.H., Dong, V.C., al., e., 2006. Fatal outcome of human influenza A (H5N1) is associated with high viral load and hypercytokinemia. Nat. Med 12, 1203-1207.
Dortmans, J.C.F.M., Dekkers, J., Ambepitiya Wickramasinghe, I.N., M.H;, V., Rottier, P.J.M., van Kuppeveld, F.J.M., de Vries, E., de Haan, C.A.M., 2013. Adaptation of novel H7N9 influenza A virus to human receptors. Scientific Reports 3.
Dudek, T., Knipe, D.M., 2006. Replication-defective viruses as vaccines and vaccine vectors. Virology 344, 230-239.
Dufour, J.H., Dziejman, M., Liu, M.T., Leung, J.H., Lane, T.E., Luster, A.D., 2002. IFN-γ-Inducible Protein 10 (IP-10; CXCL10)-Deficient Mice Reveal a Role for IP-10 in Effector T Cell Generation and Trafficking. The Journal of Immunology 168, 3195-3204.
Edigner, T.O., Pohl, M.O., Stertz, S., 2014. Entry of influenza A virus: host factors and antiviral targets. Journal of General Virology 95, 263-277.
Fan, R.L., Valkenburg, S.A., Wong, C.K., Li, O.T., Nicholls, J.M., Rabadan, R., Peiris, J.S., Poon, L.L., 2015. Generation of Live Attenuated Influenza Virus by Using Codon Usage Bias. J Virol 89, 10762-10773.
FAO, 2020. H7N9 situation update.
Ferguson, L., Olivier, A.K., Genova, S., Epperson, W.B., Smith, D.R., Schneider, L., Barton, K., McCuan, K., Webby, R.J., Wan, X.F., 2016. Pathogenesis of Influenza D Virus in Cattle. JVI 90.
Frensing, T., Kupke, S.Y., Bachmann, M., Fritzsche, S., Gallo-Ramirez, L.E., Reichl, U., 2016. Influenza virus intracellular replication dynamics, release kinetics, and particle morphology during propagation in MDCK cells. Applied Microbiology Biotechnology 100, 7181-7192.
Fukushi, M., Ito, T., Kitazawa, T., Miyoshi-Akiyama, T., Kirikae, T., Yamashita, M., Kudo, K., 2011. Serial histopathological examination of the lungs of mice infected with influenza A virus PR8 strain. PLoS One 6, e21207.

Gabriel, G., Garn, H., Wegmann, M., Renz, H., Herwig, A., Klenk, H.D., Stech, J., 2008. The potential of a protease activation mutant of a highly pathogenic avian influenza virus for a pandemic live vaccine. Vaccine 26, 956-965.
Gamblin, S.J., Skehel, J.J., 2010. Influenza Hemagglutinin and Neuraminidase Membrane Glycoproteins. J Biol Chem 285, 28403-28409.
Gao, D., Chen, Y., Han, D., Qi, Q., Sun, X., Zhang, H., Feng, H., Wang, M., 2017. Membrane-anchored stalk domain of influenza HA enhanced immune responses in mice. Microbial Pathogenesis 113, 421-426.
Gao, R., Cao, B., Hu, Y., Feng, Z., Wang, D., Hu, W., Chen, J., Jie, Z., Qiu, H., Xu, K., Xu, X., Lu, H., Zhu, W., Gao, Z., Xiang, N., Shen, Y., He, Z., Gu, Y., Zhang, Z., Yang, Y., Zhao, X., Zhou, L., Li, X., Zou, S., Zhang, Y., Li, X., Yang, L., Guo, J., Dong, J., Li, Q., Dong, L., Zhu, Y., Bai, T., Wang, S., Hao, P., Yang, W., Zhang, Y., Han, J., Yu, H., Li, D., Gao, G.F., Wu, G., Wang, Y., Yuan, Z., Shu, Y., 2013. Human Infection with a Novel Avian-Origin Influenza A (H7N9) Virus. New England Journal of Medicine 368, 1888-1897.
Geeraedts, F., Bungener, L., Pool, J., ter Veer, W., Wilschut, J., Huckriede, A., 2008. Whole inactivated virus influenza vaccine is superior to subunit vaccine in inducing immune responses and secretion of proinflammatory cytokines by DCs. Influenza Other Respir Viruses 2, 41-51.
Graef, K.M., Vreede, F.T., Y.F;, L., McCall, A.W., Carr, S.M., Subbarao, K., Fodor, E., 2010. The PB2 subunit of the influenze virus RNA polymerase affects virulence by interacting with the mitochondrial antiviral signaling protein and inhibiting expression of beta interferon. J Virol 84, 8433-8445.
Gramegna, A., Amati, F., Terranova, L., Sotgiu, G., Tarsia, P., Miglietta, D., Calderazzo, M.A., Aliberti, S., Blasi, F., 2017. Neutrophil elastase in bronchiectasis. Respir. Res 18.
Grove, J., Marsh, M., 2011. The cell biology of receptor-mediated virus entry. JCB 195, 1071.
Groves, H.T., McDonald, J.U., Langat, P., Kinnear, E., Kellam, P., McCauley, J., Ellis, J., Thompson, C., Elderfield, R., Parker, L., Barclay, W., Tregoning, J.S., 2018. Mouse Models of Influenza Infection with Circulating Strains to Test Seasonal Vaccine Efficacy. Frontiers in Immunology 9.
Guan, Y., Smith, G.J.D., 2013. The emergence and diversification of panzootic H5N1 influenza viruses. Virus Res 178, 35-43.
Hai, R., Schmolke, M., Leyva-Grado, V.H., Thangavel, R.R., Margine, I., Jaffe, E.L., Krammer, F., Solórzano, A., Garcia-Sastre, A., Palese, P., Bouvier, N.M., 2013. Influenza A(H7N9) virus gains neuraminidase inhibitor resistance without loss of in vivo virulence or transmissibility. Nat Commun 4.
Hai, R., Schmolke, M., Varga, Z.T., Manicassamy, B., Wang, T.T., Belser, J.A., Pearce, M.B., Garcia-Sastre, A., Tumpey, T.M., Palese, P., 2010. PB1-F2 expression by the 2009 pandemic H1N1 influenza virus has minimal impact on virulence in animal models. J Virol 84, 4442-4450.
Hamilton, B.S., Whittaker, G.R., Daniel, S., 2012. Influenza Virus-Mediated Membrane Fusion: Determinants of Hemagglutinin Fusogenic Activity and Experimental Approaches for Assessing Virus Fusion. Viruses 4, 1144-1168.
Hatta, M., Gao, P., Halfmann, P., Kawaoka, Y., 2001a. Molecular basis for high virulence of Hong Kong H5N1 influenza A viruses. Science 293, 1840-1842.
Hatta, M., Gao, P., Halfmann, P., Kawaoka, Y., 2001b. Molecular basis for high virulence of Hong Kong H5N1 influenza A viruses. Science 293, 1840-1842.
Hay, A.J., Lomniczi, B., Bellamy, A.R., Skehel, J.J., 1977. Transcription of the influenza virus genome. Virology 83, 337-355.

Herz, C., Stavnezer, E., Krug, R.M., 1981. Influenza Virus, an RNA Virus, Synthesizes Its Messenger RNA in the Nucleus of Infected Cells Cell 26, 391-400.
Hoffmann, E., Neumann, G., Kawaoka, Y., Hobom, G., Webster, R.G., 2000. A DNA transfection system for generation of influenza A virus from eight plasmids. PNAS 97, 6108-6113.
Hoffmann, E., Stech, J., Guan, Y., Webster, R.G., Perez, D.R., 2001. Universal primer set for the full-length amplification of all influenza A viruses. Arch Virol 146, 2275-2289.
Huarte, M., Sanz-Ezquerro, J.J., Roncal, F., Ortin, J., Nieto, A., 2001. PA Subunit from Influenza Virus Polymerase Complex Interacts with a Cellular Protein with Homology to a Family of Transcriptional Activators. Journal of General Virology 75, 8597-8604.
Idriss, H.T., Naismith, J.K., 2000. TNFα and the TNF receptor superfamily: Structure‐function relationship(s). Microscopy Research and Technique 50, 184-195.
Isakova-Sivak, I., Rudenko, L., 2017. Tackling a novel lethal virus: a focus on H7N9 vaccine development. Expert Rev Vaccines 16, 709-721.
Iwasaki, A., Pillai, P.S., 2014. Innate immunity to influenza virus infection. Nat Rev Immunol 14, 315-328.
Jagger, B.W., Wise, H.M., Kash, J.C., Walters, K.A., Wills, N.M., Xiao, Y., Dunfee, R.L., Schwartzman, L.M., Ozinsky, A., Bell, G.L., Dalton, R.M., Lo, A., Efstathiou, S., Atkins, J.F., Firth, A.E., Taubenberger, J.K., Digard, P., 2012. An overlapping protein-coding region in influenza A virus segment 3 modu-lates the host response. Science 337, 199-204.
Jang, Y.H., Seong, B., 2012. Principles underlying rational design of live attenuated influenza vaccines. Clin Exp Vaccine Res 1, 35-49.
Jin, H., Lu, B., Zhou, H., Ma, C., Zhao, J., Yang, C.F., Kemble, G., Greenberg, H., 2003. Multiple amino acid residues confer temperature sensitivity to human influenza virus vaccine strains (FluMist) derived from cold-adapted A/Ann Arbor/6/60. Virology 306, 18-24.
Jin, Y., Ren, H., Teng, Y., Hu, M., Peng, X., Yue, J., Liang, L., 2017. Novel reassortment of avian influenza A(H7N9) virus with subtype H6N6 and H5N6 viruses circulating in Guangdong Province, China. Journal of Infection 75, 179-182.
Kaplanski, G., 2018. Interleukin-18: Biological properties and role in disease pathogenesis. Immunological Reviews 281, 138-153.
Kärber, G., 1931. Beitrag zur kollektiven Behandlung pharmakologischer Reihenversuche. Naunyn-Schmiedebergs Arch. Exp. Pathol. Pharmakol. 162, 480-483.
Katsura, H., Iwatsuki-Horimoto, K., Fukuyama, S., Watanabe, S., Sakabe, S., Hatta, Y., Murakami, S., Shimojima, M., Horimoto, T., Kawaoka, Y., 2012. A replication-incompetent virus possessing an uncleavable hemagglutinin as an influenza vaccine. Vaccine 30, 6027-6033.
King, J.C., Lagos, R., Bernstein, D.I., Piedra, P.A., Kotloff, K., Bryant, M., Cho, I., Belshe, R.B., 1998. Safety and immunogenicity of low and high doses of trivalent live cold-adapted influenza vaccine administered intranasally as drops or spray to healthy children. J Infect Dis 177, 1394-1397.
Krammer, F., Smith, G.J.D., Fouchier, R.A.M., Peiris, M., Kedzierska, K., Doherty, P.C., Palese, P., Shaw, M.L., Treanor, J., Webster, R.G., García-Sastre, A., 2018. Influenza. Nat Rev Dis Primers 4, 3.
Kreijtz, J.H.C.M., Fouchier, R.A.M., Rimmelzwaan, G.F., 2011. Immune responses to influenza virus infection. Virus Research 162, 19-30.
Kuhn, C., Senior, R.M., 1978. The role of elastases in the development of emphysema. Lung 155, 185-187.

Lee, A.J., Chen, B., Chew, M.V., Barra, N.G., Shenouda, M.M., Nham, T., van Rooijen, N., Jordana, M., Mossman, K.L., Schreiber, R.D., Mack, M., Ashkar, A.A., 2017a. Inflammatory monocytes require type I interferon receptor signaling to activate NK cells via IL-18 during a mucosal viral infection. J Exp Med 214, 1153-1167.
Lee, C.Y., An, S.H., Kim, I., Go, D.M., Kim, D.Y., Choi, J.G., Lee, Y.J., Kim, J.H., Kwon, H.J., 2017b. Prerequisites for the acquisition of mammalian pathogenicity by influenza A virus with a prototypic avian PB2 gene. Nature 7.
Lee, L.Y.Y., Izzard, L., Hurt, A.C., 2018. A Review of DNA Vaccines Against Influenza. Front Immunol 9.
Li, J., Yu, M., Zheng, W., Liu, W., 2015. Nucleocytoplasmic Shuttling of Influenza A Virus Proteins. Viruses 7, 2668-2682.
Lin, D., Lan, J., Zhang, Z., 2007. Structure and Function of the NS1 Protein of Influenza A Virus. Acta Biochim Biophys 39, 155-162.
Liu, G., Lu, Y., Thulasi Raman, S.N., Xu, F., Wu, Q., Li, Z., Brownlie, R., Liu, Q., Zhou, Y., 2018. Nuclear-resident RIG-I senses viral replication inducing antiviral immunity. Nat. Commun. 9, 3199.
Loo, Y.M., Gale, M., 2011. Immune Signaling by RIG-I-like Receptors. Immunity 34, 680-692.
Lorenzo, M.M.G., Fenton, M.J., 2013. Immunobiology of Influenza Vaccines. Chest 143, 502-510.
Lu, Y., Landreth, S., Gaba, A., Hlasny, M., Liu, G., Huang, Y., Zhou, Y., 2019. In Vivo Characterization of Avian Influenza A (H5N1) and (H7N9) Viruses Isolated from Canadian Travelers. Viruses 11, 193.
Ma, W., Kahn, R.E., Richt, J.A., 2009. The pig as a mixing vessel for influenza viruses: Human and veterinary implications. J Mol Genet Med 3, 158-166.
Maassab, H.F., Bryant, M.L., 1999. The development of live attenuated cold-adapted influenza virus vaccine for humans. Rev Med Virol 9, 237-244.
Maier, H.J., Kashiwagi, T., Hara, K., Brownlee, G.G., 2008. Differential role of the influenza A virus polymerase PA subunit for vRNA and cRNA promoter binding. Virology 370, 194-204.
Mamerow, S., Scheffter, R., Röhrs, S., Stech, O., Blohm, U., Schwaiger, T., Schröder, C., Ulrich, R., Schinköthe, J., Beer, M., Mettenleiter, T.C., Stech, J., 2019. Double-attenuated influenza virus elicits broad protection against challenge viruses with different serotypes in swine. Vet Microbiol 231, 160-168.
Manzoor, R., Igarashi, M., Takada, A., 2017. Influenza A Virus M2 Protein: Roles from Ingress to Egress. Int J Mol Sci 18, 2649.
Masic, A., Babiuk, L.A., Zhou, Y., 2008. Reverse genetics-generated elastase-dependent swine influenza viruses are attenuated in pigs. Journal of General Virology 90, 375-385.
Masic, A., Booth, J.S., Mutwiri, G.K., Babiuk, L.A., Zhou, Y., 2009. Elastase-dependent Live Attenuated Swine Influenza A Viruses Are Immunogenic and Confer Protection against Swine Influenza A Virus Infection in Pigs. Journal of Virology 83, 10198-10210.
Masic, A., Lu, X., Li, J., Mutwiri, G.K., Babiuk, L.A., 2010. Immunogenicity and protective efficacy of an elastase-dependent live attenuated swine influenza virus vaccine administered intranasally in pigs. Vaccine 28, 7098-7108.
Masic, A., Pyo, H.M., Babiuk, S., Zhou, Y., 2013. An eight-segment swine influenza virus harboring H1 and H3 hemgglutinins is attenuated and protective against H1N1 and H3N2 subtypes in pigs. J Virol 87, 10114-10125.

Matrosovich, M.N., Matrosovich, T.Y., Gray, T., Roberts, N.A., Klenk, H.D., 2004. Neuraminidase Is Important for the Initiation of Influenza Virus Infection in Human Airway Epithelium. J Virol 78, 12665-12667.
Maurer-Stroh, S., Li, Y., Bastien, N., Gunalan, V., Lee, R.T., Eisenhaber, F., Booth, T.F., 2014. Potential human adaptation mutation of influenza A(H5N1) virus, Canada. Emerg. Infect. Dis. 20, 1580-1582.
Meliopoulos, V.A., Karlsson, E.A., Kercher, L., Cline, T., Freiden, P., Duan, S., Vogel, P., Webby, R.J., Guan, Y., Peiris, M., Thomas, P.G., Schultz-Cherry, S., 2014. Human H7N9 and H5N1 Influenza Viruses Differ in Induction of Cytokines and Tissue Tropism. Journal of Virology 88, 12982-12991.
Mohn, K.G.I., Smith, I., Sjursen, H., Cox, R.J., 2018. Immune responses after live attenuated influenza vaccination. Hum Vaccin Immunother 14, 571-578.
Moore, D.L., 2018. Vaccine recommendations for children and youth for the 2018/2019 influenza season. Canadian Paediatric Society.
Mountford, A.P., Fisher, A., Wilson, R.A., 1994. The profile of IgG1 and IgG2a antibody responses in mice exposed to Schistosoma mansoni. Parasite Immunol 16, 521-527.
Mueller, S., Coleman, J.R., Papamichail, D., Ward, C.B., Nimnual, A., Futcher, B., Skiena, S., Wimmer, E., 2011. Live Attenuated Influenza Vaccines by Computer-Aided Rational Design. Nat Biotechnol 28, 723-726.
Muramatsu, M., Yoshida, R., Yokoyama, A., Miyamoto, H., Kajihara, M., Maruyama, J., Nao, N., Manzoor, R., Takada, A., 2014. Comparison of Antiviral Activity between IgA and IgG Specific to Influenza Virus Hemagglutinin: Increased Potential of IgA for Heterosubtypic Immunity. PLos One 9, e85582.
Muramoto, Y., Noda, T., Kawakami, E., Akkina, R., Kawaoka, Y., 2013. Identificationof novel influenza A virus proteins translated from PA mRNA. J Virol 87, 2455-2462.
Murray, P.R., Rosenthal, K.S., Pfaller, M.A., 2013. Medical Microbiology. Elsevier 7, 524-532.
Nakatsu, S., Murakami, S., Shindo, K., Horimoto, T., Sagara, H., Noda, T., Kawaoka, Y., 2018. Influenza C and D Viruses Package Eight Organized Ribonucleoprotein Complexes. JVI 92, e02084-02017.
Neumann, G., Hughes, M.T., Kawaoka, Y., 2000. Influenza A virus NS2 protein mediates vRNP nuclear export through NES-independent interaction with hCRM1. EMBO J 19, 6751-6758.
Nilsson, B.E., Velthuis, A.J.W.T., Fodor, E., 2017. Role of the PB2 627 Domain in Influenza A Virus Polymerase Function. Journal of Virology 91, e02467-02416.
Noda, T., 2011. Native Morphology of Influenza Virions. Front Microbiol 2.
Nogales, A., Baker, S.F., Ortiz-Riaño, E., Dewhurst, S., Topham, D.J., Martínez-Sobrido, L., 2014. Influenza A virus attenuation by codon deoptimization of the NS gene for vaccine development. J Virol 88, 10525-10540.
Offlu, 2019. Influenza A Cleavage Sites. OIE FAO network of expertise on animal influenza
Ohkura, T., Momose, F., Ichikawa, R., Takeuchi, K., Morikawa, Y., 2014. Influenza A Virus Hemagglutinin and Neuraminidase Mutually Accelerate Their Apical Targeting through Clustering of Lipid Rafts. JVI 88, 10039-10055.
Opitz, B., Rejaibi, A., Dauber, B., Eckhard, J., Vinzing, M., Schmeck, B., Hippenstiel, S., Suttorp, N., Wolff, T., 2007. IFN? induction by influenza A virus is mediated by RIG-I which is regulated by the viral NS1 protein. Cellular Microbiology 9, 930-938.
Osterholm, M.T., Kelley, N.S., Sommer, A., Belongia, E.A., 2012. Efficacy and effectiveness of influenza vaccines: a systematic review and meta-analysis. Lancet Infect Dis 12, 36-44.

Pabbaraju, K., Tellier, R., Wong, S., Li, Y., Bastien, N., Tang, J.W., Drews, S.J., Jang, Y., Davis, C.T., Fonseca, K., al., e., 2014a. Full-Genome Analysis of Avian Influenza A(H5N1) Virus from a Human, North America, 2013. Emerg. Infect. Dis. 20, 887-891.
Pabbaraju, K., Tellier, R., Wong, S., Li, Y., Bastien, N., Tang, J.W., Drews, S.J., Jang, Y., Davis, C.T., Fonseca, K., Tipples, G.A., 2014b. Full-Genome Analysis of Avian Influenza A(H5N1) Virus from a Human, North America, 2013. Emerging Infectious Diseases 20.
Park, H.S., Liu, G., Thulasi Raman, S.N., Landreth, S., Liu, Q., Zhou, Y., 2018. NS1 Protein of 2009 Pandemic Influenza A Virus Inhibits Porcine NLRP3 Inflammasome-Mediated Interleukin-1 Beta Production by Suppressing ASC Ubiquitination. J Virol 92, e00022-00018.
Paterson, D., Fodor, E., 2012. Emerging Roles for the Influenza A Virus Nuclear Export Protein (NEP). PLOS 8.
Perrone, L.A., Plowden, J.K., Garcia-Sastre, A., Katz, J.M., Tumpey, T.M., 2008a. H5N1 and 1918 pandemic influenza virus infection results in early and excessive infiltration of macrophages and neutrophils in the lungs of mice. Plos Pathog 4.
Perrone, L.A., Plowden, J.K., Garcia-Sastre, A., Katz, J.M., Tumpey, T.M., 2008b. H5N1 and 1918 pandemic influenza virus infection results in early and excessive infiltration of macrophages and neutrophils in the lungs of mice.
. PLoS Pathog 4.
PHAC, 2017a. Canadian Immunization Guide Chapter on Influenza and Statement on Seasonal Influenza Vaccine for 2017-2018.
PHAC, 2017b. Canadian Immunization Guide: Part 1- Key Immunization Information. Government of Canada.
PHAC, 2018. Canada's pandemic laboratory strategy. The Public Health Agency of Canada 44-1: Emergency planning.
PHAC, 2019. Canadian Immunization Guide Chapter on Influenza and Statement on Seasonal Influenza Vaccine for 2019–2020.
Pinto, L.H., Holsinger, L.J., Lamb, R.A., 1992. Influenza virus M2 protein has ion channel activity. Cell 69, 517-528.
Portela, A., Digard, P., 2002. The influenza virus nucleoprotein: a multifunctional RNA-binding protein pivotal to virus replication. Journal of General Virology 83, 723-734.
Price, G.E., Gaszewska-Mastarlarz, A., Moskophidis, D., 2000. The Role of Alpha/Beta and Gamma Interferons in Development of Immunity to Influenza A Virus in Mice. J Virol 74, 3996-4003.
Pyo, H.M., Hlasny, M., Zhou, Y., 2015. Influence of maternally-derived antibodies on live attenuated influenza vaccine efficacy in pigs. Vaccine 33, 3667-3672.
Pyo, H.M., Zhou, Y., 2014. Protective efficacy of intranasally administered bivalent live influenza vaccine and immunological mechanisms underlying the protection. Vaccine 32, 3835-3842.
Qi, W., Jia, W., Liu, D., Li, J., Bi, Y., Xie, S., Li, B., Hu, T., Du, Y., Xing, L., Zhang, J., Zhang, F., Wei, X., Eden, J.S., Li, H., Tian, H., Li, W., Su, G., Lao, G., Xu, C., Xu, B., Liu, W., Zhang, G., Ren, T., Holmes, E.C., Cui, J., Shi, W., Gao, G.F., Liao, M., 2018. Emergence and Adaptation of a Novel Highly Pathogenic H7N9 Influenza Virus in Birds and Humans from a 2013 Human-Infecting Low-Pathogenic Ancestor. J Virol 92, e00921-00917.
Racaniello, V., 2009. Pathogenesis of influenza in humans. Virology Blog.

Rao, X., Huang, X., Zhou, Z., Lin, X., 2013. An improvement of the 2ˆ(–delta delta CT) method for quantitative real-time polymerase chain reaction data analysis. Biostat Bioinforma Biomath 3, 71-85.
Regan, J.F., Liang, Y., Parslow, T.G., 2006. Defective assembly of influenza A virus due to a mutation in the polymerase subunit PA. J Virol 80, 252-261.
Reich, S., Guilligay, D., Pflug, A., Malet, H., Berger, I., Crépin, T., Hart, D., Lunardi, T., Nanao, M., Ruigrok, R.W.H., Cusack, S., 2014. Structural insight into cap-snatching and RNA synthesis by influenza polymerase. Nature 516, 361-366.
Rodriguez, L., Nogales, A., Martínez-Sobrido, L., 2017. Influenza A Virus Studies in a Mouse Model of Infection. J. Vis. Exp 127.
Romangnani, S., 2000. T-cell subsets (Th1 versus Th2). Ann Allergy Asthma Immunol 85, 9-18.
Rowe, T., Banner, D., Farooqui, A., Ng, D.C., Kelvin, A.A., Rubino, S., Huang, S.S., Fang, Y., Kelvin, D.J., 2010. In vivo ribavirin activity against severe pandemic H1N1 Influenza A/Mexico/4108/2009. J Gen Virol 91, 2898-2906.
Saito, L.B., Diaz-Satizabal, L., Evseev, D., Fleming-Canepa, X., Mao, S., Webster, R.G., Magor, K.E., 2018. IFN and cytokine responses in ducks to genetically similar H5N1 influenza A viruses of varying pathogenicity. Journal of General Virology 99, 464-474.
Samji, T., 2009. Influenza A: Understanding the Viral Life Cycle. Yale J Biol Med 82, 153-159.
Scholtissek, C., 1995. Molecular evolution of influenza viruses. Virus Genes 11, 209-215.
Selman, M., Dankar, S.K., Forbes, N.E., Jia, J.J., Brown, E.G., 2012. Adaptive mutation in influenza A virus non-structural gene is linked to host switching and induces a novel protein by alternative splicing. Emerging Microbes and Infections 1.
Shao, W., Li, W., Goraya, M.U., Wang, S., Chen, J.L., 2017. Evolution of Influenza A Virus by Mutation and Re-Assortment. Int J Mol Sci 18, 1650.
Shi, M., Jagger, B.W., Wise, H.M., Digard, P., Holmes, E.C., Taubenberger, J.K., 2012. Evolutionary conservation of the PA-X open reading frame in segment3 of influenza A virus. J Virol 86, 12411-12413.
Shimizu, T., Takizawa, N., Watanabe, K., Nagata, K., Kobayashi, N., 2011. Crucial role of the influenza virus NS2 (NEP) C-terminal domain in M1 binding and nuclear export of vRNP. FEBS Lett 585, 41-46.
Sieczkarski, S.B., Whittaker, G.R., 2002. Influenza virus can enter and infect cells in the absence of clathrin-mediated endocytosis. J Virol 76, 10455-10464.
Skehel, J.J., Wiley, D.C., 2000. Receptor binding and membrane fusion in virus entry: the influenza hemagglutinin. Annu Rev Biochem 69, 531-569.
Skountzou, I., Satyabhama, L., Stavropoulou, A., Ashraf, Z., Esser, E.S., Vassilieva, E., Koutsonanos, D., Compans, R., Jacob, J., 2014. Influenza Virus-Specific Neutralizing IgM Antibodies Persist for a Lifetime. Clin Vaccine Immunol 21, 1481-1489.
Skowronski, D.M., Chambers, C., Gustafson, R., Purych, D.B., Tang, P., Bastien, N., Krajden, M., Li, Y., 2016. Avian Influenza A(H7N9) Virus Infection in 2 Travelers Returning from China to Canada, January 2015. Emerging Infectious Diseases 22.
Sokol, P.A., Kooi, C., Hodges, R.S., Cachia, P., Woods, D.E., 2000. Immunization with a Pseudomonas aeruginosa Elastase Peptide Reduces Severity of Experimental Lung Infections Due to P. aeruginosa or Burkholderia cepacia. The Journal of Infectious Diseases 181, 1682-1692.

Solorzano, A., Webby, R.J., Lager, K.M., Janke, B.H., Garcia-Sastre, A., Richt, A.J., 2005. Mutations in the NS1 protein of swine influenza virus impair anti-interferon activity and confer attenuation in pigs. J Virol 79, 7535-7543.
Spearman, C., 1908. The Method of 'Right and Wrong Cases' ('Constant Stimuli') without Gauss's Formulae. Br. J. Psychol. 1904-1920 2, 227-242.
Spickler, A.R., 2016. Avian Influenza. The Center for Food Security & Public Health.
Sridhar, S., Brokstad, K.A., Cox, R.J., 2015. Influenza Vaccination Strategies: Comparing Inactivated and Live Attenuated Influenza Vaccines. Vaccines (BaseI) 3, 373-389.
Stech, J., Garn, H., Herwig, A., Stech, O., Dauber, B., Wolff, T., Mettenleiter, T.C., Klenk, H.D., 2011. Influenza B Virus With Modified Hemagglutinin Cleavage Site as a Novel Attenuated Live Vaccine. The Journal of Infectious Diseases 204, 1483-1490.
Stech, J., Garn, H., Wegmann, M., Wagner, R., Klenk, H.D., 2005. A new approach to an influenza live vaccine: modification of the cleavage site of hemagglutinin. nature medicine 11, 683-689.
Stegmann, T., 2000. Membrane fusion mechanisms: the influenza hemagglutinin paradigm and its implications for intracellular fusion. Traffic 1, 598-604.
Su, S., Gu, M., Liu, D., Cui, J., Gao, G.F., Zhou, J., Liu, X., 2017. Epidemiology, Evolution, and Pathogenesis of H7N9 Influenza Viruses in Five Epidemic Waves since 2013 in China. Trends in Microbiology 25.
Subbarao, K., 2019. The Critical Interspecies Transmission Barrier at the Animal–Human Interface. Trop Med Infect Dis 4, 72.
Sun, X., Belser, J.A., Pappas, C., Pulit-Penaloza, J.A., Brock, N., Zeng, H., Creager, H.M., Le, S., Wilson, M., Lewis, A., Stark, T.J., Shieh, W., Barnes, J., Tumpey, T.M., Maines, T.R., 2018. Risk assessment of fifth-wave H7N9 influenza A viruses in mammalian models. Journal of Virology.
Takatsu, K., 2011. Interleukin-5 and IL-5 receptor in health and diseases. Proc Jpn Acad Ser B Phys Biol Sci 87, 463-485.
Tamada, T., K, T., K, K., A, M., O, T., I, K., K, R., T, T., 2009. Combined High-Resolution Neutron and X-ray Analysis of Inhibited Elastase Confirms the Active-Site Oxyanion Hole but Rules against a Low-Barrier Hydrogen Bond. Journal of the American Chemical Society 131, 11033-11040.
Tang, J., Zhang, J., Zhou, J., Zhu, W., Yang, L., Shumei, Z., Wei, H., Xin, L., Huang, W., Li, X., Cheng, Y., Wang, D., 2019. Highly pathogenic avian influenza H7N9 viruses with reduced susceptibility to neuraminidase inhibitors showed comparable replication capacity to their sensitive counterparts. Virology 16.
Taniguchi, T., Takaoka, A., 2002. The interferon-α/β system in antiviral responses: a multimodal machinery of gene regulation by the IRF family of transcription factors. Current Opinion in Immunology 14, 111-116.
Tau, G., Rothman, P., 1999. Biologic functions of the IFN-γ receptors. Allergy 54, 1233-1251.
Tauber, S., Ligertwood, Y., Quigg-Nocol, M., Dutia, B.M., Elliott, R.M., 2012. Behaviour of influenza A viruses differentially expressing segment 2gene products in vitro and in vivo. J Gen Virol 93, 840-849.
Thangavel, R.R., Bouvier, N.M., 2014. Animal models for influenza virus pathogenesis, transmission, and immunology. J Immunol Methods 0, 60-79.
Thomas, P.G., Keating, R., Hulse-Post, D.J., Doherty, P.C., 2006. Cell-mediated Protection in Influenza Infection. Emerg Infect Dis 12, 48-54.

Treanor, J.J., Kotloff, K., Betts, R.F., Belshe, R., Newman, F., Iacuzio, D., Wittes, J., Bryant, M., 1999. Evaluation of trivalent, live, cold-adapted (CAIV-T) and inactivated (TIV) influenza vaccines in prevention of virus infection and illness following challenge of adults with wild-type influenza A (H1N1), A (H3N2), and B viruses. Vaccine 18, 899-906.
Tripp, R.A., Tompkins, S.M., 2009. Animal models for evaluation of influenza vaccines. Curr Top Microbiol Immunol 333, 397-412.
Van Reeth, K., Braeckmans, D., Cox, E., Van Borm, S., van den Berg, T., Goddeeris, B., Vleeschauwer, A.D., 2009. Prior infection with an H1N1 swine influenza virus partially protects pigs against a low pathogenic H5N1 avian influenza virus. Vaccine 27, 6330-6339.
Van Reeth, K., Van Gucht, S., Pensaert, M., 2002. Correlations between lung proinflammatory cytokine levels, virus replication, and disease after swine influenza virus challenge of vaccination-immune pigs. Viral Immunol 15, 583-594.
van Riet, E., Ainai, A., Suzuki, T., Hasegawa, H., 2012. Mucosal IgG responses in influenza virus infections; thoughts for vaccine design. Vaccine 30, 5898-5900.
Varga, Z.T., Ramos, I., Hai, R., Schmolke, M., García-Sastre, A., Fernandez-Sesma, A., Palese, P., 2011. The Influenza Virus Protein PB1-F2 Inhibits the Induction of Type I Interferon at the Level of the MAVS Adaptor Protein. PLOS Pathogens 7, e1002067.
Vasin, A.V., Temkina, O.A., Egorov, V.V., Klotchenko, S.A., Plotnikova, M.A., Kiselev, O.I., 2014. Molecular mechanisms enhancing the proteome of influenza A viruses: an overview of recently discovered proteins. Virus Res 185, 53-63.
Victor, S.T., Watanabe, S., Katsura, H., Ozawa, M., Kawaoka, Y., 2012. A Replication-Incompetent PB2-Knockout Influenza A Virus Vaccine Vector. J Virol 86, 4123-4128.
Vivier, E., Tomasello, E., Baratin, M., Walzer, T., Ugolini, S., 2008. Functions of natural killer cells. Nat Immunol 9, 503-510.
Vries, E.D., Tscherne, D.M., Wienholts, M.J., Cobos-Jiménez, V., Scholte, F., García-Sastre, A., Rottier, P.J.M., C.A.M;, d.H., 2011. Dissection of the Influenza A Virus Endocytic Routes Reveals Macropinocytosis as an Alternative Entry Pathway. PLos Pathog 7, e1001329.
Wacheck, V., Egorov, A., Groiss, F., Pfeiffer, A., Fuereder, T., Hoeflmayer, D., Kundi, M., Popow-Kraupp, T., Redlberger-Fritz, M., Mueller, C.A., Cinatl, J., Michaelis, M., Geiler, J., Bergmann, M., Romanova, J., Roethl, E., Morokutti, A., Wolschek, M., Ferko, B., Seipelt, J., Dick-Gudenus, R., Muster, T., 2010. A novel type of influenza vaccine: safety and immunogenicity of replication-deficient influenza virus created by deletion of the interferon antagonist NS1. J Infect Dis 201, 354-362.
Watanabe, K., Shimizu, T., Noda, S., Tsukahara, F., Maru, Y., Kobayashi, N., 2014. Nuclear export of the influenza virus ribonucleoprotein complex: Interaction of Hsc70 with viral proteins M1 and NS2. FERBS Open Bio 4, 683-688.
Watanabe, T., Wantanabe, S., Neumann, G., Kida, H., Kawaoka, Y., 2001. Immunogenicity and Protective Efficacy of ReplicationIncompetent Influenza Virus-Like Particles. JVI 76, 767-773.
Weber, F., Haller, O., 2007. Viral suppression of the interferon system. Biochimie 89, 836-842.
Webster, R.G., Bean, W.J., Gorman, O.T., Chambers, T.M., Kawaoka, Y., 1992a. Evolution and ecology of influenza A viruses. Microbiol Rev 56, 152-179.
Webster, R.G., Bean, W.J., Gorman, O.T., Chambers, T.M., Kawaoka, Y., 1992b. Evolution and Ecology of Influenza A Viruses. Microbiological Reviews 56, 152-179.
WHO, Cumulative Number of Confirmed Human Cases for Avian Influenza A(H5N1) Reported to WHO, 2003–2018.
WHO, 2017. Human infection with avian influenza A(H7N9) virus – China.

WHO, 2019. Summary of status of development and availability of avian influenza A(H7N9) candidate vaccine viruses. WHO.
Wise, H.M., Foeglein, A., Sun, J., Dalton, R.M., Patel, S., Howard, W., Anderson, E.C., Barclay, W.S., Digard, P., 2009. A complicated message: Identification of a novel PB1-related protein translated from influenza A virus segment 2 mRNA. J Virol 83, 8021-8031.
Wong, S.S., Webby, R.J., 2013. Traditional and New Influenza Vaccines. Clinical Microbiology Reviews 26, 476-492.
Wu, W.W., Sun, Y.H., Pante, N., 2007. Nuclear import of influenza A viral ribonucleoprotein complexes is mediated by two nuclear localization sequences on viral nucleoprotein. Virol J 4, 49.
Yang, Y., Wong, G., Yang, L., Tan, S., Li, J., Bai, B., Xu, Z., Li, H., Xu, W., Zhao, X., Quan, C., Zheng, H., Liu, J.W., Liu, W., Liu, L., Liu, Y., Bi, Y., Gao, G.F., 2019. Comparison between human infections caused by highly and low pathogenic H7N9 avian influenza viruses in Wave Five: Clinical and virological findings. Journal of Infection 78, 241-248.
Yasuda, J., Nakada, S., Kato, A., Toyoda, T., Ishihama, A., 1993. Molecular assembly of influenza virus: association of the NS2 protein with virion matrix. Virology 196, 249-255.
York, A., Fodor, E., 2013. Biogenesis, assembly, and export of viral messenger ribonucleoproteins in the influenza A virus infected cell. RNA Biol 10, 1274-1282.
Zeng, H., Belser, J.A., Goldsmith, C.S., Gustin, K.M., Veguilla, V., Katz, J.M., Tumpey, T.M., 2015. A(H7N9) Virus Results in Early Induction of Proinflammatory Cytokine Responses in both Human Lung Epithelial and Endothelial Cells and Shows Increased Human Adaptation Compared with Avian H5N1 Virus. Journal of Virology 89, 4655-4667.
Zhang, F., Bi, Y., Wang, J., Wong, G., Shi, W., Hu, F., Yang, Y., Yang, L., Deng, X., Jiang, S., He, X., Liu, Y., Yin, C., Zhong, N., Gao, G.F., 2017. Human infections with recently-emerging highly pathogenic H7N9 avian influenza virus in China. J Infect 75, 71-75.
Zheng, H., Xinhua, O., Rusheng, Z., Dong, Y., Lingzhi, L., Ruchun, L., Yelan, L., Jingfang, C., Biancheng, S., 2019. Evolved avian influenza virus (H7N9) isolated from human cases in a middle Yangtze River city in China, from February to April 2017. Heliyon 5, e01253.
Zhu, Y., Qi, X., Cui, L., Zhou, M., Wang, H., 2013. Human co-infection with novel avian influenza A H7N9 and influenza A H3N2 viruses in Jiangsu province, China. The Lancet 381, 2134.

APPENDIX

A. ACHIEVEMENTS DURING THE STUDY

A.1 Publications

Lu, Y., **Landreth, S**., Liu, G., Brownlie, R., Gaba, A., van den Hurk, S.V.D.L., Gerdts, V., Zhou, Y., 2020. Innate immunemodulator containing adjuvant formulated HA based vaccine protects mice from lethal infection of highly pathogenic avian influenza H5N1 virus. *Vaccine.* 38 (10).

Lu, Y*., **Landreth, S***., Gaba, A., Hlasny, M., Liu, G., Huang, Y., Zhou, Y., 2019. In Vivo Characterization of Avian Influenza A (H5N1) and (H7N9) Viruses Isolated from Canadian Travelers. *Viruses*. 11, 193. * Contributed equally

Park, H.S., Liu, G., Raman, S.N.T., **Landreth, S.L**, Liu, Q., Zhou, Y., 2018. NS1 Protein of 2009 Pandemic Influenza A Virus Inhibits Porcine NLRP3 Inflammasome-Mediated Interleukin-1 Beta Production by Suppressing ASC Ubiquitination. *Journal of Virology*. 82 (8), e00022-18.

A.2 Presentations

Landreth, S., Lu, Y., Pandey, K., Zhou, Y. A recombinant mutant H7N9 influenza virus confers complete protection against challenge with influenza H7N9 virus in mouse. Abstract submitted for the American Society for Virology conference, Colorado State University, Fort Collins, Colorado, United States, June 13-17, 2020.

Tian, X., **Landreth, S.,** Lu, Y., Pandey, K., Zhou, Y. A Replication Defective Influenza Virus Harboring H5 and H7 Hemagglutinins Provides Protection against H7N9 and H5N1 Virus Infection in mice. Abstract submitted for the American Society for Virology conference, Colorado State University, Fort Collins, Colorado, United States, June 13-17, 2020.

Landreth, S., Detmer, S., Gerdts, V., Zhou, Y. Development of replication defective influenza virus vaccine for swine. Poster presentation at the Banff Pork Seminar in the Fairmont Banff Springs Hotel, Banff, Alberta, Canada, January 7-9, 2020.

Landreth, S., Gaba, A., Zhou, Y. Development of a novel live attenuated influenza vaccine against H1N2 and H3N2 in pigs. Oral presentation at the Lister Center, University of Alberta, Edmonton, Alberta, Canada, June 4, 2019.

Landreth, S., Lu, Y., Gaba, A., Zhou, Y. Development of a novel vaccine against low pathogenic avian influenza (LPAI) H7N9 viruses. Poster presentation at the Health and Life Science Research Expo, University of Saskatchewan, Saskatoon, Saskatchewan, Canada, May 2, 2019.

Landreth, S., Lu, Y., Gaba, A., Zhou, Y. Development of a highly pathogenic avian H7N9 influenza disease model in mouse. Oral presentation at the 5th International One Health Congress, TCU Place, Saskatoon, Saskatchewan, Canada, June 22-25, 2018.

Landreth, S., Lu, Y., Gaba, A., Zhou, Y. Development of a mouse disease model for the highly pathogenic avian H7N9 influenza. Poster presentation at the Health and Life Science Research Expo, University of Saskatchewan, Saskatoon, Saskatchewan, Canada, May 3, 2018.

Landreth, S., Lu, Y., Zhou, Y. Development of a novel H7N9 influenza vaccine. Poster presentation at the School of Public Health poster day, University of Saskatchewan, Saskatoon, Saskatchewan, Canada, October 20, 2017.

A.3 Scholarships

School of Public Health scholarship ($8000) from the School of Public Health, Vaccinology & Immunotherapeutics, University of Saskatchewan, 2017.

A.4 Awards

First place in Basic Sciences Category 4 ($200) for a poster presentation at the Health and Life Science Research Expo, University of Saskatchewan, 2019.